DEVELOPMENT OF WASTE-HEAT THERMOELECTRIC POWER GENERATION SYSTEM FOR BIOMASS POWER PLANTS

BANCHOB SUKPRAPAPORN

A Thesis Submitted to the Graduate School of Naresuan University
In Partial Fulfillment of the Requirements for the Doctor of Philosophy
Degree in Renewable Energy
September 2014
Copyright 2014 by Naresuan University

Thesis entitled "Development of Waste-heat Thermoelectric Power Generation System for Biomass Power Plants" By Banchob Sukprapaporn has been approved by the Graduate School as partial fulfillment of the requirements for the Doctor of Philosophy in Renewable Energy of Naresuan University

Oral Defense Committee

........................P. Promvonge........................ Chair

(Associate Professor Pongjet Promvonge, Ph.D)

.... Advisor

(Pisit Maneechot, Ph.D.)

.... Co – Advisor

(Assistant Professor Nipon Ketjoy, Dr-ing.)

.... Co – Advisor

(Assistant Professor Sarayooth Vaivudh, Ph.D.)

Approved

....

(Panu Putthawong, Ph.D.)
Associate Dean for Administration and Planning
for Dean of the Graduate School

29 | September 2014

ACKNOWLEDGEMENT
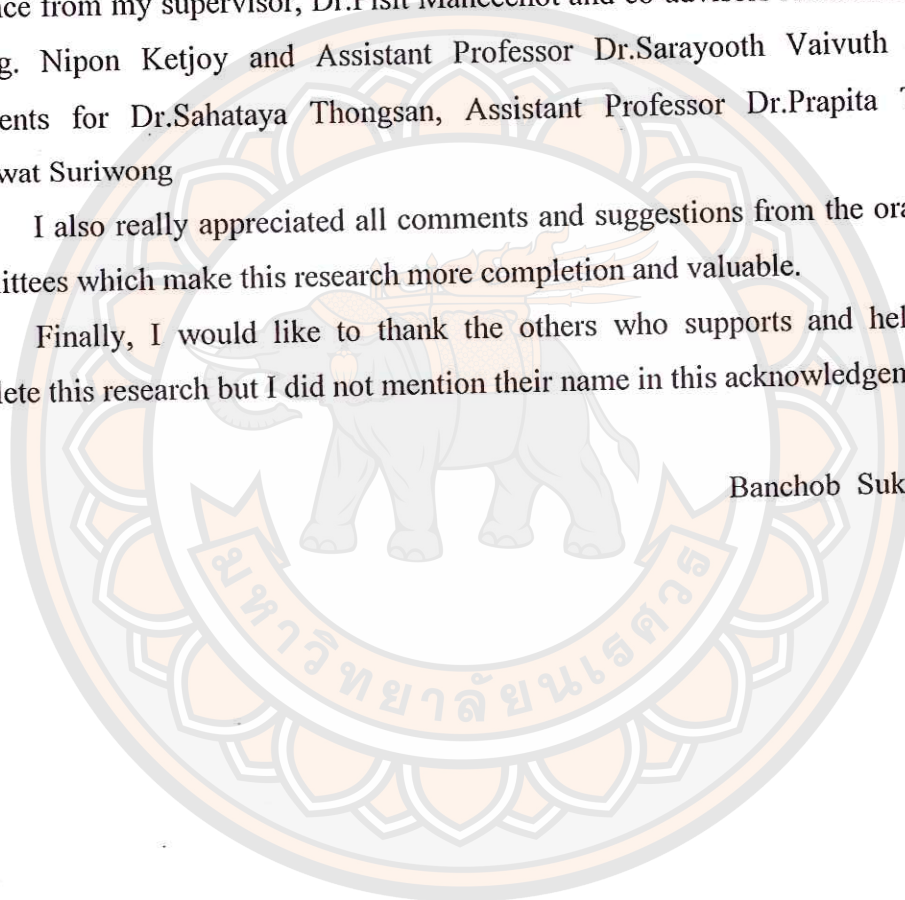
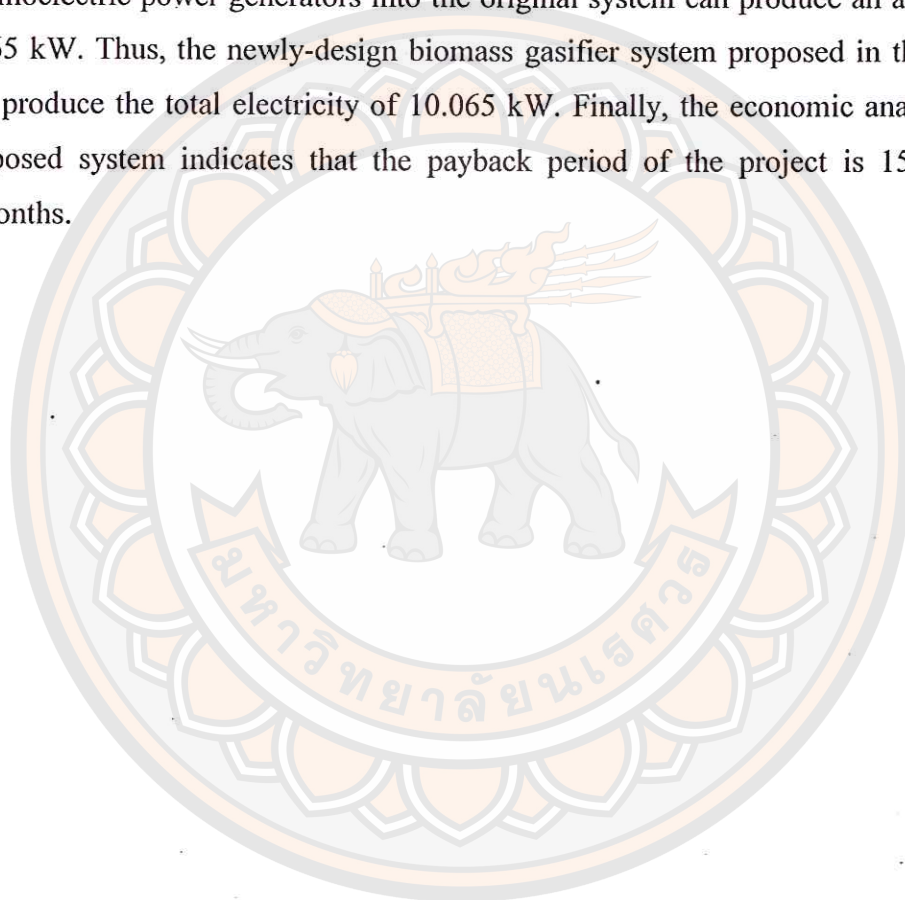| Title	DEVELOPMENT OF WASTE-HEAT THERMOELECTRIC POWER GENERATION SYSTEM FOR BIOMASS POWER PLANTS
Author	Banchob Sukprapaporn
Advisor	Pisit Maneechot, Ph.D
Co- Advisor	Assistant Professor Nipon Ketjoy, Dr.-Ing
	Assistant Professor Sarayooth Vaivudh, Ph.D
Academic Paper	Thesis Ph.D. in Renewable, Naresuan University, 2014
Keywords	Thermoelectric power generator (TEG), Waste-heat, Biomass gasifier

ABSTRACT

A synthesis gas or syngas produced from a biomass gasifier system usually has a very high temperature and need to be cooled by a cooling system. Thus, a biomass gasifier system loses approximately 60-65% of thermal energy to its surrounding environment. This waste-heat can be recovered for several purposes such as power generation by using thermoelectric devices. This research has an objective to design a suitable geometry of a heat duct that can be used with a flat-shaped thermoelectric power generator (TEG) model HZ-14. We found that a square cross-sectional duct is the most suitable geometry, because a temperature profile along its length is the most stable even though it has the lowest average temperature compared with a triangular and a circular cross-sectional ducts. In order to improve the efficiency of heat transfer of a square cross-sectional duct, a swirl or a wedge cores were installed and tested whether which type of ducts can create a turbulent flow. A swirl core could create a turbulent flow and improved the efficiency of heat transfer by increasing the average temperature inside a square cross-sectional duct for approximately 16-22%. Moreover, flow directions of a cooling system were also tested whether a pararell flow or a counter flow can create a stable profile of temperature differences along the length of a heat duct. A counter flow contributes to the most stable temperature difference profile. In conclusion, a square cross-sectional duct is the most suitable geometry. Installation of a swirl core inside a heat duct can

increase an average temperature and improve the efficiency of heat transfer of a heat duct. Using a counter flow of a cooling system contributes to the most stable temperature difference profile along the length of a heat duct. A total thermal energy produced from a biomass gasifier system was 42.547 kW, while waste-heat was 23.288 kW. The thermoelectric power generators could recover only 1.254 kW and generate 0.065 kW of electricity which is equal to 5.18% efficiency. The original biomass gasifier system can generate 10 kW of electricity, while the installation of thermoelectric power generators into the original system can produce an additional of 0.065 kW. Thus, the newly-design biomass gasifier system proposed in this research can produce the total electricity of 10.065 kW. Finally, the economic analysis of the proposed system indicates that the payback period of the project is 15 years and 5 months.

LIST OF CONTENT

LIST OF CONTENT (CONT.)

LIST OF TABLES

LIST OF TABLES (CONT.)

LIST OF FIGURES

LIST OF FIGURES (CONT.)

LIST OF FIGURES (CONT.)

ABBREVIATIONS

A	=	Area (m^2)
P	=	Power (Watt)
E , v	=	Electrical Potential (Voltage)
R , r	=	Resistor (Ω)
L	=	Inductor (H)
I , i	=	Electrical Current (A)
V	=	Voltage (V)
E	=	Thermal Conductance (W/m^2, kW/m^2K)
cp	=	Specific Heat (J/kg.K)
E	=	Energy (J, Joule)
Q	=	Heat Flow (J/kg)
k	=	Conductivity of Material (W/m.K)
P	=	Density (kg/m^3)
a , S	=	Thermo Power (V/K)
c	=	Heat Capacity of Thermopile (J/K)
a , S	=	Thermo Power (V/K)
CFM	=	Liquid or Air Flow Rate (Ft^3/minute)
H	=	Enthalpy (kJ/kg)
h	=	Latent Heat (kJ/kg)
S	=	Entropy (kJ/K)
u	=	Internal Energy (Joule)
S	=	Seebeck Coefficient (V/K)
l	=	Length of the Thermo Element (m)
lc	=	Thickness of the Contact Layer (m)
$\Re$	=	Electrical Resistivity of the Thermo Element (Ω.m)
λ	=	Thermal Conductivity of the Thermo Element (W/m.K)
λc	=	Thermal Conductivity of the Contact (W/m.K)

CHAPTER I

INTRODUCTION

Rationale of the Study

Thailand imports most of fossil fuels, such as oil and gas, from foreign countries. In 2011, the imported fossil fuels was equivalent to 1,845 thousand barrels (KBD) of oil per day [1] or a total of 1.2 trillion baht per year. [2] However, Thailand is also a country of a very high agricultural output with a vast harvest area of approximately 238,794 km^2 [3]. Thailand's important agricultural products are rice, sugar cane, maize, cassava, rubber and palm oil which can produce large amounts of raw materials and waste. These agricultural products can be used for fuel and biogas production by using a fermentation system or synthesis gas production by using a biomass gasifier system.
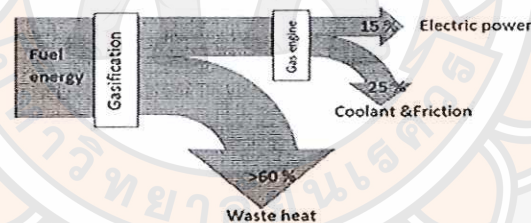
Figure 1 Waste-heat of a biomass gasifier system

As shown in the Figure 1, a biomass gasifier system loses approximately 60-65% of thermal energy to its surrounding environment [4] and 25% by coolant and friction. This waste-heat can be recovered for power generation by using a thermoelectric power generator or TEG. The thermoelectric power generator can convert thermal energy into electricity. Thermoelectric power generators can also be integrated into the original biomass gasifier system. Even though the installation of thermoelectric devices into the original system are not complicate, design of a heat duct that has a suitable geometry is necessary. A suitable design of duct can improve the efficiency

of heat transfer of a heat duct. In conclusion, the integration of thermoelectric power generators into the original system can save the initial cost and improve the total efficiency of a biomass gasifier system.
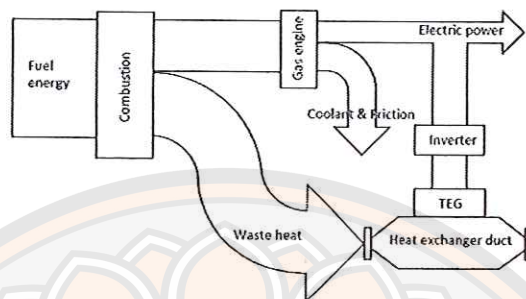
Figure 2 Waste-heat recovery from a biomass gasifier system

Waste-heat can be recovered for several purposes such as using in drying processes, heating water or generating power from thermoelectric devices. A thermoelectric device employs the Seebeck effect, which is the direct conversion of temperature differences into electricity or vice versa. A thermoelectric device has two sides (cool and hot sides) made of different types of materials. The efficiency of a thermoelectric device depends on temperature differences (ΔT) between the two sides. The integration of thermoelectric devices into the original biomass gasifier system as shown in the Figure 2 can increase the total power output of the gasifier system. Moreover, the newly-design system for a small-scaled biomass gasifier system may be able to operate without reliance on an external power sources, which is suitable for remote areas.

Problem Statement

The integration of thermoelectric devices into the original biomass gasifier system requires modification of a heat duct. In this research, different geometries of a heat duct which are circular, triangular and square cross-sectional ducts were designed. Their thermal conductivity were tested to find the most suitable geometry. Installation of a swirl core and a wedge core were made in order to improve the efficiency of heat transfer of a heat duct. Flow directions of a water cooling system

were also tested whether a parallel flow or a counter flow contribute to the most stable temperature difference profile along the length of a heat duct. Moreover, the economic analysis of the integrated system was analyzed to determine whether it is economically reasonable to invest money in the newly-design system or not.

Purpose of the Study

1. To determine and utilize waste-heat from a biomass power plant, and to generate electricity from thermoelectric devices combining to the original biomass gasifier system.

2. To design and fabricate a heat transfer system to utilize waste-heat from a biomass gasifier system.

3. To evaluate the economic analysis of the integrated system combining the thermoelectric devices into the original biomass gasifier system.

Scopes of the Study

1. Testing and measuring the power generation of a 10 kW small biomass gasifier system.

2. Designing equipments such as heat ducts and cooling pipes for waste-heat recovery from biomass gasifier system for power generation. Testing equipments for thermoelectric power generation.

3. Evaluating the economic analysis of the thermoelectric devices integrated to the original biomass gasifier system by the 3 economic indicators which are the Payback period (PB), the Net Present Value (NPV) and the Internal Rate of Return (IRR).

Expected Benefits

1. To use waste-heat from the biomass gasifier system by analyzing and designing a heat duct, a cooling pipe and flow directions of a water cooling system.

2. To know main features of the thermoelectric properties.

3. To determine the performance of thermal energy conversion to electricity.

4. Analysis of strengths and weaknesses of the biomass gasifier system and the cost effectiveness of investment and operation.

CHAPTER II

LITERATURE REVIEWS

In this chapter, researches related to this thesis including topics of materials, experimental procedures and scientific principles such as principles of biomass gasifier system, thermoelectric power generation and heat transfer in a heat duct will be discussed. The content of this chapter is divided into the following topics;

Biomass

Biomass is an organic matter that stores energy in a form of chemical substances. Plants, which are major sources of biomass contributing to approximately 10-14% of the total energy supply, convert carbon dioxide, water and light into carbohydrate during the photosynthesis [5]. To release energy stored in carbohydrates, breaking down of chemical bonding is necessary. However, there are several methods of breaking the chemical bonding such as fermentation and combustion. Moreover, agricultural products are one of the most important parts of the economy of Thailand. During 1998-2000, agricultural products accounted for approximately 10.1-11.2% of Thailand's GDP [6].

In general, there are three major categories of biomass which are woody, non-woody and animal waste [7]. However, biomass can also be classified according to their sources as follows;

1. Agricultural waste such as rice husk, rice straw, corn cob, cassava, peanut shell, coconut shell cotton seed etc.

2. Agro-industrial waste such as bagasse from sugar production, food waste rejected from production lines etc.

3. Domestic waste such as municipal waste and animal feces.

4. Aquatic biomass such as algae, water hyacinth etc.

There are two categories of methods available for conversion of biomass into energy sources, which are bio-chemical methods and thermo-chemical methods. The bio-chemical methods are fermentation as a means for breaking down the chemical bonding of biomass such as ethanol or methane production through anaerobic digestion, while the thermo-chemical methods are directed combustion, gasification, pyrolysis and liquefaction instead of fermentation. Moreover, the conversion of biomass into thermal energy can be categorized into three methods which are direct combustion, gasification and cogeneration.

1. Direct combustion

The direct combustion is the most commonly used method which biomass, in a form of solid fuel, by direct burning in a furnace. Heat production from combustion will be turned water into a high-pressure steam for driving a steam turbine for power generation. Steam will be delivered through a condenser and become water droplets. After temperature and pressure of water is low. It will flowed to a boiler and repeated step again. The types of a furnace is depended on sizes of biomass fuel. Wood scraps which a relatively large size are suitable for a kiln gasification system, while rice husk or sawdust which a small size are suitable with a fluidized-bed system.

2. Gasification

The gasification is a process of reacting biomass with high temperatures under limited amount of air without combustion. The resulting gas mixture of carbon monoxide, hydrogen and methane is called a synthetic gas or syngas.

3. Cogeneration system

The cogeneration system is the use of a heat engine to generated electricity and thermal energy at the same time. The total energy efficiency of cogeneration system is approximately 80% which is high compared to 40% of the system that uses electricity alone.

Biomass Gasification System

The biomass gasifier system is produced thermal energy by blowing air into a furnace under limit amounts of oxygen without fully combustion. The gasifier system can be classified into categories as follows;

1. Updraft or counter-current gasification

A small gas stove is produced simplest by blowing the air flow up through a wire rack on the top of gas stove. The fuel will be fed in to the top of the stove then moves down to bottom. This system is called counter flow or also called a countercurrent gasifier. The bottom layer is the combustion zone, and next to reduction zone, pyrolysis zone and drying zone respectively. The combustion occurs on the grate when the fuel this area is called the combustion zone. [8]
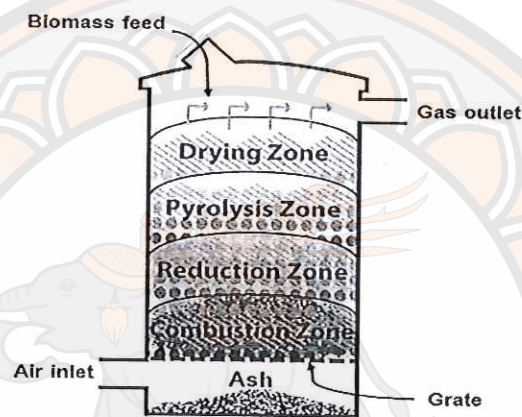
Figure 3 Updraft gasification.

2. Downdraft gasification

This stove is designed for eliminate the tar fuel. The air will be flowed down in the same route as the flow of fuel, which run from the top of gas stove to the bottom. This is called a co-current gasifier system. In combustion zone, the fuel with the air mixing will be flowed from the combustion zone and reduction zone to the bottom. The temperature combustion in the range between 900-1200 °C. The gas can be applied to the internal combustion engine. The disadvantage of this type of gas stove the combustion will burned on bottleneck. Thus, it is necessary to used material which durable with high temperature, also melt and sticks together and causes clots in the bottleneck. The gas stove is produced gas temperature of between 450 °C to 550 °C. [8]
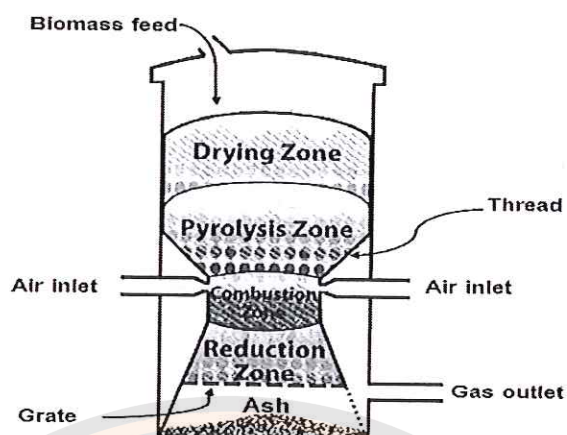
Figure 4 Downdraft gasification.

3. Cross-draft gasification

This biomass system the fuel will be fed from the top to bottom. The direction of air flow is flowed perpendicular to the axis of the furnace or the air will flowed transverse to the flow of the fuel and sent directly to the combustion zone and also to the reduction zone. Both floors will be laid as a small layer. The average temperature is not high. The advantages are small and light weight. It can produced gas faster with low tar and oil. [8]
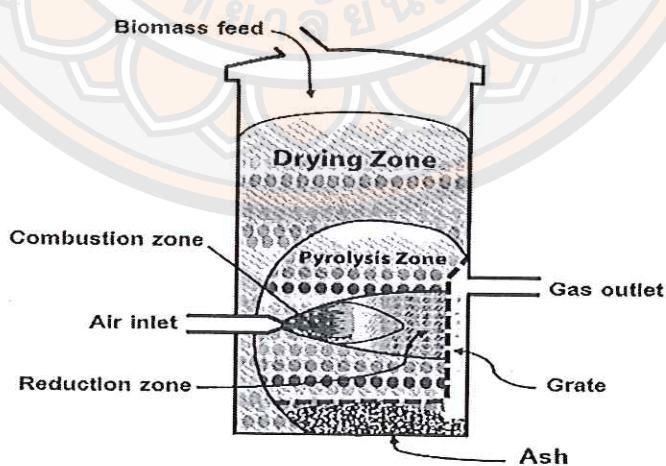
Figure 5 Cross-draft gasification.

4. Fluidized-bed gasification

This furnace, the temperature is easy to control. The temperature is below the melting point of the ash. It will prevented the capture of slag fuel ash which, is occurred in a gasification furnace may cause many problems. Due to the high speed of the air inside the furnace, ash and dust need will be removed from the process by using a dust trap. This control system is complex and difficult to used, and expensive.
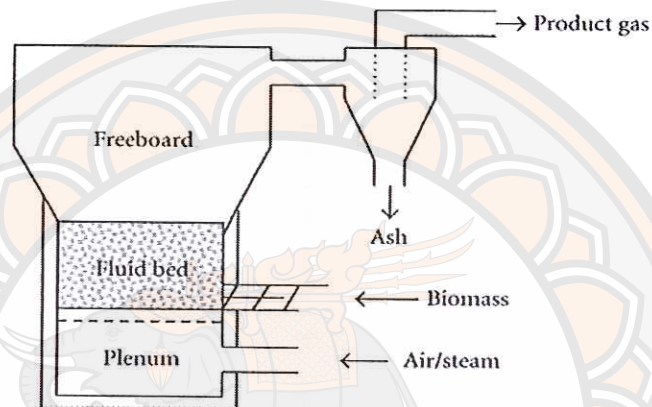
Figure 6 Fluidized-bed gasification.

5. Suspended gasification

The principle of this gas stove, the air is swirled across the oven, each section. This system is a completed combustion process. The fuel are used coal or small fuels, such as sawdust, rice husk. [8]
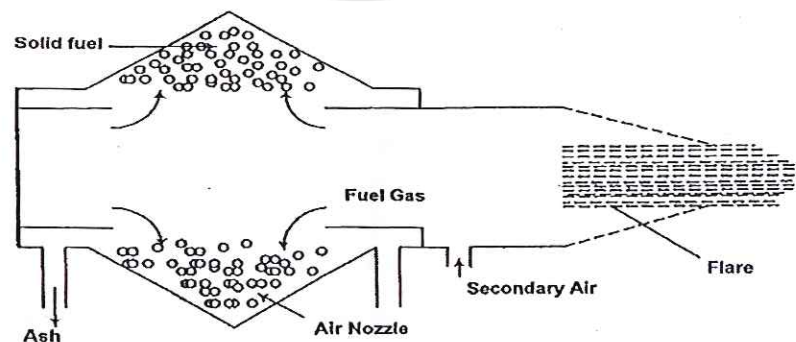
Figure 7 Suspended gasification.

The produced gas can be used as fuel for the gas turbine, for power generation and for gas engines. Many of international attention have been focused on electricity produced by the use of gas turbines. This can be seen by the increasing number of gas turbine power plant. However, there have been problems with the produced gas as fuel for electricity. These problems include dust and tar contamination in large quantities. This causes problems for the engine producing electricity. Also the built up of slag means the furnace has to be shutdown frequently to remove the slag. Correction of the gas filters due to the high temperature of the biogas it also a problem.

In Thailand, the electricity power plant by using the producer gas has been undertaken for more than 20 years. Rice husks are offer used to produce fuel, because Thailand has a lot of rice. Many of modern rice mills are uses rice husk in the biomass gasifier process, which is then used power gasoline engine to produce electricity for used in the mill.

Benefits of Using Biomass to Produce Electricity

Mainly of biomass is agricultural products, which it can supply fuel across the country in different for each region. Possible it will required for use the biomass to produce electricity in the future for the following reasons.

1. Thailand is an agricultural country. The biomass and a byproduct of agriculture are still cheap.

2. Fuel that imported from abroad will get more expensive. To reduce costs, biomass has received more attention as an alternative energy source.

3. Environmental awareness. It is low particular emitted waste from power plant. The advantages of biomass are stayed in this field. It is a natural material. When burning biomass, Carbon dioxide is return to the plant that have been used and rotation continuous.

Thermoelectric Generator (TEG)

A thermoelectric device is a solid state material that can achieve energy conversion known as the Seebeck effect. It was discovered by Thomas Seebeck in 1821, when a temperature by a process difference is occured at the hot-cold junction of the two dissimilar materials (P-type and N-type semiconductors), electrical potential will be generated in the Figure 8 explain the thermoelectric power generation.
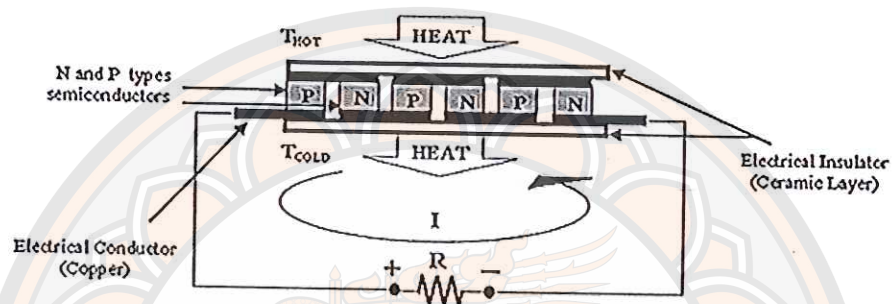
Figure 8 Thermoelectric module in generator mode.

In 1834, Jean Charles Athannase Peltier found that electric current can be produced at the hot-cold junction of two dissimilar metals. The proportionality constant was shown as the Peltier coefficient. Twenty years later, William Thomson was proposed a comprehensive explanation of the Seebeck and Peltier effects, and described their inter-relationships through thermodynamics which is a phenomenon known as thermoelectric effect. These three effects can be represented mathematically as follows.

$$dE = \alpha(h\text{-}c)dT \qquad \text{[Eq.1]}$$

$$dQ = \pi(h\text{-}c)dI \qquad \text{[Eq.2]}$$

$$dQ = \beta(h\text{-}c)dI \; T/\partial x \; dx \qquad \text{[Eq.3]}$$

Where. α (h-c) = The Seebeck coefficient

π (h-c) = Peltier coefficient

β (h-c) = Thomson coefficient

x = Conductor length

I = Electric current

E = Electric potential

h, c = Hot-cold junction's temp. [9]

In 1910, Altenkirch was provided a theoretical description of the thermoelectric effect and in 1948 Loffe proposed a new theory that thermoelectric generating material needs high a Seebeck coefficient (α), high electrical conductivity (σ), and low thermal conductivity (κ). The efficiency of thermoelectric material can be defined as shown in the Figure 9 and the power generation as an equation.

$$\text{Figure of merit (Z)} = (\alpha^2 \sigma)/k \qquad \text{[Eq.4]}$$
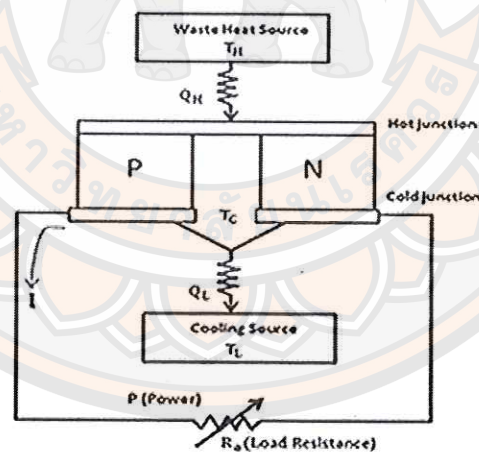
Figure 9 Basic concept of thermoelectric generation. [10]

The principle of thermoelectric generation can be described through the Seebeck and Thomson effects that electricity can be generated by temperature difference on both sides of the thermoelectric material as shown in the Figure 9. The waste heat source (QH) and cooling source (QL) can be calculated as follow.

$$QH = \alpha I \bar{T} H + \kappa(\bar{T}H - \bar{T}L) - 1/1 I^2 R_{TEG} \qquad \text{[Eq.5]}$$

$$QL = \alpha I \bar{T} L + \kappa(\bar{T}H - \bar{T}L) + 1/1 I^2 R_{TEG} \qquad \text{[Eq.6]}$$

The principle of thermoelectric generation can be described through the Seebeck and Thomson effects being that electricity can be generated by temperature difference on both sides of the thermoelectric module (ΔT). [11] The hot side of the thermoelectric unit will be archived from a heat source and the cold side of the thermoelectric unit must be cooled by the air, water or oil. The temperature between a both sides of the thermoelectric device can generated electricity. The power output is depended on the temperature difference between both sides of the device.

Thermoelectric Material Property

1. The Seebeck coefficient is defined as the Seebeck voltage per unit. Temperature is measured and the magnitude of an induced electric power for response to the temperature difference across that material. The thermo power has a units of voltage per kelvin (V/K), although it is more often given in microvolts per kelvin (μV/K). This is represented by the Greek letter α. Most of materials, conductor and semiconductor have Seebeck coefficients. It has been found that Seebeck coefficients metals range from extremely small values to approximately 80 (μV/K). For semiconductors, the range is up to 900 (μV/K). The materials specifically developed for thermoelectric applications have Seebeck coefficient of approximately 100-500 (μV/K).

Table 1 Seebeck coefficient of some semiconductor. [12]

Semiconductors	Seebeck coefficient (μV/k)	Semiconductors	Seebeck coefficient (μV/k)
Se	900	$Pb_{09}Ge_{33}Se_{58}$	-1360
Te	500	$Pb_{13}Ge_{29}Se_{58}$	-1710
Ge	300	$Pb_{15}Ge_{37}Se_{58}$	-1990
N-type Bi_2Te_3	-230	$SnSb_4Te_7$	25
P-type $Bi_{2x}Sb_xTe_3$	300	$SnSi_4Te_7$	120
P-type Sb_2Te_3	185	$SnSi_3Sb_1Te_7$	151
PbTe	-180	$SnSi_{2.5}Sb_{1.5}Te_7$	110
$Pb_{03}Ge_{39}Se_{58}$	1670	$SnSi_2Sb_2Te_7$	90
$Pb_{06}Ge_{36}Se_{58}$	1410	$PbBi_4Te_7$	-53

2. Thermal conductivity is the quantity of heat that passed in unit time through a plate of a particular area and thickness where the opposite side differ in temperature one kelvin. For a plate of thermal conductivity k, area A and thickness L, the conductance calculate is kA/L, measured in W·K-1 (equivalent to: W/°C). The thermal conductance of that particular construction is the inverse of the thermal resistance. Represented by the Greek letter κ for thermoelectric applications, a substance should possessed the lowest thermal conductivity attainable. Most semiconductors exhibit thermal conductivity in the range 0.01-0.1 and the range in metals are approximately an order of a higher magnitude. [13]

3. Electrical resistivity known as resistivity, specific occurs when electrical resistance or volume resistivity the flow of electric current (A) has low resistivity indicates a material that allows the movement of electric charge. In commonly represented by the Greek letter ρ (rho). The SI unit of electrical resistivity is ohm-meter (Ω-m) although others unit as ohm-centimeter (Ω-cm) are also in used. In the process of maximization of the Figure of merit of semiconductors, found that the optimum range of electrical resistivity from 10.2 to 10.3 Ω-cm (3). Most of metals are

exhibited resistance about one thousand as great. Semiconductors whose resistivity between 0.01 and 0.1 Ω-cm. [13]

4. The thermoelectric figure of merit can be expressed in terms of a number of parameters such as reduced Fermi energy, reduced energy gap, thermal conductivity, effective of mass and controls the change in composition and dopant of material Consequently, if the order parameters are fixed, then the Figure of merit can optimized with respect to variations in the reduced Fermi energy and reduce energy gap. [13] The efficiency can be expressed as a function of the temperature over which this operate is called goodness factor or thermoelectric Figure-of-merit of the thermoelectric material (Z).

$$Z = \frac{\alpha^2}{(\rho k)}$$ [Eq.7]

Where
α = Seebeck coefficient $(\frac{V}{K})$

P = Electrical Resistivity (Ω-m)

k = Thermal conductivity $(\frac{W}{wK})$

The materials are used to make a thermocouple with different features according to the type of metal will be focus on the thermal conductivity, that can be measured at high temperatures, but thermoelectric device focus on the seebeck coefficient, which is a semiconductor materials, that it has limitation in choosing the materials in high efficiency as shown in the Figure. [13]
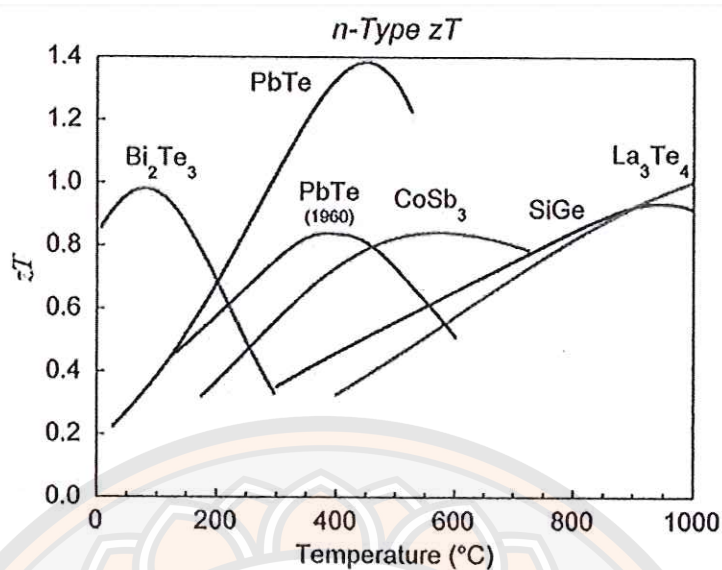
Figure 10 The efficiency of thermoelectric material. [13]

The target of thermoelectric module is used to the waste heat recovery market. The HZ-14 is made from bismuth telluride alloys and consists of 98 couples, when applies to any heat source, the module is required a heat flux of about 8 Watt per cm^2. At a temperature difference of 200°C the module is converted 5% of the thermal energy that pass through in to electricity will generated a maximum power 13 Watt of electrical power. When the thermoelectric device has properly installation, can be run for tens of thousands hours. [14]Thermoelectric device was generated electric power and can be calculated by using equation as follow.

$$P = I^2 R \qquad\qquad\text{[Eq.8]}$$

Benefits of Thermoelectric Device

Thermoelectric device is a modern technology in development. There are two type of construction. One for application is used in the cooling systems and another for generate electricity, the advantages of these devices which are beneficial to use are the following.

1. High reliability. Thermoelectric devices as solid-state which work in a heat pump they have a structure made of a semiconductor which is doped with a material difference between the two types of the structure. The two types of N-type and P-type materials will be computability for high quality. The manufacturers can be guarantee the performance for up to 20 year.

2. Flexibility. The function, applications of the thermoelectric components can be connect in series and parallel, they can be used with the DC voltage system.

3. Environmentally friendly. The materials of thermoelectric component is obtained from natural material. The silicon and ceramic can be able to recycle or destroy, then convert back to their original condition. Material is not toxic or dangerous chemically they can be used safely.

4. Light weight. A thermoelectric device is used a lightweight structure. Each module can provided high power and installed easily without need for big and strong body thus can be saved for the cost of the building of the piece as well.

5. Small size. Each module of the thermoelectric device is small in ranging from 40-80mm^2, with a thickness of about 4-10 mm, which it can be installed in a small areas.

6. Noiseless operating. The equipment of the thermoelectric device have not a moving parts. It does not cause noise on vibration. It does not cause problems when use in environments that require silence. In addition, the thermoelectric devices can also be used in various environments, including areas with as well as noise and vibration. It can also use in area where these are intense radio wave frequency.

Heat Transfer of TEG

The heat transfer means the energy transfer due to the temperature difference. The transfer of thermal energy from a higher temperature to a lower when the two mediums reach the same temperature. The heat transfer mechanism can be used in three basic ways. The conduction is used to transfer heat through a solid material such as metal, concrete or mediums of various natural materials. The convection is the heat transferred by using the medium material such as liquid and gas in heat transference; these include water, oil, steam, air and gas. The radiation is the transfer of heat from one point to another point by means of thermal radiation frequency and clearly

observes radiation from the sun, the heat transfer by radiation transmit through a high frequency in the Infrared and microwave range.

In heat conduction through solid medium materials, there is a different rate of conduction. This is an important for make effect the heat transfer in medium, thickness of material, types of materials and the amount heat transmitted.

Heat transfer by conduction will be transferred in an opaque object. The grade of the temperature can occur in a solid, liquid and gas, but due to current flow occurs optimally in liquids and gases. The solid opaque materials do not moved. The heat will be transferred by conduction only. The rate of heat transferred by conduction of heat is proportional to the gradient of temperature (Temperature gradient) multiply with area of the heat flow as equation.

$$Rate\ of\ heat\ conduction\ \alpha = \frac{(Area)(Temperature\ difference)}{Thickness} \qquad [Eq.9]$$

$$\dot{Q}_{cond} = A\frac{dT}{dX} \qquad [Eq.10]$$

Where

$\dot{Q}_{cond}$	=	Rate of heat conduction, (W. or J/s)
A	=	Area of temperature passes (m^2)
T	=	Temperature (k)
x	=	Thickness of material (m)

The rate of heat conduction through material, the proportion will be make the temperature difference across the layer and the heat transfer area. It is inversely proportional to the thickness of the layer material. It can be written as an equation.
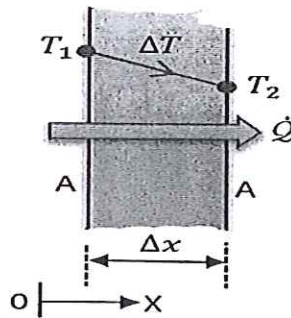
Figure 11 Rate of heat conduction in the medium.

$$\dot{Q}_{cond} = kA\frac{T_1 - T_2}{\Delta x} = -kA\frac{\Delta T}{\Delta x}$$ [Eq.11]

Where k =   Thermal conductivity of materials

dT/dx =   Temperature gradient (negative when temperature decreases with increases X)

Heat is conducted in the direction of the decreasing temperature heat transfer. Figure 12 is the normal direction of heat transfer in materials.

(a) copper   (b) silicon
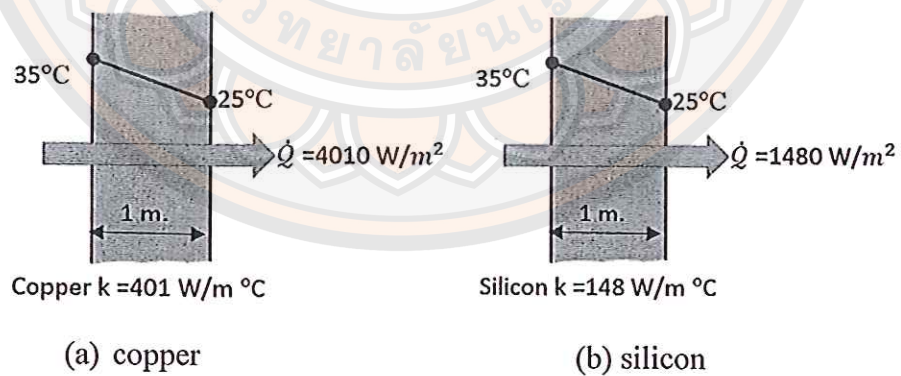
Figure 12 Thermal conductivity of material.

The thermal conductivity of materials varies over a wide range, as shown in the Figure 13 the thermal conductivity of gases such as air will be vary by a factor of 104 from those of pure metals such as copper. Note that pure crystals and metals have the highest thermal conductivity but gases and insulating materials are still lowest.
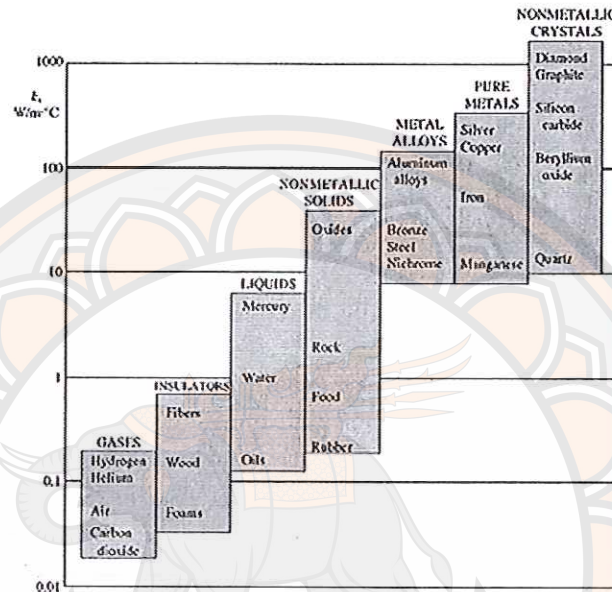
Figure 13 The range of thermal conductivity of various materials. [15]

The Heat ducts to use in industry can divided in to the group according to the shape of the device. The heat exchanger of the fluid as shown on the chart as follow.
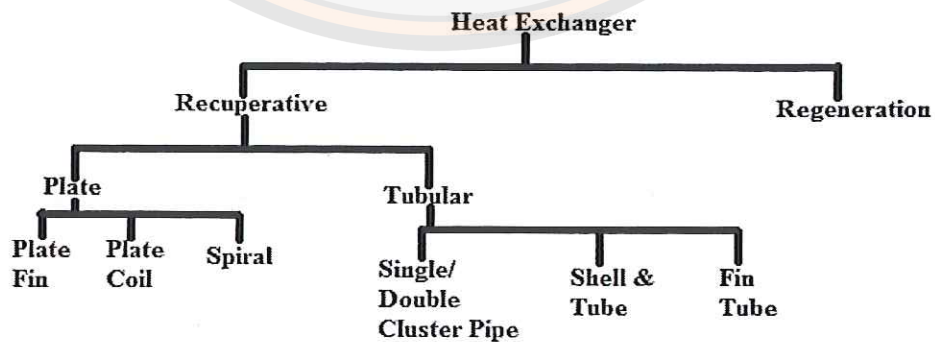
Figure 14 Type of heat exchangers. [16]

The Heat Exchanger

Normally, the two fluids pipe can be classified into four basic types in the Figure 15(a) illustrate idealized counter flow exchanger in which the two fluids flow parallel to each other but in opposite directions. This type of flow arrangement is allowed the largest change in temperature of both fluids, therefore most of efficient where the efficiency is the amount of actual heat transfer compared with the theoretical maximum amount of heat that can be transferred. In parallel flow heat exchangers, the streams will flow parallel to each other and in the same direction as shown in the Figure 15(b); this is less efficient than counter flow.

(a) Counter flow   (b)Parallel flow

(c)Cross flow   (d) Hybrids flow
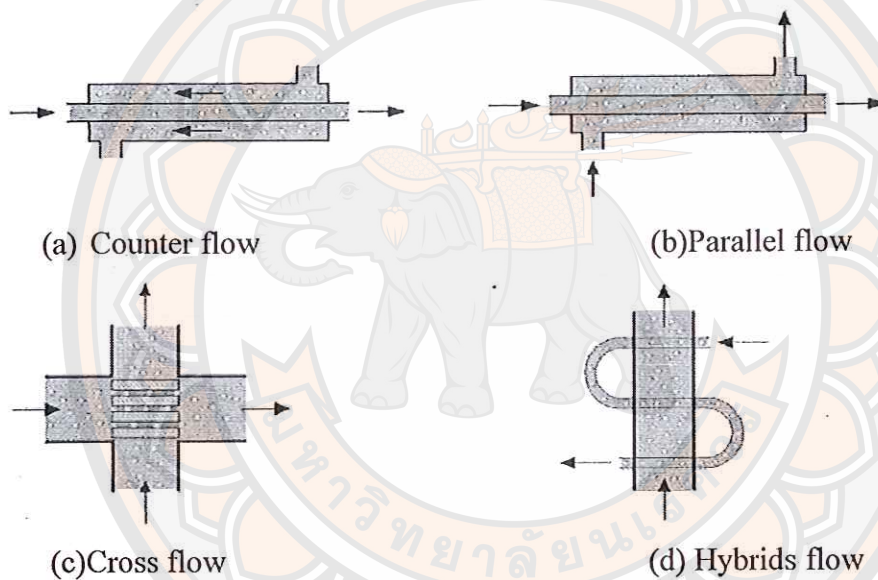
Figure 15 Type of heat exchanger flow. [17]

According to the Figure 15(c) the cross flow heat exchanger is intermediate in efficiency between counter flow and parallel flow exchangers. In these unit, the stream flow at right angle to each other. The fourth type in the Figure 15(d) is used in industrial heat exchangers, hybrids of the above flow types are often found. These are the combined cross flow and counter flow or multi pass flow heat exchangers.

Fluid Flow in Pipe

Fluid that flows in limited or low speed is called a lamina flow rate. When the flow rate up is called a turbulent flow. Fluid motion is not uniform. A transformation of the flow is cause by friction. This is cause by the flow of liquid through a solid uneven surface.

Osborne Reynolds (1842-1912) the physicist was the first proved the variables used to control flow and correlate this information to predict the flow and also found that the phenomenon of the flow is generated by a balance between inertia, friction and the viscosity of the fluid. Thus leading to the definition of the term no unit is called the Reynolds number indicates the ratio between the viscosity and inertia of movement speed. This causes will make the laminar flow to become a turbulent flow.
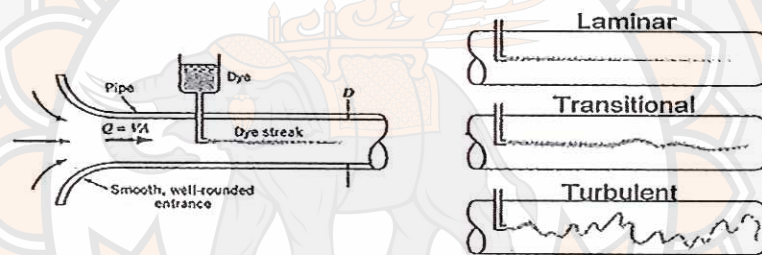
Figure 16 Type of current flow in pipe. [18]

The performance of fluid flow is influenced by a dimensionless unit which called the Reynolds number. It can defined as the ratio of the liquid's inertial forces to drag forces.

a) Uniform Lamina flow   b) Non-uniform Lamina flow   c) Turbulent flow
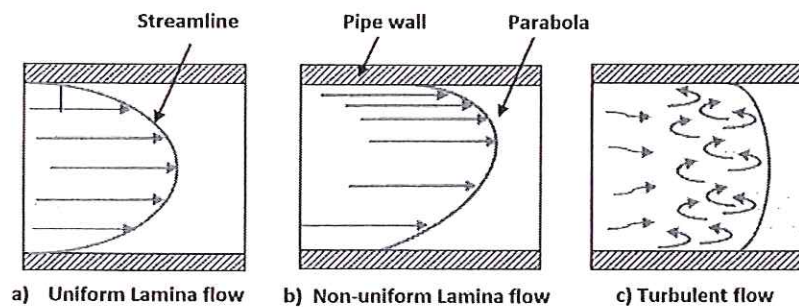
Figure 17 The shape of liquid and gas flow in tube.

The flow rate and the specific gravity are inertial forces, and the diameter of pipe and viscosity are dragged forces. When the diameter of pipe is constant. At the low velocities or high viscosities, the fluid will flow low speed and smoothly. The layers with the highest velocity at the center of the pipe and low velocities at the wall of pipe, where the viscous forces will be restrained fluid flow. This type of flow is called laminar flow. The Re values are approximately below 2300. A characteristic of laminar flow is fluid flowed in the parabolic shape the velocity profile as shown in the Figure 17 However; most applications involve turbulent flow, with the Re values above 2300. Turbulent flow occurs at high velocities or low viscosities. The fluid flow will break up into turbulent eddies that flow through the pipe with the same average velocity. The velocity profile is flowed uniform in the pipe. A transition zone exists between turbulent and laminar flows depending on the piping configuration and other installation conditions. The flow may be either turbulent or laminar in this zone. The laminar and turbulent flow are two types normally encounter in liquid flow measured. Most applications involve turbulent flow, with the Re values above 2300. Viscous liquids usually exhibit laminar flow, with the Re values below 2300. The transition zone between the two levels may be either laminar or turbulent as shown in the Equation 12. [51]

$$Re = \frac{3160 \times Q \times G_t}{D \times \mu} \qquad \text{[Eq.12]}$$

Where
Re = Reynolds number
Q = liquid's flow rate, (*gpm*)
Gt = liquid's specific gravity
D = inside pipe diameter, (*inch*)
μ = liquid's viscosity, (centipoise: *cp*)

When Liquid or gas was flowed through the pipe usually applied to heating or cooling a fluid or gas flow in the pipeline to determine by the value of the Re. Where the Re is the dimensionless unit given by the ratio of the force due to the inertia force to the viscosity of the fluid. It is used as a criterion to distinguish whether the flow is

laminar flow or turbulent flow. The Re of the flow in the pipe can be calculated by the Equation 13.

$$Re = \frac{\rho V_{avg}D}{\mu} = \frac{V_{avg}D}{v}$$ [Eq.13]

Where V_{avg} = mean velocity

ρ = The density of the fluid.

D = Diameter pipe. (Wet line).

$V = \mu/\rho$ = kinematic viscosity of the fluid

For lamina flow in pipes: Re < 2,300. Flow transition length: 2,300> Re> 10,000 and turbulent flow Re> 10,000.

And $Re = \frac{\rho V_{avg}D}{\mu} = \frac{V_{avg}D_h}{v}$ (Flow in non-circular pipe) [Eq.14]

By $D_h = \frac{4A_c}{P}$

When A_c = Cross section area of duct

P = border line of box

When hot or cold fluids at temperature T flow through a pipe, temperature of the fluid will change. If the pipe wall temperature, Ts is constant, temperature of the fluid will gradually change, as in the case of fluid velocity shown in the Figure 18.

(a)Actual   (b) Ideal
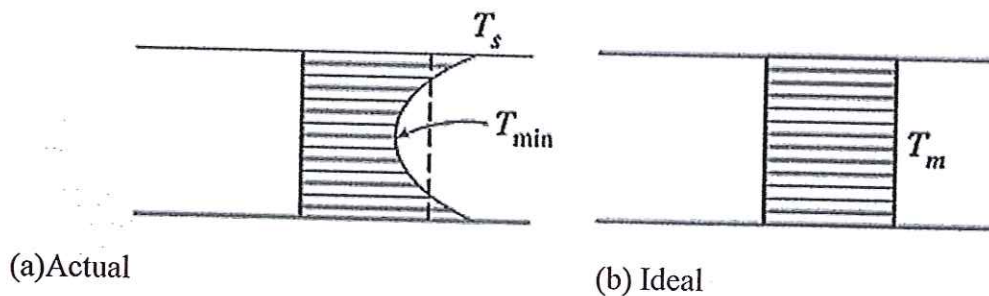
Figure 18 Temperature profile of fluid in pipe.

Thermal Entrance Region

When hot or cold fluids at temperature T the temperature of the fluid flowing through the tube will be changed. If the pipe wall temperature Ts, which is constant. Temperature of the fluid will gradually change, as in the case of the fluid velocity as shown in the Figure 19. Temperature profiles change from the regular (uniform) to a complete development (fully developed region) called thermal entry length (Lt) and show that.

$$\frac{L_t}{D} = 0.05 \, RePr \qquad\qquad\qquad \text{[Eq.15]}$$
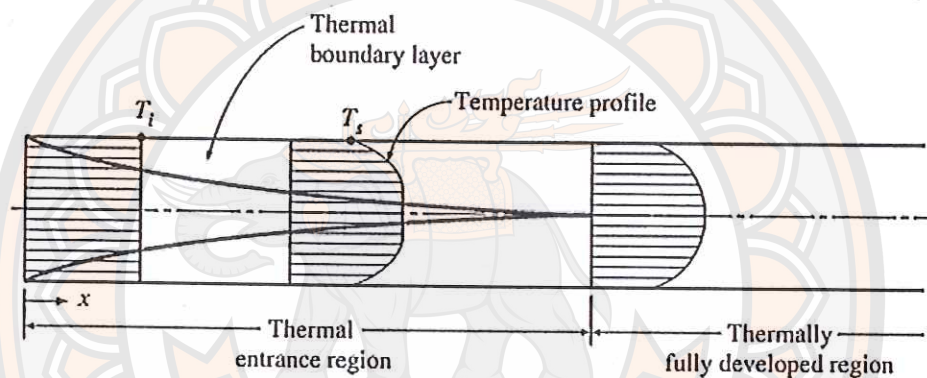
Figure 19 Develop region profile of fluid flow.

General Thermal Analysis

Consider, the equation of energy conservation for the steady flow of a fluid is flowing within a pipe as shown in the Figure 20.
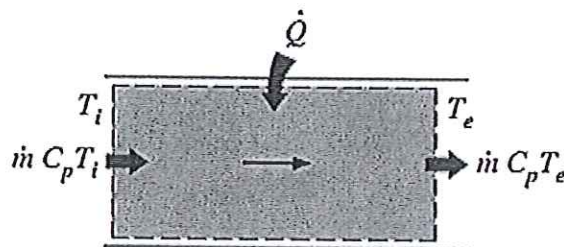
Figure 20 Thermal transfer to fluid.

Energy balance: $\dot{Q} = \dot{m}C_p(T_e - T_i)$ (Watt) [Eq.16]

When

T_e and T_i Average temperature of the fluid at the entrance and exit, respectively and the rate of heat transfer into or out of the liquid tank. Observe that the temperature of the fluid in the pipe will be fixed in no case of the interaction process between the pipes.

Surface Heat Flux

The surface heat flux is the amount of heat per unit area on the materials. The unit is Watt/m^2 . It can find by the Equation 17.

$$q_s = h_x(T_s - T_m)(W/m^2)$$ [Eq.17]

In the case of heat transfer analysis. Can be divided into two cases, including a case study.

1. Constant surface heat flux (q=constant)

In cases where q_s is a constant heat transfer rate. It can be calculated by the Equation 18.

$$q = q_s A_s = \dot{m}C_p(T_e - T_i)$$ [Eq.18]

When the average temperature at the exit of the pipe is given by the Equation 19.

$$T_e = T_i + \frac{q_s A_s}{mCC_p}$$ [Eq.19]

Pipe surface temperature in the case of constant surface heat flux q_s. It can calculated by the Equation 20-21.

$$q_s = h(T_s - T_m)$$ [Eq.20]

To that

$$T_s = T_m + \frac{q_s}{h} \qquad \text{[Eq.21]}$$
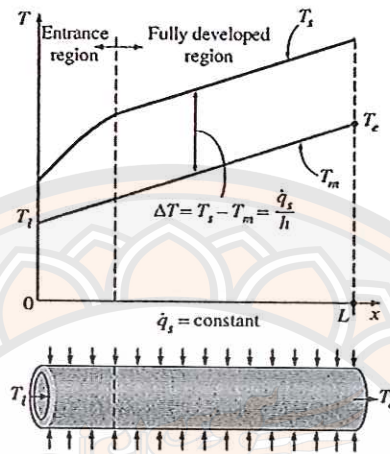
Figure 21 Variation of the tube surface and fluid temperatures:

According to the Figure 21. The fully develop region surface temperature(T_s) is flowed increase on the distance and the fluid moves; with at this region $T_s - T_m$ are constants. This equation will be true when fluid properties are constant during the flow.

The average temperature slop (T_m) on the graph T_x . The diagram from the energy balance in a small area with thickness d_x as shown in the Figure 22 and can be found by the Equation 22.
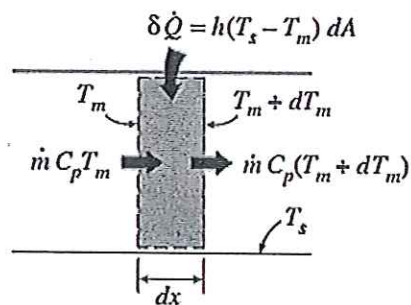
Figure 22 Energy interactions of control volume.

$$\dot{m}C_p dT_m = q_s dA_s = q_s(pdx) \qquad \text{[Eq.22]}$$

$$\frac{dT_m}{dx} = \frac{q_s p}{\dot{m}C_p} = constant \ t \qquad \text{[Eq.23]}$$

When

$p =$ is perimeter of the tube

Note q_s and h is constant Therefore, differentiation equations

$$\frac{dt_m}{dx} = \frac{dT_s}{dx} = constant \ t \qquad \text{[Eq.24]}$$

$$\frac{\partial}{\partial_k}\left(\frac{T_s - T}{T_s - T_m}\right) = 0 \qquad \frac{1}{T_s - T_m}\left(\frac{\partial T_s}{\partial k} - \frac{\partial T}{\partial k}\right) = 0 \qquad \frac{\partial T_s}{\partial k} = \frac{\partial T}{\partial k}$$

To that $\dfrac{\partial T}{\partial x} = \dfrac{dT_m}{dx} = \dfrac{dT_s}{dx} = \dfrac{q_s p}{\dot{m}C_p} = constant \ t$ [Eq.25]

The equation conclude that fully develop flow in a pipe under a constant surface of heat flux, the temperature gradient depends on the distance of X, and the model of temperature profile will not change by the length of the pipe as shown in the Figure 23 below.
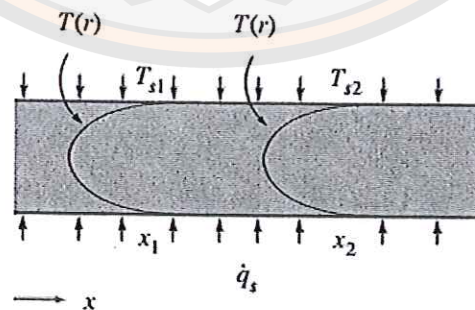
Figure 23 The fully development region in pipe.

The shape of the temperature profile is remain unchanged in the fully developed region of a tube subject to constant surface of heat flux.

2. Constant Surface Temperature (T_s= Constant)

From the Newton's law of cooling system. It can calculated the rate of heat transfer into or out of the fluid flowing through the pipe. It can be calculated by the Equation 26.

$$q = hA_s\Delta T_{avg} = hA_s(T_s - T_m)_{avg} \qquad [Eq.26]$$

When h = the average heat transfer coefficient.

A_s = the surface area for heat transfer tube and the average temperature difference between the fluid and the surface.

Analysis of Heat Exchangers

In designing or selecting a heat exchangers are used in engineering. There must be a way of predicting the exit temperature of the hot and cold fluids. Determine the rate of heat transfer between the hot fluid and cold when the rate of the fluid mass flow is known. The heat exchanger is usually used for a long time without changing in working conditions. Therefore, one might suppose that a device has a steady flow properties. The temperature at the inlet or entrance constant. Unchanged kinetic energy and specific heat to the average fluid is constant. Thermal conductivity along the axis of the pipe is not important and cannot calculated. Finally, assuming the outer surface of the heat exchanger is well insulation so that protect heat loss of heat transfer fluid to the two type. The rate of heat transfer from the hot fluid to cold fluid. Heat transfer rate can be found by the Equation 27-28.

$$\dot{Q} = \dot{m}_c C_{pc}(T_{c,out} - T_{c,in}) \qquad [Eq.27]$$

And

$$\dot{Q} = \dot{m}_h C_{ph}(T_{h,out} - T_{h,in}) \qquad [Eq.28]$$

When h and c subscript is the hot and cool fluid.

$$\dot{m}_c, \dot{m}_h = \text{mass flow rate}$$
$$C_{pc}, C_{ph} = \text{specific heats}$$
$$T_{c.out}, T_{h,out} = \text{average outlet temperature}$$
$$T_{c.in}, T_{h,in} = \text{average inlet temperature}$$

Heat exchangers will be located in a twin tube attach together. The fluid flow may flow in following is called parallel flow and opposite direction flow is called counter flow. Both direction flow is shown in the Figure 24 as follow.
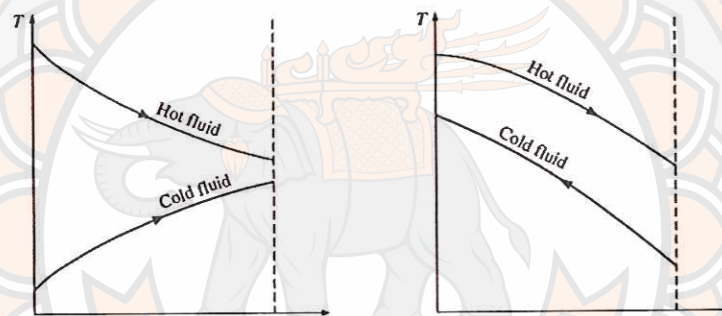
Figure 24 The direction flow of heat exchanger.

In the analysis of heat exchangers. In order to include the mass flow rate and specific heat of the fluid together for ease of calculation. The number call. Rate of heat (Heat Capacity Rate), C as follow.

$$C = \dot{m}C_p \qquad \text{[Eq.29]}$$

For hot fluid $C_h = m_h C_{ph}$ and cool fluid $C_C = m_C C_{pC}$, this equation in the form of heat capacity is the ability to shown the difference in the case of the rate flow and the heat capacity is the same, as shown in the Figure 25.

$$\dot{Q} = C_c(T_{c,out} - T_{c,in}) \qquad \text{[Eq.30]}$$

And

$$\dot{Q} = C_h(T_{h,out} - T_{h,in})$$ [Eq.31]
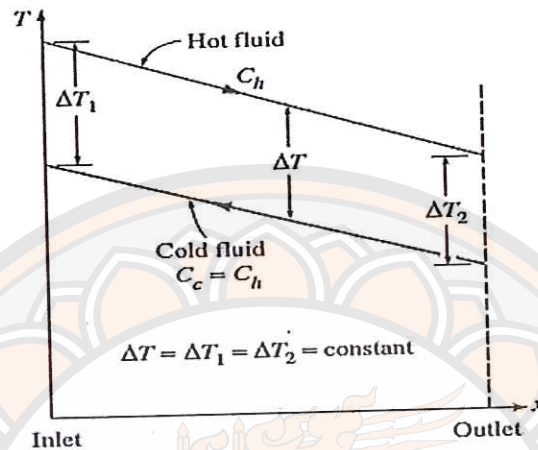
Figure 25 The temperature of counter flow.

Economic Evaluation

The measuring of implementation for energy projects need a minimum standard "Bottom line" of performance configurations and shown the cost benefit to make sure that the implementation of projects has economic potential. The value of implementation is a reason to bring a degree of uniformity to the procedures for financial evaluation of energy production projects and an evaluation of the cost-effectiveness for completion and investment. "Life Cycle Costing" is seen as the most reliable methodology for determine the cost effectiveness of energy management projects for institutional, government commercial and industrial applications. Life cycle costing methodology is involved adding up all the costs of a project over the term of the evaluation, with the costs in one-year will be discounted back to the base period. The discounting process seeks to reflect the time value for money and reduce all future sums of money to an equivalent sum of money in the base period (e.g. in today's dollars or dollars at the start of the project). This discounting process estimates the present value of future costs. The following assumptions are made in this approach. Initial capital costs are consider as a lump sum at the start of the analysis.

1. Others non-recurring costs as replacement of plant and equipment probably require during the period of the analysis.

2. All recurring costs (e.g. energy costs and operating and maintenance costs) begin to accumulate in the first period.

3. Costs in any period are lump together and consider to occur at theend of that period.

4. Input such as salvage values are consider as negative costs.

5. The rate at which costs increase may differ between energy and othersrecurring costs.

Present Value

Present value is the value of a future transaction discounted to some base date. It is reflected a time value for money. The present day equivalent of a future cost, i.e. the present value can be thought of as the of amount money that would be invested today, at an interest rate equal to the discount rate, in order to have the money available to meet the future cost at the time when it was predicted to occur. The value can be find by the Equation 32.

$$Present\ Value = \frac{F_n}{(1+r)^n} \qquad \text{[Eq.32]}$$

Where F_n = cash flow, or any other value in year n.

n = year

r = discount rate

$1/(1+r)^n$ is define as the single payment present worth factor.

If inflation is consider, the single payment present worth factor can be included the effects of both inflation and discount rate, and becomes a function of r, a, and n.

$$\frac{(1+a)^n}{(1+r)^n} \quad or \quad \left(\frac{1+a}{1+r}\right)^n \qquad \text{[Eq.33]}$$

Where r = discount rate

a = escalation / inflation rate

n = year

Another term often use in discounted cash flow calculations is the escalated ratio, d.

$$d = \frac{1+a}{1+r}$$ [Eq.34]

Where a = inflation / escalation rate and

r = discount rate.

Net Present Cost

The Net Present Cost (NPC) of a project is the sum of the Present Value of all costs over the period of interest, including residual values as negative costs. The total Net Present Cost of a project is a summation of all cost components including.

1. Capital investment cost.
2. Non-fuel operation and maintenance cost.
3. Replacement cost.
4. Energy cost. (fuel cost plus any associated cost)
5. Any other cost such as legal fees, etc.

If a number of options are considered then the option with the lowest. The Net Present Cost is the most favorable financial option.

Net Present Value

The Net Present Value (NPV) of a project is the sum of the present values of all the benefits associated with the project less the sum of present values of all costs associated with the project. In a project with a single capital outlay of "C" at the start of the project and annual financial savings that will be increased at a rate of "a" from an initial Figure of "S", the Net Present Value can be given by the following equation.

$$NPV = -C + \sum_{1-1}^{n} \left(\frac{1+a}{1+r}\right)^{i} \times S \qquad \text{[Eq.35]}$$

Where $\sum_{1-1}^{n} \left(\frac{1+a}{1+r}\right)^{i}$ = PWF (a, r, n) is the present worth factor for a series of regular payments / savings. PWF (a, r, n) probably referred to as the net present cost factor and the value can be determined from the Tables (e.g. see the standard) or from the formula.

$$\text{PWF } (a, r, n) = \frac{1-\left(\frac{1+a}{1+r}\right)^{n}}{\left(\frac{1+a}{1+r}\right)-1} \qquad \text{[Eq.36]}$$

If the NPV of a project is positive, then the project will provided a net financial benefit for the company. Such as an approach can be used when evaluate energy management options, which will involve the initial capital expense and produced subsequent energy savings.

Payback Period

The Payback Period (PB) takes into account the time taken to payback the capital Investment "C" on the basis of equal annual payments, the annual payments being the estimated savings. The simple Payback Period is given by the Equation 37.

$$T = \frac{C}{S} \qquad \text{[Eq.37]}$$

Where
C = Capital Investment
S = Estimated savings
T = Time period in years

Annual Equivalent Cost

This is a variation of the NPV method which may be more meaningful to many people. Costs and savings are reduced to a series of equal annual payments which when discount and summed have the same total value as the initial outlay. This is equivalent to the calculation of a bank loan.

The capital recovery factor (CRF), which is the reciprocal of the PWF, is used to convert a single payment "C" into the equivalent annual payment "A".

$$A = C \times CRF(a,r,n) \qquad \text{[Eq.38]}$$

$$= C \times 1/PWF(a,r,n) \qquad \text{[Eq.39]}$$

Compare Tariffs and Generated Cost of Energy

It is important to note that there exists a significant difference between the "tariffs" which must be charged to recoup energy costs and the often quoted "generate" cost of energy. The difference stems from the public utility need to discount their annual revenue, which is successes through the sale of units of electricity (kWh). The following examples illustrates the difference.

Tariff (P_0) = tariff which recover the NPC over "n" years in PV terms.

$$NPC = (P_0 \times kWh) + (P_0 \times kWh)\frac{(1+a)^1}{(1+r)} + (P_0 \times kWh)\frac{(1+a)^2}{(1+r)} + \cdots +$$

$$(P_0 \times kWh)\frac{(1+a)^n}{(1+r)} \qquad \text{[Eq.40]}$$

Therefore,

$$P_0 = \frac{NPC}{discounted\ kWh} = \frac{NPC}{kWh\left(1+\frac{1+a}{1+r}+\left(\frac{1+a}{1+r}\right)^2+\cdots+\left(\frac{1+a}{1+r}\right)^n\right)} \qquad \text{[Eq.41]}$$

Generate cost (G_0) – kWh is not discount.

Therefore,

$$G_0 = \frac{NPC}{Total\ kWh} \qquad \text{[Eq.42]}$$

Where   *Total kWh = kWh/yrs. × "n" years.*

Benefit-Cost Analysis

The benefit-cost analysis is known as a cost-benefit analysis (CBA) or a benefit-cost analysis (BCA). Performing one is critical to any project. When performing a cost-benefit analysis make a comparative assessment of all the benefits anticipate from the project and all the costs to introduce the project, to perform and support the changes resulting from project.

Cost benefit analysis is a technique for finding costs and social benefits paid out in cash (monetary social cost and benefit) of investment projects in a given period of time. Principles of cost benefit analysis are a key criteria.

1. Use as a tool to evaluate the program in view of economic analysis, or evaluation of social or welfare benefit. This is a technique used in projects, business and government spending projects.

2. Use as a tool to bring out the impact of the project to the outside. (externally) to be consider in the implementation of the project, including impacts on people or the environment outside the project couple with the economic costs and benefits to the project and bring the two parts to be included in the decision to implement the project or not. In this sense and the second part will be included in the decision to implement the project or not, in this sense, cost benefit analysis is estimated the impact on social welfare of the investment in the project.

3. Navigating the vagaries of time frame consider in terms of the economic value of the discount period, benefit delay or even more in the future or to cut costs

by period in the future.

Benefit Analysis.

Step 1. Calculated the social benefits of the project. Social benefits imply.

1. Visible direct benefits.

2. Benefits that is not visible. The indirect benefits or benefits to person who fall outside the target.

Step 2. To calculated the social costs incurred, cost comprises direct visible costs and the Invisible or indirect costs. The project implement in step 1 and step 2 are important step one must have the confidence that they can gather and calculated the social benefits and social costs completely.

Step 3. Calculated the analysis sensitivity. Assess the nature of events or results that may not happen. Assess the size of the uncertainty, to measure the true value of the costs and benefits as to ensure the accuracy of the calculation in Step 1-2.

Step 4. The depreciation by taking into account the financial value of the benefit discounting the future time. One is the reduction of the value of the costs and benefits that accumulate over time. The fee is discount back to present value to a lower value, where is different. The value of future benefits will be reduced indefinitely. If the time period is greater this causes a discount future value.

Step 5. Compared the benefits expect against cost. This indicates that the cost has been deducted from the benefits already. The net social rate of return is positive or negative. If the value of social returns are positive. It is estimate that the project is worthwhile.

Step 6. Compared between the returns of the investment project in considering whether the project can be implemented to achieve social benefits. In such cases, to consider projects with lower costs or a return on investment that is worth the input.

Table 2 Cost and benefit analysis.

Field	Cost		Benefit	
	Non current	Recurrent	Non current	Recurrent
Personal	xxx	xxx	xxx	xxx
Spare parts	xxx	xxx	xxx	xxx
Subcontractung	xxx	xxx	xxx	xxx
Computerized maintainance management	xxx	xxx	xxx	xxx
Tools	xxx	xxx	xxx	xxx
Measuring instruments	xxx	xxx	xxx	xxx
Equipments	xxx	xxx	xxx	xxx
Training	xxx	xxx	xxx	xxx
Others	xxx	xxx	xxx	xxx
Total	xxx	xxx	xxx	xxx

Literatures Review

There are a variety of applications including the application of heat from the car, the source of heat from the cooking stove, of solar energy or the waste-heat from industrial factories from, research laboratories which are as follows.

J. C. Bass., et al. [20] presented in proceeding of the 13th International conference on thermoelectric applications to truck essential power 1 kW generator mounted on 141 commins NTC 350 engine. The generator built up with Hi-Z 14 type modules, which were reformed so as to have a high durability under the use of harsh conditions. The generator was coupled directly to the exhaust gas outlet of the engine turbocharger. The main structure of the generator was a cylindrical steel casting body having surface resisted with nickel. The total length is 47 cm. the diameter is 22 cm. and the weight was 13.6 kg.

K. Ikoma et al. [21] the Nissan motor group developed a prototype generator for gasoline engine vehicle. The size of the module was 20 mm. square and 9.2 mm.in height. The module consists of 8 couples of p-type and n-type Si-Ge elements. The elements were electrically connected in series using mo electrode by brazing method. The maximum electric power of the module was approximately 1.2 W, at the temperature difference 563 K between the hot and cold side of the module. A thermoelectric generator had been made using 72 units of the present module. The module was arranged between an exhaust pipe with a rectangle cross sectionand a water jacket around the exhaust pipe. The volume of the generator was 440 x 180 x 170 mm^3. Generated electric power of the present generator was 35.6 W, when the exhaust gas was introduced into the generator under the condition corresponding to 60 km/hr. hill climb mode of 3000 cc. gasoline engine vehicle. The heat exchange efficiency of the generator was estimated at 11% of the primary exhaust gas energy flux. The generated power was 0.9% of the heat flux through the generator.

Chih Wu, et al. [22] researched analysis of waste-heat thermoelectric power generation a real thermoelectric power generator utilizing waste-heat is proposed. The generator was treated as an external and internal irreversible heat engine. The specific power output of the generator was analyzed and compared with that of the Carnot, end reversible and external reversible thermoelectric heat engines.

Jin-Kuk Kim., et al. [23] researched on cooling systems to date had focused on the individual components of cooling systems, not the system as a whole. Cooling water systems should be designed and operated with consideration of all the cooling system components because of the interactions between cooling water networks and the cooling tower performance. In re-circulating cooling water systems, cooling Water from the cooling tower was supplied to a network of coolers that usually had a parallel configuration. However, re-use of cooling water between different cooling duties enables cooling water networks to be designed with series arrangements. This allows better cooling tower performance and increased cooling tower capacity, both in the context of new design and retro. A methodology has been developed for the design of cooling networks to satisfy any supply conditions for the cooling tower. A model of cooling tower performance allows interactions between the performance of the cooling tower and the design of cooling water networks to be explored systematically. In debottlenecking situations, better design of the cooling network using the new method, including increasing cooling tower blow down, taking hot blow down and strategic use of air coolers, can all be used to avoid investment in new cooling tower capacity and to improve the performance of the cooling tower in a systematic way.

Douglas T., et al. [24] conducted research in optimization of cross flow heat exchangers for thermoelectric waste heat recovery. Thermoelectric waste heat recovery was investigated for current thermoelectric materials with advanced heat exchangers. Numerical heat exchanger models integrated with models for Bi_2Te_3 thermoelectric modules were validated against experimental data from previous cross flow heat exchanger studies as well as experiments using thermoelectric between counter flow hot water and cooling air flow channels. The models were used in optimization studies of thermoelectric waste-heat recovery with air cooling in a cross flow heat exchanger. Power losses from an air fan and a fluid pump result in an optimal configuration at intermediate cooling air and hot fluid flows. Results show that heat exchangers with Bi_2Te_3 thermoelectric scan achieve net power densities over 40 W/l.

Chuang Yu., et al. [25] conducted research of thermoelectric automotive waste-heat energy recovery using maximum power point tracking, a thermoelectric waste-heat energy recovery system for internal combustion engine automobiles, including gasoline vehicles and hybrid electric vehicles. The key was to directly convert the heat energy from automotive waste-heat to electrical energy using a thermoelectric generator, which was then regulated by a DC–DC up converter to charge a battery using maximum power point tracking. Hence, the electrical power stored in the battery could be maximized. Both analysis and experimental results demonstrate that the proposed system could work well under different working conditions, and was promising for automotive industry.

Panya Yodovard. [26] conducted research in thermoelectric power generation by using two scale thermoelectric generations the first was use Bi_2Te_3 thermoelectric module property testing by using LPG gas. And the second to study for large scale of waste-heat recovery data from 27000 factories in the potential for thermoelectric generation.

Somchai maneewan. [27] conducted to research in mathematical modeling of a roof-integrated solar thermoelectric generation. Study the system performance of a roof-integrated first to prove the feasibility of this concept and develop mathematical model set energy balance equation for thermoelectric module (TEG) and study in the characteristic and the number of thermoelectric module under Thailand weather condition.

Xiaolong Gou., et al. [28] conducted research in modeling, experimental study and optimization on low-temperature waste heat thermoelectric generator system, thermoelectric generator for waste heat recovery in industry area, and a low-temperature waste heat thermoelectric generator setup had been constructed. Through the comparison of results between theoretic analysis and experiment, testing results and discussion show the promising potential of using thermoelectric generator for low-temperature waste heat recovery, especially in industrial fields.

Basel I., et al. [29] conducted research into novel technologies of generating electrical power. Thermoelectric power generators have emerged as a promising alternative green technology due to their distinct advantages. Thermoelectric power generation offer a potential application in the direct conversion of waste-heat energy

into electrical power where was unnecessary to consider the cost of the thermal energy input. The application of this alternative green technology in converting waste-heat energy directly into electrical power can also improve the overall efficiencies of energy conversion systems. In this paper, a background on the basic concepts of thermoelectric power generation is presented and recent patents of thermoelectric power generation with their important and relevant.

In biomass gasifier system, hot gas produced from the system need to be cooled down. This situation leaves a large amount of excessive heat from the system. The most efficient cooling systems are cooling by water. Since water has lower temperature compared with hot gas, heat will transfer from hot gas to water. The thermoelectric effect reveals that temperature difference in the cooling system can be used in power generation. There are several studies that proposed the applications of thermoelectric technology in several systems such as power generation from an excessive heat of automobiles, solar panels and other heat sources. Even though biomass gasifier system already has equipments suitable for working with a very high temperature. Power generation from biomass gasifier system still need to be improved by changing or installation of additional equipments such as heat pipes or chilled-water-pipes. Thus, this research provides a design of the power generation system using thermoelectric technology with the small-scaled biomass gasifier system, and the economic analysis of the newly-design power generation system.

CHAPTER III

RESEARCH METHODOLOGY

This research has the purpose of the study to power generation from waste-heat of a small-scaled biomass power plant by using thermoelectric devices. The operations of this research were conducted as follows;

```
                    ┌──────────┐
                    │  Start   │
                    └──────────┘
                         │
                         ▼
┌──────────────────────────┐   ┌──────────────────────────────┐
│ 1. Performance of the     │   │ 2. Thermoelectric device     │
│    original Biomass       │   │    testing                   │
│    gasifier system.       │   │                              │
└──────────────────────────┘   └──────────────────────────────┘
                         │
                         ▼
┌─────────────────────────────────────────────────────────┐
│ 3 Heat duct design.                                      │
│    3.1 Heat duct design and testing.                     │
│    3.2 Effects of two type cores insertion in the duct.  │
│    3.3 Flow directions of a water cooling system.        │
│    3.4 Performance of the thermoelectric devices.        │
└─────────────────────────────────────────────────────────┘
                         │
                         ▼
        ┌──────────────────────────────────────┐
        │ 4 Thermoelectric Power Generation     │
        │   from Waste Heat of Biomass Gasifier │
        │   Plant.                              │
        └──────────────────────────────────────┘
                         │
                         ▼
            ┌──────────────────────────┐
            │  5. Economic Analysis.    │
            └──────────────────────────┘
                         │
                         ▼
                    ┌──────────┐
                    │   End    │
                    └──────────┘
```

Figure 26 The operation processes of this research.

Experimental design

1. Performance of the original biomass gasifier system.

A synthetic gas or syngas is a resulting gas mixture of a biomass gasifier system. The syngas usually has a high temperature and need to be cooled by a cooling system. A cooling process results in loss of waste-heat to the surrounding environment. This waste-heat can be used for several purposes. This research has an objective to study power generation from waste-heat by using thermoelectric devices. Benefits of using the integrated system, the combining of the thermoelectric devices into the original biomass gasifier system, are mobility and simplicity. Even though the original biomass gasifier system as shown in the Figure 27 requires little maintainance, it consumes large amounts of power supply and has to connect to the external power generation system. However, the integrated system may be able to rely on its own power source.
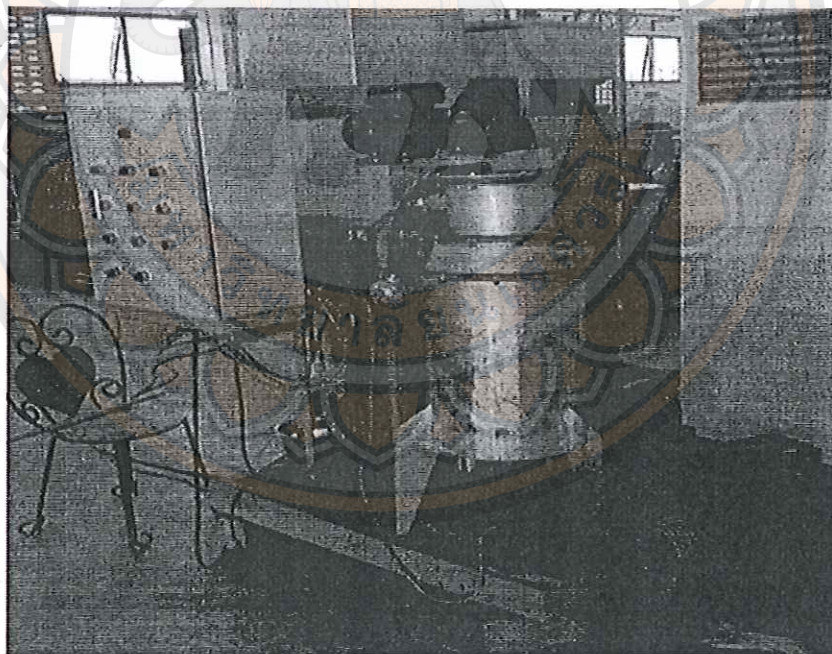
Figure 27 A small-scaled biomass gasifier system.

The schematic of a biomass gasifier system is shown in the Figure 28. In the integrated system, thermoelectric devices were placed on the surface of a heat duct. Since the surface of a heat duct has a very high temperature, the thermoelectric devices can convert thermal energy into large amounts of electricity. The installation of the thermoelectric devices at this position has no negative effects to regular functions of the biomass gasifier system.
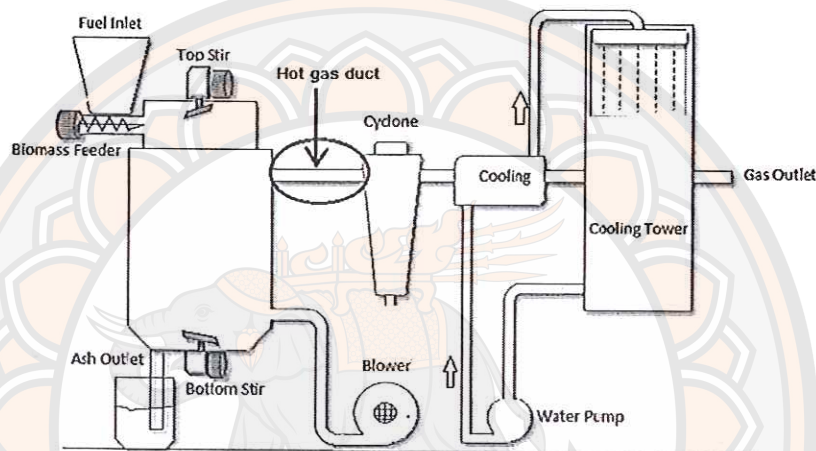
Figure 28 A small-scaled biomass gasifier system.

The performance of a small-scaled biomass gasifier system as shown in the Figure 27-28 was tested by using wood chips as fuels and feed them to the gasifier system with a rate of 4 kg/hr. This gasifier system produced a synthetic gas at a temperature of 150°C, while a temperature at the outlet was 41°C. Flow rate of a synthetic gas was of 257 CFM. The resulting gas was tested with a gasoline engine and a 10 kW dynamo.

2. Thermoelectric device testing

The thermoelectric device was tested to determine the ability to convert thermal energy into electricity.

In this experiment, a thermoelectric device was placed between a heat sink connected with a water cooling system and a hot plate as shown in the Figure 29. Temperatures and flow rates of water at the inlet and the outlet of a water cooling

system, and temperatures on the surface of a hot plate were measured by digital thermometers. The electric current of a power source was measured by AC ammeter, while the power output was measured by a DC voltmeter. A DC ammeter was also used to measure the electric current that flows across the resistive load. The experiments were conducted at different levels of temperatures from 100 - 280°C. The temperatures were increased 10° C per step. All experimental data was recorded for further analysis. The equipment use in the experiment were listed as follows;

1. A 750 W hotplate with an electric dimmer switch.
2. A thermoelectric device.
3. A heat sink connected with a cooling pipe.
4. A water pump.
5. A digital DC voltmeter and a DC ammeter.
6. A 1.5 ohm 10 W resistive load and a cable wire.
7. A digital thermometer with a thermocouple transducer.
8. A water tank.
9. A stopwatch.
10. A flow meter.
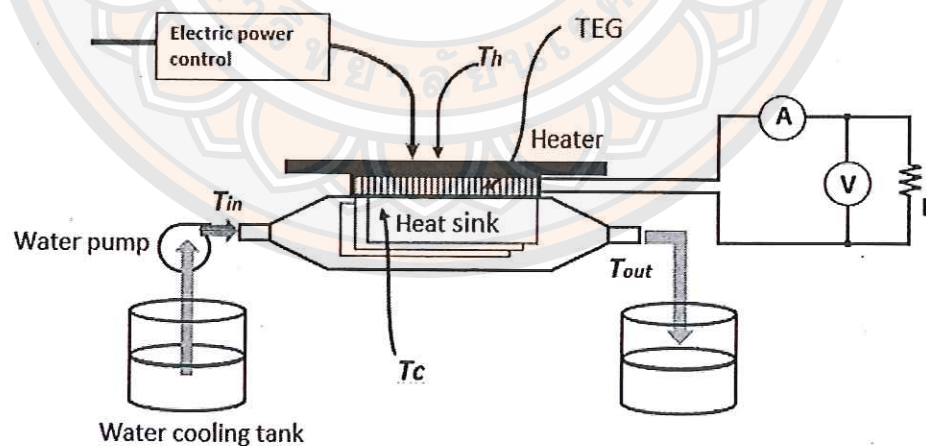
Figure 29 Thermoelectric property testing.

3. Heat duct design

In order to design a suitable geometry of a heat duct that can be used with thermoelectric devices, a triangular, a circular and a square cross-sectional ducts were designed as shown in the Figure 30. Temperatures along the length of these three ducts were measured. The effects of a laminar and a turbulent flows, and directions of a water of a cooling system to the efficiency of heat transfer in a heat duct were investigated. The experiments were conducted as follows;

3.1 Heat duct design and testing

A model of the thermoelectric devices used in the experiments have to be considered. There are several model available as shown in the Table 3. The model HZ-14 with a size of 6.27×6.27 cm^2 was selected, because it has the lowest price per watt for a desired size. These thermoelectric devices will be placed on the surface of heat ducts, the appropriate distance between each thermoelectric device is necessary to calculate. The suitable distance between each device was 7.5 cm. Temperatures along the length of heat ducts were measured on the positions that the thermoelectric devices will be installed as shown in the Figure 32.

Table 3 Characteristics of the thermoelectric devices. [18]

Model	Length(cm.)	Width(cm.)	High(cm.)	Weight (g.)	Power (Watt)
HZ-2	2.9	2.9	.508	13.5	2
HZ-9	6.27	6.27	.651	10.5	9
HZ-14	6.27	6.27	.508	8.2	13
HZ-20	7.5	7.5	.508	11.5	20

All heat ducts must have equal width (10 cm) and length (40 cm), and also have sufficient spaces for the installation of 5 thermoelectric devices. The Dimension of heat ducts are shown in the Table 4.

Table 4 Dimension of heat ducts.

Duct	Radius (cm.)	High (cm.)	Width (cm.)	Depth (cm.)	Length (cm.)	Volume (cm^3)	Cross-sectional area (cm^2)
1. Circular	1.5	-	-	-	40	282.8	7.07
2. Triangular	-	8.7	10	-	40	1750	43.5
4. Square	-	-	10	10	40	4000	100
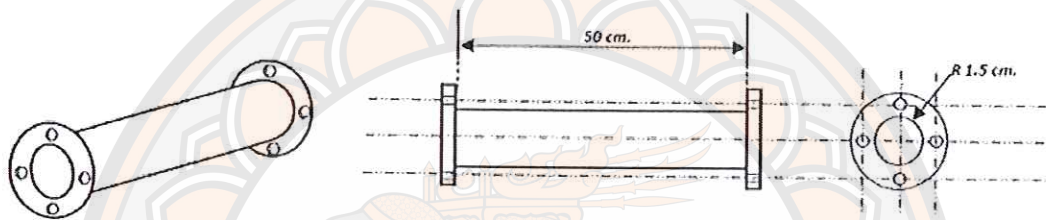
(a) A circular cross-sectional duct.
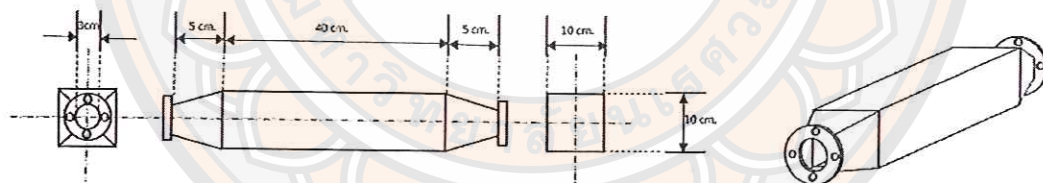
(b) A square cross-sectional duct.
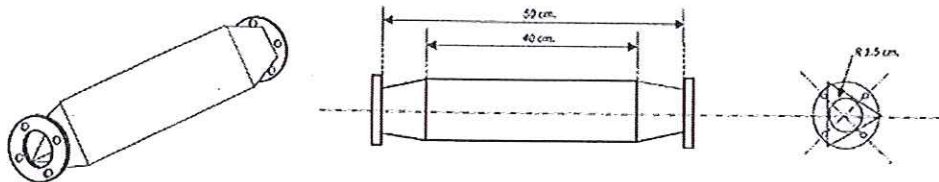
(c) A triangular cross-sectional duct.

Figure 30 The schematic of heat ducts.

To select a suitable material as shown in the Table 5 for the fabrication of heat ducts, thermal conductivity, corrosion resistance, heat resistance and price should be considered.

Table 5 Thermal conductivity of materials.

Materials	Temperature -t- (°F)	Thermal Conductivity-k- (Btu/ (hr.°F ft.))
Aluminum, pure	68	118
	200	124
	400	144
Aluminum Bronze	68	44
Carbon Steel, max 0.5% C	68	31
Carbon Steel, max 1.5% C	68	21
	752	19
	2192	17
Cast Iron, gray	70	27 - 46
Copper, pure	68	223
	572	213
	1112	204
Iron, pure	68	42
	572	32
	1832	20
Stainless Steel	68	7-26

In this study, carbon steel was selected, because it has the most suitable thermal conductivity and can withstand temperatures used in the experiments. Moreover, carbon steel is easy for fabrication and modification such as cutting, drilling, welding and bending.
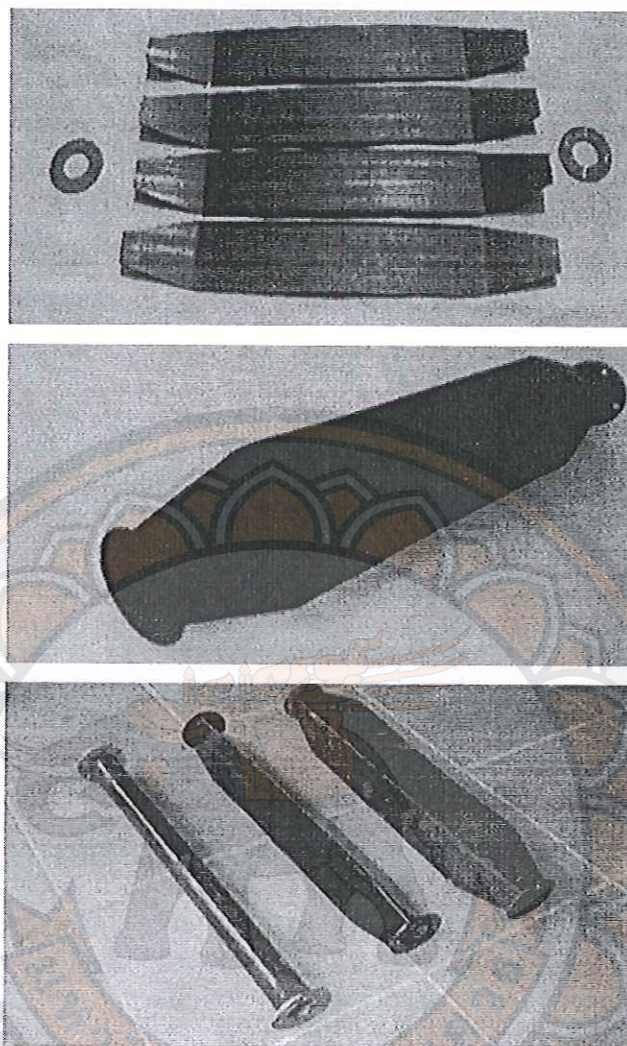
Figure 31 Heat ducts fabricated from carbon steel.

To examine and compare thermal conductivity of each geometry, three types of heat ducts were placed on a gas stove. Thermocouples were connected to positions that the thermoelectric devices will be installed as shown in the Figure 32. Thermocouples were used to measure temperatures along the length of heat ducts. The temperatures used in the experiments were also change by adjustment of gas levels from level 1 to 2 and 3. The experiments were performed several times by changing the order of gas levels from 1-2-3 to 3-2-1 in order to eliminate the influence of the external temperature. The ambient temperature was 34° C and only changed less than 1° C during the experiment.
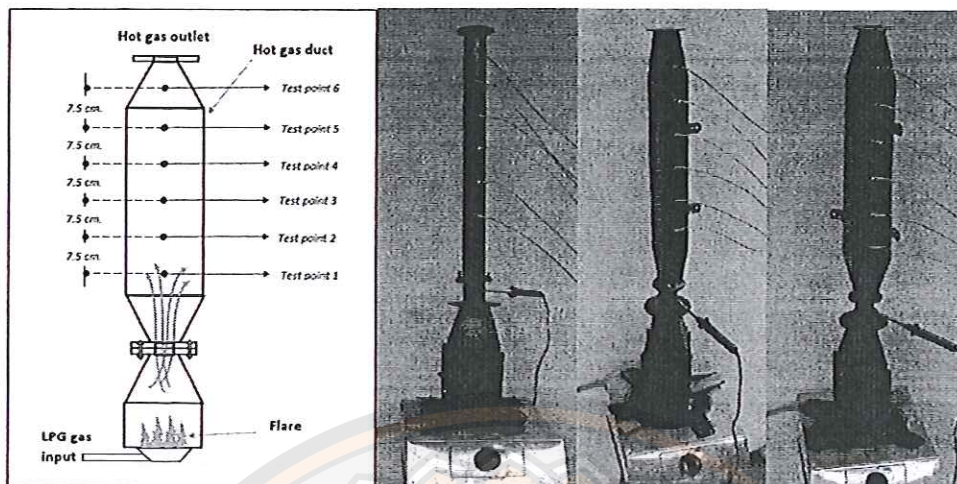
Figure 32 Thermal conductivity of different geometries.

3.2 Effects of two type cores insertion in the duct.

A square cross-sectional duct which is the most suitable geometry, as explained in the chapter 4, was used in the experiments afterward. To increase the efficiency of heat transfer in a square cross-sectional duct, a wedge and a swirl core were installed to examine whether which type of cores can create a turbulent flow. A turbulent flow can improve the efficiency of heat transfer. The schematic and the installations of a swirl and a wedge cores into a square cross-sectional duct are shown in the Figure 33.
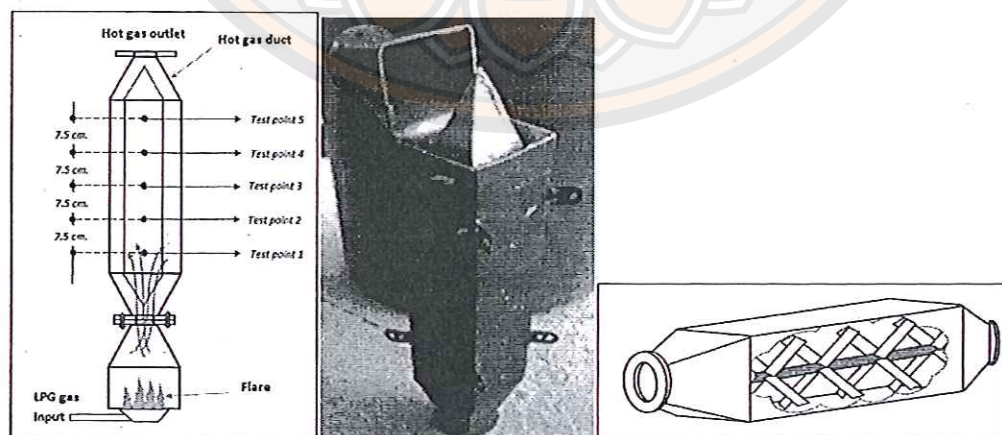
Figure 33 The schematic and the installation of a wedge core and a swirl core.

3.3 Cooling system design

A biomass gasifier system uses a cooling system to lower temperature of hot gas. A cooling system can be integrated to the gasifier system by simply attaching a water cooling pipe on one side of the thermoelectric devices as shown in the Figure 34. Another side of the thermoelectric devices must attach to a heat duct in order to create temperature difference according to principles of the Seebeck effect.
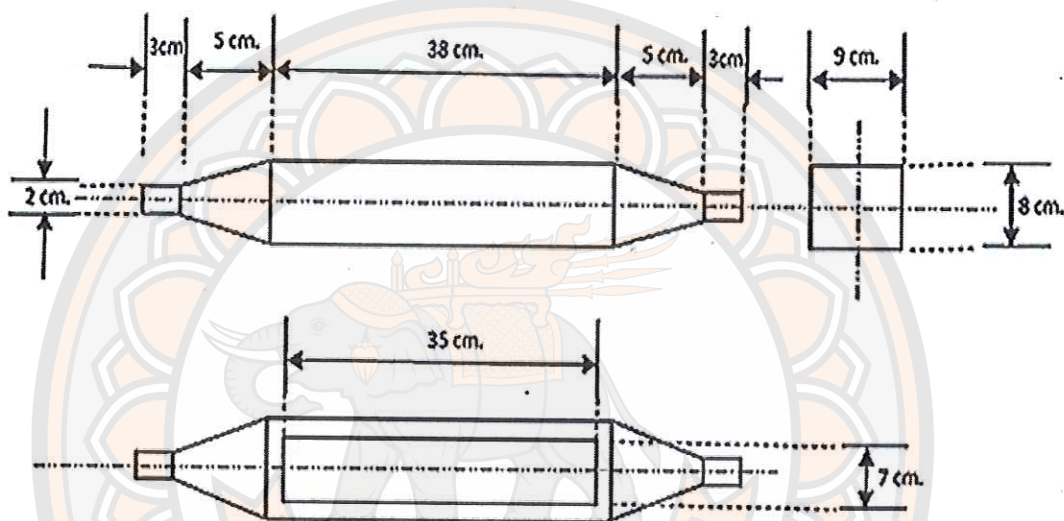
Figure 34 Cooling system design.

Since the temperature of water in a water cooling pipe is not high, a cooling pipe can be made of metal sheet coated with zinc. This make a cooling pipe light and easy to fabricate. A water cooling pipe is 3/4 smaller compared with a heat duct.

3.4 Flow directions of a cooling system

In this experiment, flow directions of a cooling system were tested whether a counter flow or a parallel flow can improve the efficiency of heat transfer. A parallel flow refers to the flow of cooling water in the same direction of hot gas, while a counter flow refers to the flow of cooling water in the opposite direction of hot gas.
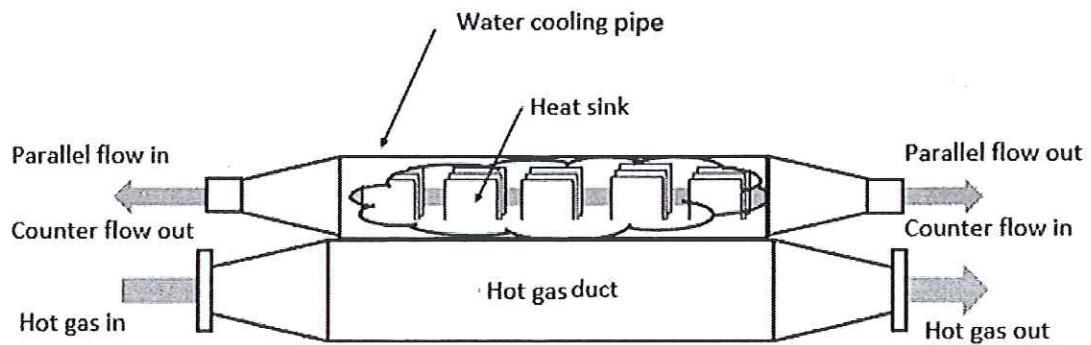
Figure 35 Flow directions of a cooling system.

The thermoelectric devices were installed on the surface of a heat duct and the heat duct was placed over a gas stove. Turn on gas to simulate gas flow as in the biomass gasifier system. Temperature profiles along the heat duct were collected for further analysis.
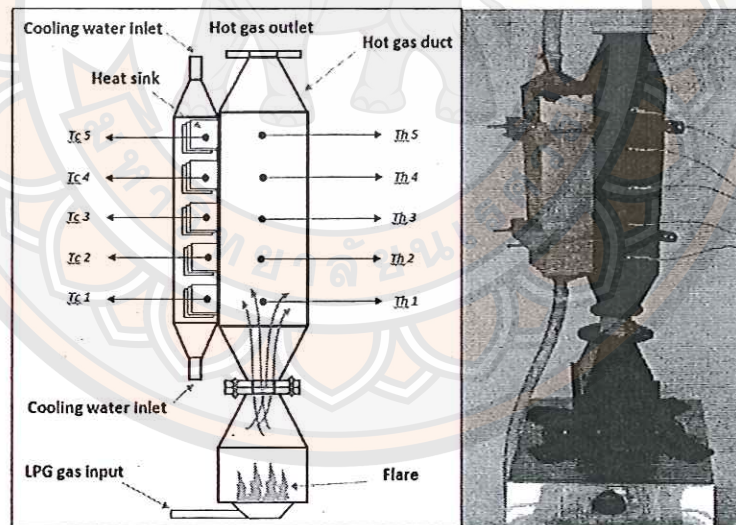
Figure 36 Flow directions of a cooling system.

3.5 Performance of the thermoelectric devices

A square cross-sectional duct is the most suitable geometry, since the temperatures along its length are nearly equal. Moreover, the thermoelectric devices call be placed on four sides of the heat duct different from other geometries. The thermoelectric power generation experiment is shown in the Figure 37.

The thermoelectric devices were installed on the surface of a square cross-sectional duct. Thermocouples were connected to the positions that the thermoelectric devices will be installed. A heat sink and a water cooling pipe were connected as shown in the Figure 37. In this experiment, a counter flow of a cooling water was used. Voltage and current of the thermoelectric devices were measured. We adjusted the temperature level of a gas stove. Temperature profiles, temperature differences and power generation can be calculated.
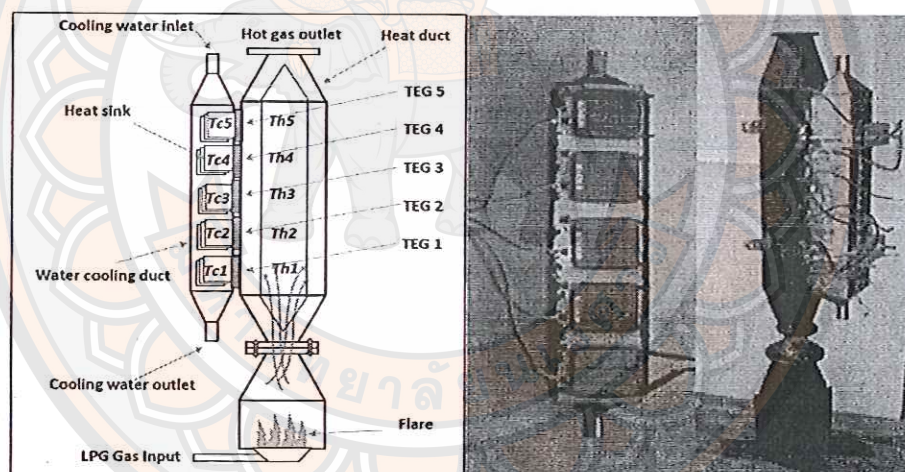
Figure 37 Thermoelectric power generation.

The power output was generated from the thermoelectric devices attached to the heat duct as shown in the Figure 37. Temperature differences between two sides of the thermoelectric devices or at the inlet and outlet of a heat duct can be collected by adding the resistive loads of 1.5 Ω., 10 W to the electric circuits of each thermoelectric devices. DC voltmeter and DC ammeter were used to measured voltage across resistive loads in serial circuits as shown in the Figure 38.
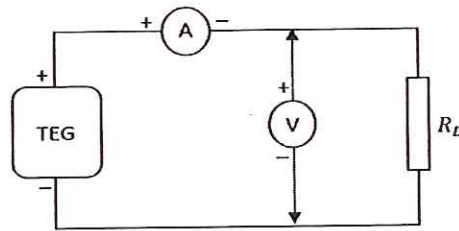
Figure 38 **The schematic of a resistive load circuit for finding the power output of a thermoelectric device.**

The efficiency of a thermoelectric electric device can be calculated by the equation as follows;

$$q = \dot{m}C_p\Delta T$$

[Eq.42]

Where,

q = The heat of a TEG.

$\dot{m}$ = The mass of a TEG. (Hz-14: 82 gm)

C_p = The capacity of a TEG. (Bi2Te3: 0.544 J/g/°C)

ΔT = The temperature difference. (°C)

And

$$\eta = \frac{E_2}{E_1} \times 100$$

[Eq.43]

Where,

η = The energy efficiency of a TEG.

E_1 = The thermal energy input. ($source = q$)

E_2 = The power output ($P \times t$).

The thermoelectric devices can be connected into a serial or a parallel circuits depending on the level of power output required.
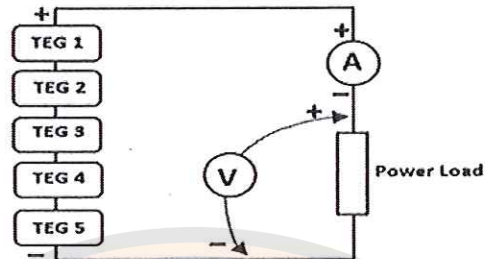
Figure 39 Measurement of power output of thermoelectric devices.

The total power output of the thermoelectric devices in a serial circuit can be calculated by the equation as follows;

$$P_{total} = P_{TEG1} + P_{TEG2} + P_{TEG3} + P_{TEG4} + P_{TEG5}$$ [Eq.44]

4. Thermoelectric power generation from waste-heat of a biomass gasifier system

In this experiment, the integrated system was introduced. A square-cross-sectional duct was used, and a water cooling system was installed as shown in the Figure 40.
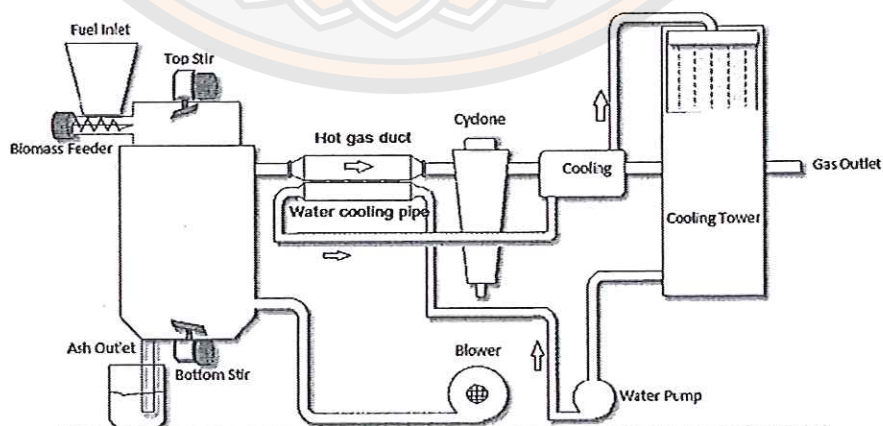
Figure 40 The integrated system.

Thermoelectric devices can be connected in a serial circuit which increases the power output or a parallel circuit which increases the output current. The level of the current and voltage can be adjusted by changing the connection of a circuit as shown in the Figure 41.
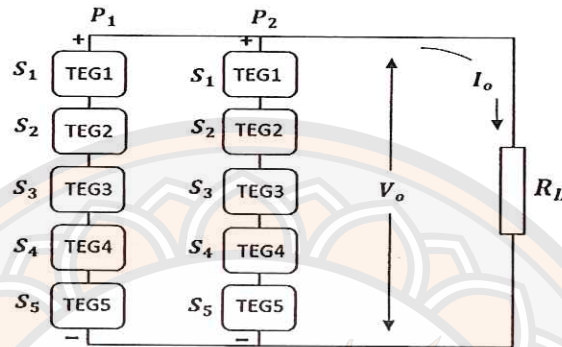
Figure 41 The thermoelectric device circuit.

The thermoelectric devices can be connected into serial and parallel circuits. The output voltage (V_o), the output current(I_o) and the output power(P_o) of the thermoelectric array can be collected by connecting the thermoelectric array to the resistive load (R_L) and calculated from the equations as follows;

$$V_o = \frac{NN_sS(T_h-T_c)}{\frac{1+2rl_c}{l}} \qquad \text{[Eq.45]}$$

$$I_o = \frac{ANN_pS(T_h-T_c)}{2\Re(n+1)(\frac{1+2rl_c}{l})} \qquad \text{[Eq.46]}$$

$$P_o = V_oI_o \qquad \text{[Eq.47]}$$

Where, N_s= Number of modules in serial connections.

N_p= Number of column in parallel connections.

S, $\Re$ and λ are the temperature dependent constants described

by Melcor in 1992 as follows;

$$S = (22224+936.6T_{avg}-0.6279T_{avg}^2) \times 10^{-9}$$ [Eq.48]

$$\mathfrak{R} = (5112+163.4T_{avg}-0.9905T_{avg}^2) \times 10^{-9}$$ [Eq.49]

$$\lambda = (62605+277.7T_{avg}-0.143T_{avg}^2) \times 10^{-9}$$ [Eq.50]

$$T_{avg} = \frac{(T_h+T_c)}{2}$$ [Eq.51]

The thermoelectric devices with n~0.1mm, r~0.2mm, and lc~0.7mm are commercially available.

The economic analysis

The economic analysis of the integration of thermoelectric devices into the original biomass gasifier system will be discussed here. The analysis includes investment factors, environmental factors, and fluctuations of money exchange rates, interest rate and burden costs to operate the project. This factors will be used to determine the investment value of the project. The primary assessment of investment factors are classified into;

1. Tangible and intangible benefits.
2. Tangible and intangible costs.

In decision making for investment in a particular project, these economic factors need to be considered;

1. Cash flow to investors.
2. Investment value.
3. Investment decisions.
4. Project implementation.
5. Project evaluation.

To compare the investment value between the original biomass gasifier system, the thermoelectric power generation system and the integrated system combining the thermoelectric power generation into the original gasifier system, these economic indicators need to be considered;

1. Payback period. (PB)
2. Net Present Value. (NPV)
3. Internal Rate of Return. (IRR)

A payback period (PB) can be calculated from initial investment and cash flow to the investor. In this research, only a formula for continuous and stable cash flow will be considered as follows;

$$Payback\ period\ (PB)\ =\ \frac{Initial\ investment}{Cash\ flow\ per\ period} \qquad [Eq.52]$$

The benefits of the PB analysis is that, investors can calculate whether it is economically reasonable to invest in a particular project and how long the payback period for that project is. The PB analysis can indicate whether the project has high successful rate or not. However, the PB analysis also has disadvantages. Because the value of money can change over time, there is a risk that cash flow to the investor in the future will decrease and extend a payback period. Moreover, there is no any criteria that can indicate whether the investment will increase the value of the project or not.

The Net Present Value (NPV) is a method to evaluate the desirability of the investment in a particular project. It can defined as follows;

$$NPV = \frac{\sum_{t=1}^{n} B_t - \sum_{t=1}^{n} C_t}{(1+i)^t} - TIC \qquad [Eq.53]$$

Where,

Bt	=	The expected benefit at the end of year n.
Ct	=	The expected cost at the end of year n.
TIC	=	The total initial investment.
i	=	The discount rate or the minimum annual return required to finance the project.
t	=	The time of the cash flow. (in years)
n	=	The total time of evaluation. (in years)

The Internal Rate of Return (IRR) is another method to measure and compare the profitability of investments. The IRR is defined as the rate of return that makes the NPV of all cash flows both negative and positive from a particular investment equal to zero.

$$NPV = \sum_{n=1}^{N} \frac{B_n - C_n}{(1+r)^n} - TIC = 0 \qquad \text{[Eq.54]}$$

Where,

r = The Internal Rate of Return. (IRR)

The economic analysis of the original biomass gasifier system, the thermoelectric power generation system and the integrated system combining the thermoelectric power generation into the original gasifier system are shown in the table 6-8. The economic life of the project, the expected period of time during which an asset is useful to the owner, is 25 years with a discount rate of 7%.

Table 6 The economic analysis of the original biomass gasifier system.

Capital Investment	The original biomass gasifier system (THB)	Detail
1) Initial Investment	600,000	Power Output = 10 kW Utilization = 80% Operation time (per day) = 24 hr or (63,360 kWh/yr.)
2) Fuel Cost	19,008	Wood chips = 600 THB/Ton
2) Operation and Maintenance Cost	120,000	(20% of the initial investment)
3) Benefit (Per year)	316,800	Electricity tariff = 5.0 THB/Unit

Table 7 The economic analysis of the thermoelectric power generation system.

Capital Investment	Thermoelectric power generation system (*The nominal capacity) (THB)	Detail
1) Initial Investment	30,000	Volume = 10 modules Power Output = 140 W or (997.92 kWh/yr)
2) Fuel Cost	-	
2) Operation and Maintenance Cost	150	(0.5% of the initial investment)
3) Benefit (per year)	4,990	Electricity tariff = 5.0 THB/Unit

Table 8 The economic analysis of the integrated system combining the
thermoelectric power generation into the original gasifier system.

Capital Investment	Integrated System (THB)	Detail
1) Initial Investment	630,000	Volume = 10 modules Power Output 140 watt or (997.92 kWh/yr.) Power Output 1 kW or (63,360 kWh/yr.)
2) Fuel Cost	19,008	
2) Operation and Maintenance Cost	120,150	(20.5% of the initial investment)
3) Benefit (Per year)	321,790	Electricity tariff = 5.0 THB/Unit

CHAPTER IV

EXPERIMENTAL RESULTS AND ANALYSIS

In this chapter, the experimental results were discussed. The content was divided into four sections consisting of the thermoelectric device testing, heat duct design and testing, performance of thermoelectric devices and the economic analysis of the investment in this project.

Performance of the original biomass gasifier system

To determine the performance of the biomass gasifier system, the experiment was performed and the experimental data were collected as described in the chapter 3. The gasifier system use wood chips as fuel with a feeding rate of 4 kg/hr. The heating value of wood chips is approximately 18,000 kg/°C or 20.934 kWh. The power output was 10 kWh. The gasifier system was connected to the external power supply. The power consumption of the biomass gasifier system was shown in the Table 9.

Table 9 Power consumption of the biomass gasifier system.

Motor	Time (minute.)	Current (A.)	Power (W)
1.Blower	60	2.9	638
2.Water pump	60	1.7	374
3.Top stir motor	6	1.3	286
4. Bottom Stir motor	6	1.3	286
5 Biomass feeder motor	19	1.4	308
Total			1892

The power consumption of the biomass gasifier system indicated that the gasifier system had to connect to the external power generation system. The total amount of power supply was 1.8 kWh. Gas flows with a rate of 257 CFM. The temperature at the outlet of 41°C, while the temperature of water at the outlet of a cooling system was 47°C. Since the small-scaled biomass gasifier system required total electricity of 63.936 kW, the efficiency of the small-scaled biomass gasifier system was 64.623 %.

Performance of thermoelectric devices

According to specifications of the thermoelectric devices model HZ-14, if the temperature difference was high as 250 °C, the thermoelectric device generated electricity of approximately 13 W. Therefore, if the temperature different between a heat duct and a cooling water system was high enough (more than 200°C), the thermoelectric devices can generate electricity with high efficiency.

Performance of the thermoelectric devices was shown in the Table 10. In this experiment, 10 thermoelectric devices were installed on two sides of a square cross-sectional duct. Each side of a heat duct has 5 thermoelectric devices. The swirl core was installed and a counter flow of a cooling system was used to create stable temperature differences along the length of the heat duct.

The output voltage and the output current were measured across the resistive load of each thermoelectric device by using DC voltmeter and DC ammeter. Power generation of each devices was shown in the Table 10. The ambient temperature was 32 °C. The total power output of the thermoelectric devices was 26.24 W.

Table 10 Performance of the thermoelectric power generation.

Column	Module	Th(°C)	Tc(°C)	ΔT1(°C)	E (V.)	I (A.)	P1 (W.)
	S 1	149	32.42	116.58	1.57	2.2	3.45
	S 2	134	32.33	101.67	1.48	1.95	2.88
P1	S 3	123.3	32.3	91	1.45	1.73	2.5
	S 4	115.6	32.28	83.32	1.47	1.54	2.26
	S 5	113	32.28	80.72	1.43	1.5	2.15
	S 1	148.5	32.4	116.1	1.59	2.15	3.42
	S 2	133.1	32.32	100.78	1.47	1.92	2.82
P2	S 3	120.2	32.29	87.91	1.43	1.71	2.45
	S 4	114	32.28	81.72	1.45	1.52	2.21
	S 5	112.5	32.28	80.22	1.41	1.49	2.1
Total		26.24 watt					

The maximum temperature of the thermoelectric devices was 149 °C. The temperature of cooling water varies in the range 32.2-32.4 °C. The temperature differences between the two sides of the thermoelectric devices were 80.22-116.58°C. Each thermoelectric device can generated electricity between 2.1-4.45 W. The Total power output of the system was 26.25 W or 1.574 kWh. The experimental results were shown in the Figure 42.
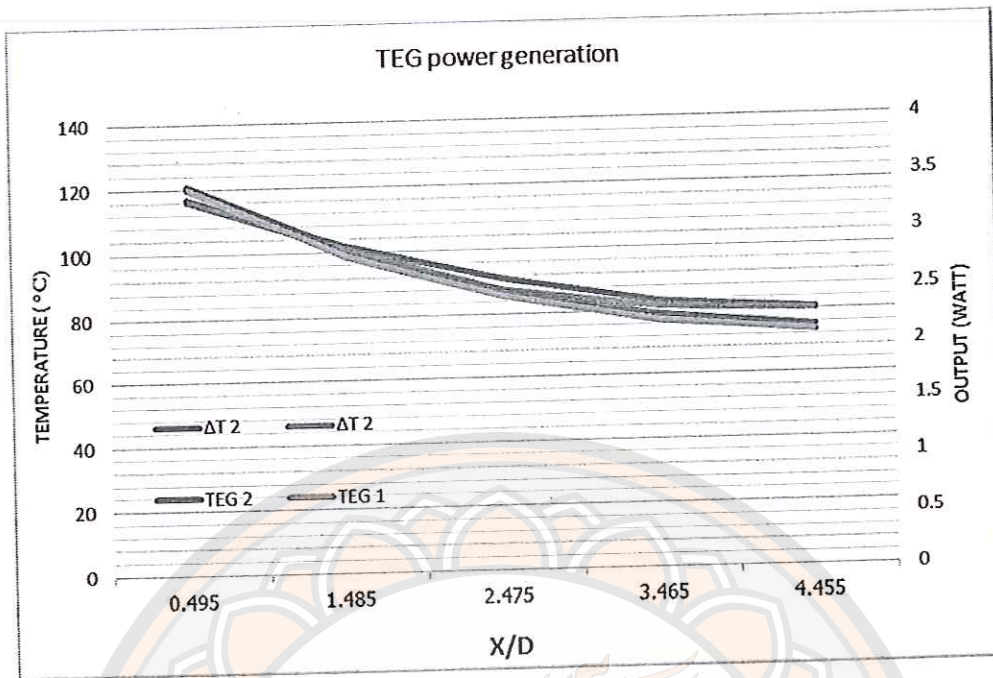
Figure 42 Power generation of thermoelectric devices.

The ability to generate electricity of a thermoelectric device depended on the temperature differences (ΔT). If the temperature difference was higher than 150°C, the thermoelectric device was generated electricity with high efficiency.

Thermoelectric device testing

The efficiency of the thermoelectric devices could be improved, if the temperature difference between the two sides of the thermoelectric device was higher than 150°C. Found that the electricity could be converted by the thermoelectric device at 50% thermal efficiency. Thermal energy can convert into. The ambient temperature was 31°C. The thermoelectric device testing of the thermoelectric devices was shown in the Table 11.

Table 11 Thermoelectric device testing.

No	Th (°C)	Tc (°C)	ΔT(°C)	Voltage (V.)	Current (A.)	Power (W.)
1	100	32.32	67.68	1.09	1.63	1.77
2	110	32.34	77.66	1.19	1.79	2.14
3	120	32.35	87.65	1.27	1.9	2.41
4	130	32.37	97.63	1.33	2	2.67
5	140	32.4	107.6	1.45	2.18	3.17
6	150	32.42	117.58	1.52	2.3	3.50
7	160	32.44	127.56	1.67	2.48	4.13
8	170	32.5	137.5	1.73	2.6	4.50
9	180	32.55	147.45	1.87	2.78	5.19
10	190	32.6	157.4	2.00	2.95	5.90
11	200	32.7	167.3	2.10	3.13	6.57
12	210	32.8	177.2	2.19	3.3	7.22
13	220	32.8	187.2	2.32	3.45	8.00
14	230	33	197	2.43	3.61	8.78
15	240	33	207	2.50	3.72	9.30
16	250	33.1	216.9	2.57	3.85	9.89
17	260	33.2	226.8	2.68	4	10.72
18	270	33.2	236.8	2.77	4.1	11.37
19	280	33.5	246.5	2.87	4.2	12.04

The temperature differences between the two sides of the thermoelectric devices were increased 10°C each step from 100-280°C. The temperature of cooling water was 32.32°C which did not different much from the ambient temperature. When the temperature at the hot side increased, the temperature of cooling water also increased to 33.5°C. The maximum temperature difference was 246.5 °C and the thermoelectric device could generate electricity of 12.04 W. The electricity generated from the thermoelectric devices was shown in the Figure 43.
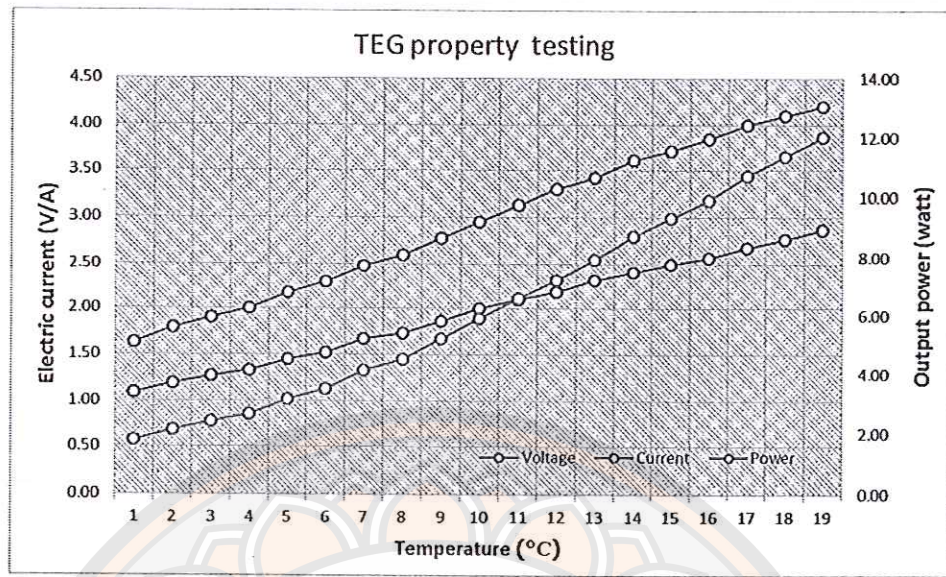
Figure 43 Thermoelectric device testing.

According to the specification of the thermoelectric device, the temperature differences between the two sides of thermoelectric devices of 250°C generated the maximum power output of 13 W. The efficiency of the thermoelectric device at a high temperature difference was 4.5%. However, in the experiment, we found that at the temperature difference of 246.5°C, a thermoelectric device generated electricity of 12.04 W. The efficiency of power generation was 4.02%.
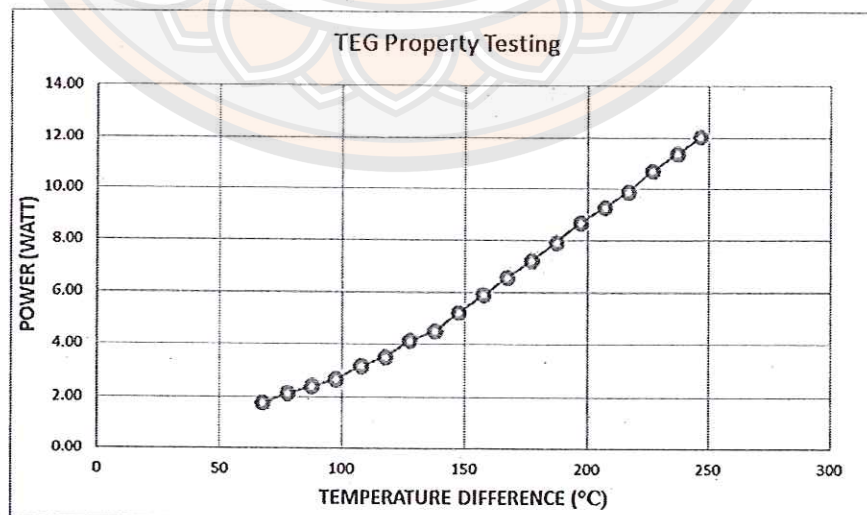
Figure 44 Power generation of the thermoelectric devices.

Hot duct and cooling pipe design

Factors were considered about hot duct design. A heat duct should have a flat surface and sufficient space for installation the thermoelectric devices. A cooling pipe had to the same shape. The hot duct and cooling pipe were designed and tested the performance as follows.

1. Heat transfer of heat ducts

The thermoelectric devices were installed on the surface of heat ducts. The distance between each thermoelectric device was 7.5 cm. The temperatures used in this experiment was separated to 3 levels which were of 230°C, 336°C, and 464°C as shown in the Table 12. The ambient temperature was 34°C.

Table 12 Temperature profiles of a circular cross-sectional duct.

Gas temp.(°C)	T1(°C)	T2(°C)	T3(°C)	T4(°C)	T5(°C)	T6(°C)
230	138	122	110	100	93	83
336	167	146	133	123	111	97
464	212	185	166	150	137	123
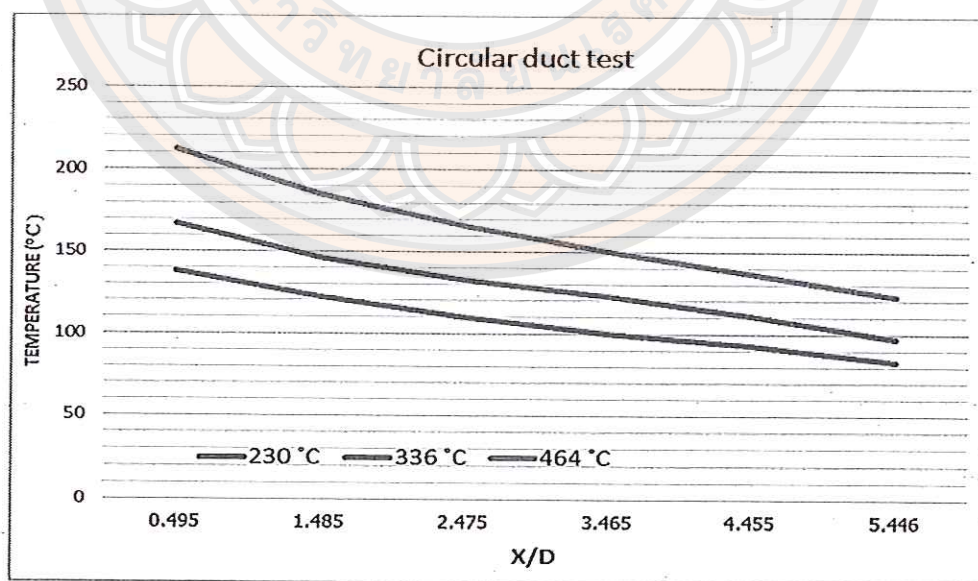
Figure 45 Temperature profiles of a circular cross-sectional duct.

The temperature profiles were measured at the positions that the thermoelectric devices installed. The temperatures along the length of heat ducts linearly decreased as shown in the Figure 45. The temperature difference at the inlet and the outlet of a circular cross-sectional duct was the highest compared with the other geometries.

Table 13 Temperature profiles of a triangular cross-sectional duct.

Gas temp.(°C)	T1(°C)	T2(°C)	T3(°C)	T4(°C)	T5(°C)	T6(°C)
247	128	121	113	100	95	88
360	157	155	138	117	113	103
474	183	182	164	140	129	123

The temperature profiles of a triangular cross-sectional duct exhibited the same features as in a square and a circular cross-sectional ducts. However, the temperature difference at the inlet and outlet of the heat duct was higher than a square cross-sectional duct.
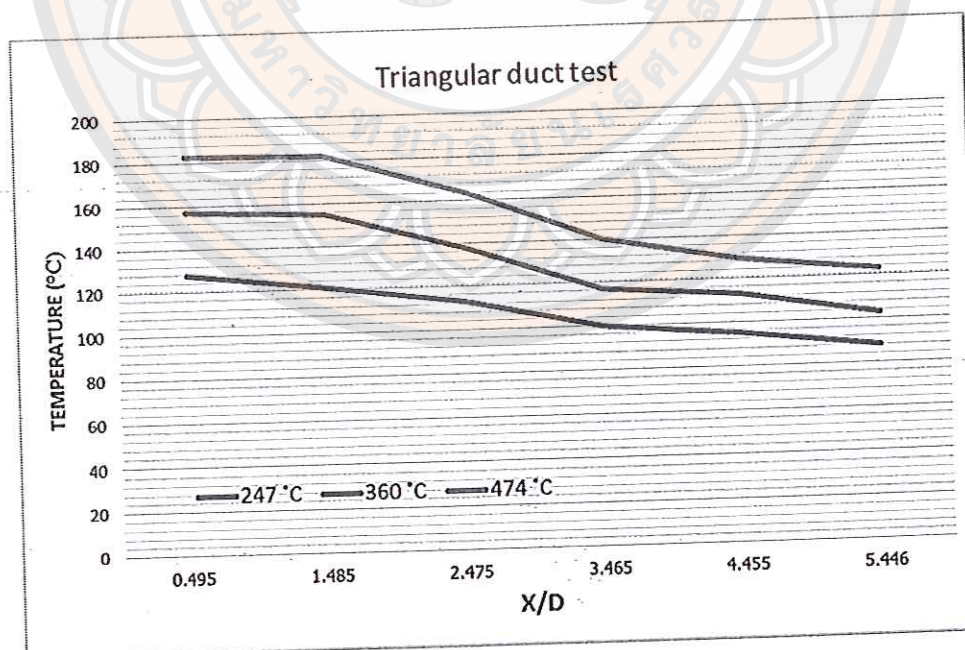
Figure 46 Temperature profiles of a triangular cross-sectional duct.

Table 14 Temperature profiles of a square cross-sectional duct.

Gas temp. (°C)	T1(°C)	T2(°C)	T3(°C)	T4(°C)	T5(°C)	T6(°C)
240	104	99	98	91	85	87
291	127	118	114	105	98	100
437	158	151	149	134	121	124

We found that the temperature profiles of a square cross-sectional duct as shown in the Figure 47 was the most stable. The temperatures along the length of the heat duct were nearly equal. Therefore, the square cross-sectional duct was a suitable geometry for power generation by using thermoelectric devices. Moreover, a square cross-sectional duct was the largest cross-sectional area compared to the other two geometries. This can improve heat transfer inside a heat duct and increase the power output of the system.
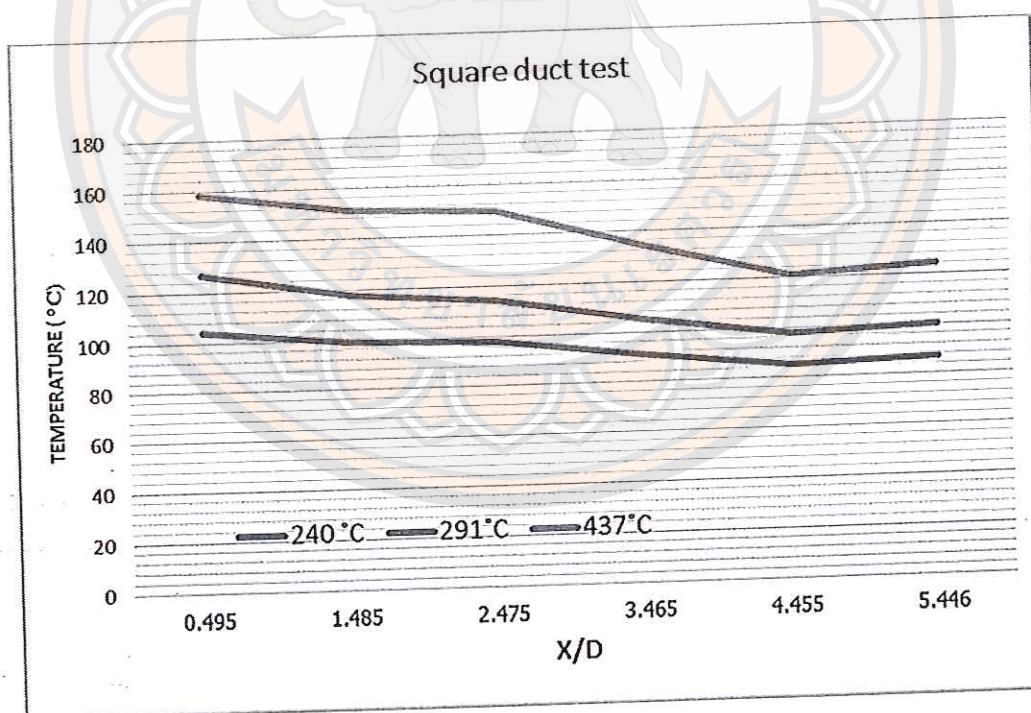
Figure 47 Temperature profiles of a square cross-sectional duct.

Table 15 Comparison the temperature profiles of different geometries.

Duct type	Temp. (°C)	T1(°C)	T2(°C)	T3(°C)	T4(°C)	T5(°C)	T6(°C)
Circular	230	133	123	104	133	123	104
Triangular	247	117	119	99	117	119	99
Square	240	105	108	98	105	108	98

The temperature profiles of all geometries shared the same feature that the temperatures at the inlet were the highest and linearly decrease to the temperature at the outlet as shown in the Table 15 and the Figure 48.
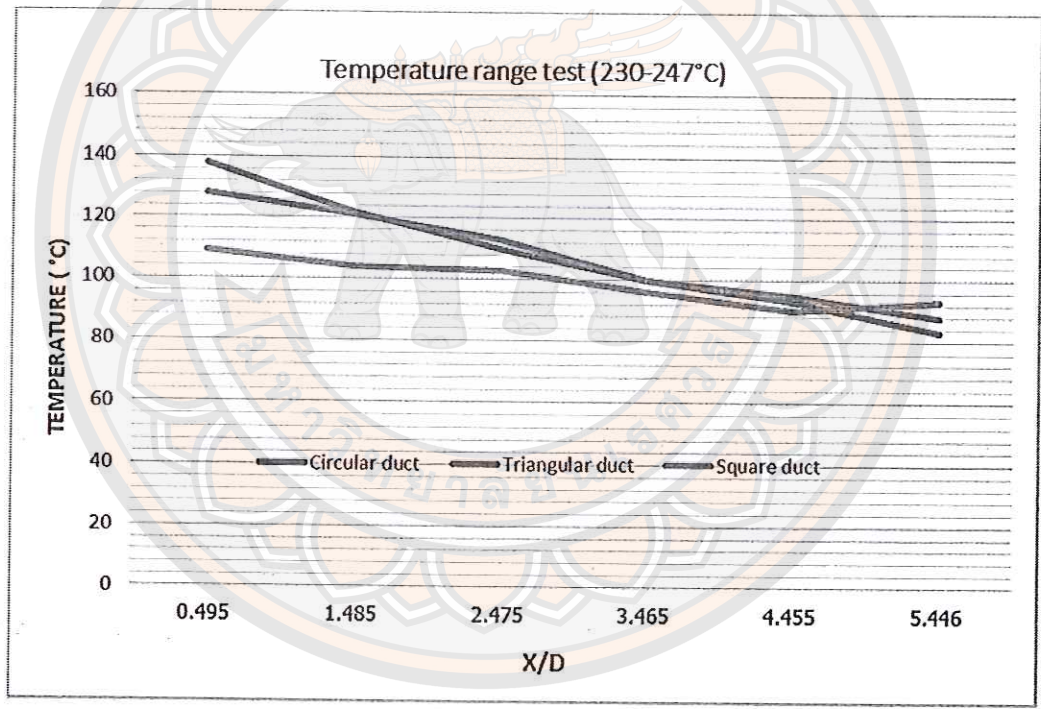
Figure 48 Temperature profiles of different geometries. (230-464°C)

Table 16 Comparison the temperature profiles of different geometries.

Duct type	Temp.(°C)	T1(°C)	T2(°C)	T3(°C)	T4(°C)	T5(°C)	T6(°C)
Circular	277	160	147	127	160	147	127
Triangular	290	140	140	118	140	140	118
Square	291	122	128	114	122	128	114

The temperature were increased to the range of 277 - 291°C as shown in the Table 16 and the Figure 49, however, the experimental results were still the same and shared feature of temperature profiles of the lower temperatures. A square cross-sectional duct was still the most suitable duct for power generation by using thermoelectric devices.
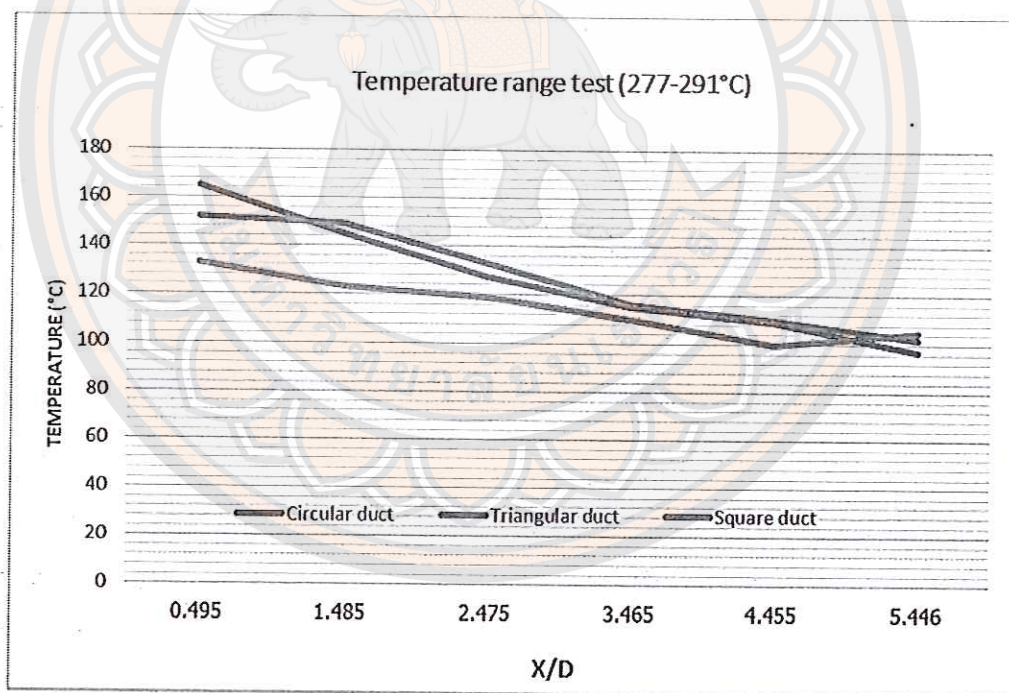
Figure 49 Temperature profiles of different geometries. (277-291°C)

2. Effects of two type cores insertion in the duct.

A square cross-sectional duct was selected for this experiment. The heat transfer of the laminar flow was lower than the turbulent flow, the average temperature could improve by creating a turbulent flow. The experiment was performed at two temperatures (180°C and 280°C). The ambient temperature was 36°C. A wedge and a swirl core were inserted to create a turbulent flow, as shown in the Table 17 and the Figure 50, a wedge core could not create the turbulent flow because the length of the heat duct was not enough, while the swirl core could create the turbulent flow and increased the average temperature of a heat duct.

In this experiment, a square cross-sectional duct was used to examine effects of a laminar and a turbulent flow on heat transfer. A turbulent flow occurs when the Reynolds number is higher than 10,000. In this study, the Reynolds number was 10,000 for a heat duct that has 100 cm in length. To reduce the length of a heat duct to 50 cm and still having a turbulent flow, the cross-sectional area was changed from 10x10 cm^2 to 5x5 cm^2.

Table 17 Temperature profiles of two type core insertion in the duct.

Core type	Temp.	T1(°C)	T2(°C)	T3(°C)	T4(°C)	T5(°C)
Wedge core 1	180°C	106	95	87	80	75
Swirl core 1	180 °C	125	113	104	92	82
Wedge core 2	280°C	136	118	106	97	90
Swirl core 2	280°C	174	145	131	115	103
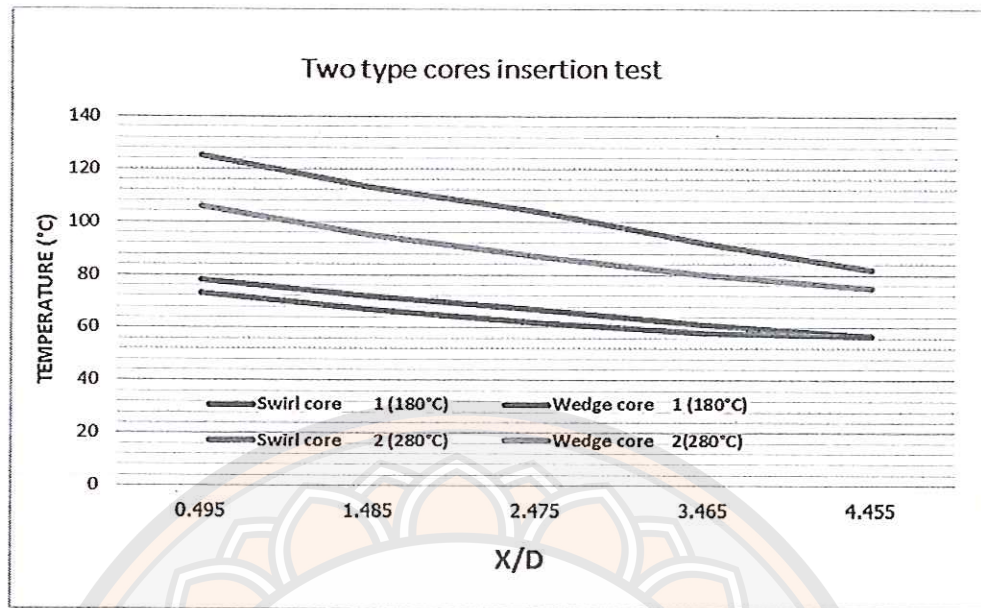
Figure 50 Temperature profiles two type cores insertion.

3. Effects of flow directions of a water cooling system on heat transfer

The directions of a water cooling system was important because different directions could affect heat transfer from a heat duct to a cooling pipe. The efficiency of heat transfer directly affected the temperature differences and amount of power output. In a regular water cooling system, there were a parallel and a counter flows. The effects of flow directions of the water cooling system to the temperature profiles of a heat duct was shown in the Table 18 and the Figure 51 for a parallel flow and in the Table 19 and the Figure 52 for a counter flow.

Table 18 Effects of a parallel flow to the temperature profiles.

Tp	$T_{h1}(°C)$	$T_{c1}(°C)$	$\Delta T_1(°C)$	$T_{h2}(°C)$	$T_{c2}(°C)$	$\Delta T_2(°C)$
T1	200	42	158	172	52	120
T2	168	45	123	149	60	89
T3	143	46	97	130	62	68
T4	132	47	85	118	63	55
T5	130	46	84	114	65	49
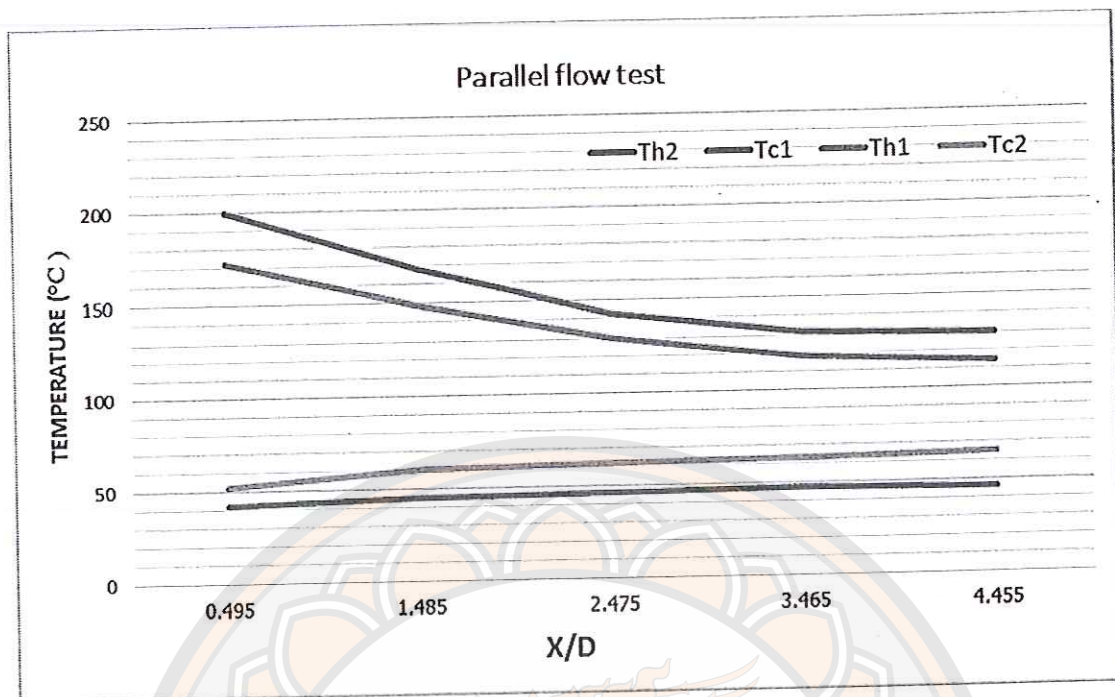
Figure 51 Effects of a parallel flow to the temperature profiles.

As shown in the Table 19 and the Figure 52, the temperature differences between a heat duct and a cooling pipe a counter flow were low, while a parallel flow increased the temperature difference. A small temperature different indicated a good heat transfer. Thus, a counter flow of a water cooling system could improve the efficiency of heat transfer inside a heat duct. Moreover, the thermoelectric devices could generate equal amounts of electricity.

Table 19 Effects of a counter flow to the temperature profiles.

Tp	T_{h1}(°C)	T_{c1}(°C)	ΔT_1(°C)	T_{h2}(°C)	T_{c2}(°C)	ΔT_2(°C)
T1	182	52	130	210	48	162
T2	158	50	108	179	46	133
T3	142	47	95	159	44	115
T4	128	44	84	144	41	103
T5	119	41	78	132	39	93
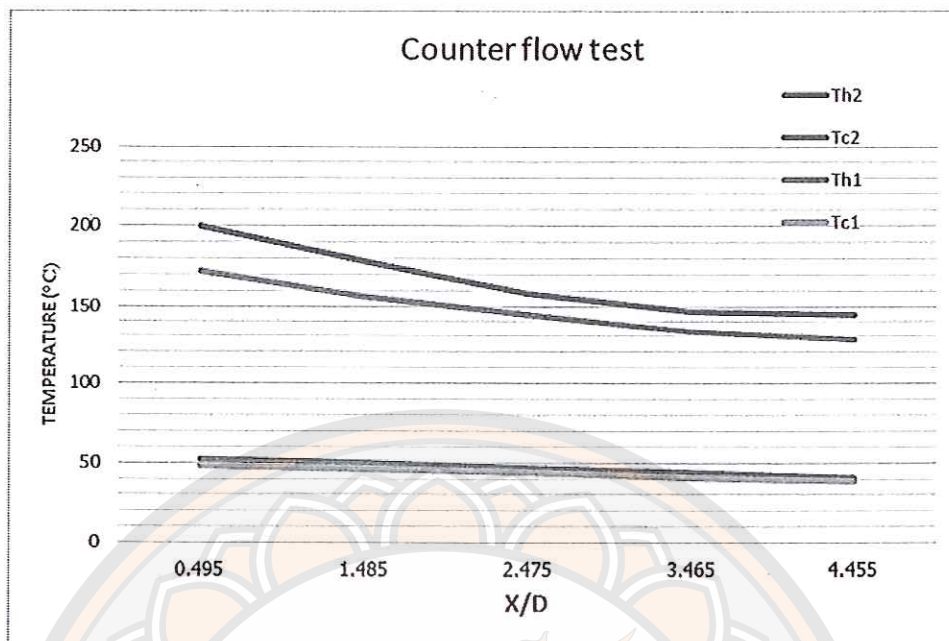
Figure 52 Effects of a counter flow to the temperature profiles.

4. Thermoelectric power generation.

In this experiment, the most suitable conditions were used which mean using a square cross-sectional duct was with a counter flow of a water cooling system. A swirl core was installed to create a turbulent flow. The temperature differences between the two sides of the thermoelectric devices were limited to not exceed 160°C. The ambient temperature was 33°C.

Table 20 Temperature profiles of the thermoelectric power generation.

Tp	Th1	Tc1	ΔT1	Th2	Tc2	ΔT2
T1	198	38	160	186	35.6	150.4
T2	178	37	141	167	36	131
T3	159	35.6	123.4	151	34.8	116.2
T4	147	34.3	112.7	140	34.2	105.8
T5	145	34.1	110.9	136	33.9	102.1

As shown in the Table 21, at the inlet of a heat duct which had the temperature difference of 16°C, the thermoelectric device could generate 6.02 W of electricity, while at the outlet which had the temperature difference of 110.9°C, the thermoelectric device could generate 3.2 W of electricity. The higher temperature difference, the higher power output generated from the thermoelectric devices. Thus, the efficiency of power generation at the inlet of a heat duct was 2.44% while at the outlet was 1.85%.
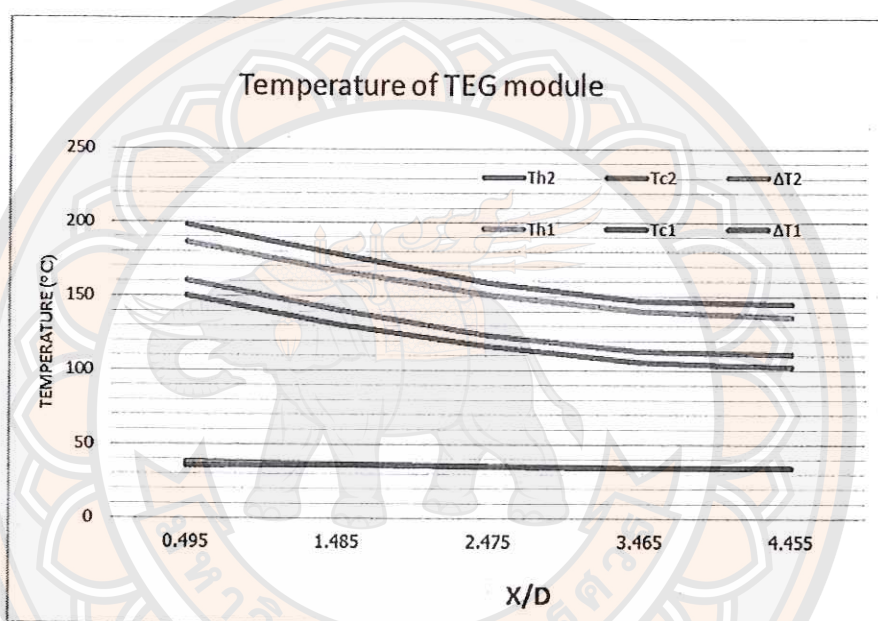
Figure 53 Temperature profiles of a heat duct.

Table 21 Performance of the thermoelectric power generation.

Tp	ΔT1 (°C)	E (V)	I (A)	P1 (W)	ΔT2 (°C)	E (V)	I (A)	P2 (W)
T1	160	1.56	3.86	6.02	150.4	1.53	3.66	5.60
T2	141	1.49	3.15	4.70	131	1.47	2.92	4.30
T3	123.4	1.43	2.69	3.85	116.2	1.38	2.54	3.50
T4	112.7	1.38	2.54	3.50	105.8	1.35	2.35	3.18
T5	110.9	1.28	2.50	3.20	102.1	1.20	2.25	2.70
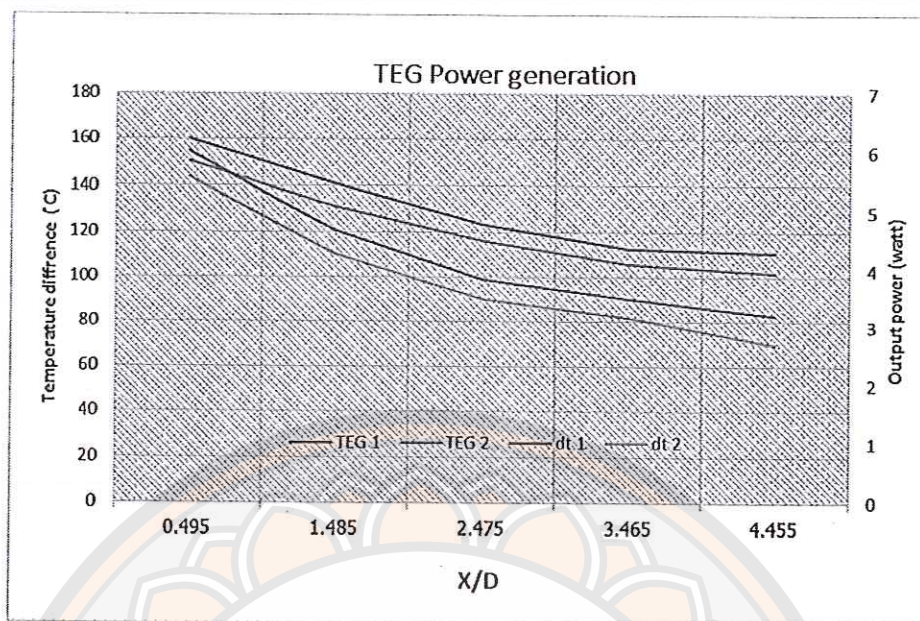
Figure 54 Temperature difference along the length of a heat duct.

The general equation of efficiency was obtained from 3 variables, 2 dependent variables and 1 independent variable as follows:

$$Efficiency = \frac{Output\ power}{Thermal\ energy}$$

An efficiency equation for electricity generation of by thermoelectric device can be written as following equation.

$$\eta_{TEG} = \frac{P}{T}$$

And

$$P = \eta_{TEG} \times T$$

When $\quad\quad\quad T = \int \Delta T,\ X/D$

The relationships temperature was the temperature difference (ΔT) and the perimeter of duct (X). The distance from the inlet of a heat duct (D) or X/D, when replace on the power equation can be described as follows;

$$P = \eta_{TEG} \times f\Delta T, X/D$$

The thermoelectric efficiency of each modules were operated in narrow range and still low between 2.38% to 3.9% as shown in Table 22 therefore the temperature difference and X/D have effected for the power output of TEG.

Table 22 The efficiency of HZ-14 module as a function of ΔT at various values of Tc.

Tc/ΔT	50 °C	100 °C	150 °C	200 °C	250 °C	275 °C
30 °C	.01212	.0234	.0334	.04196	.0467	.048
60 °C	.0119	.0227	.0317	.0381	.0412	.0413
80 °C	.0117	.0219	.0301	.0353	.037	.0364
100 °C	.0119	.022	.0294	.0336	.0339	.0328

The relationships between the temperature difference and the ratio of the outer diameter(X) to the distance from the inlet of a heat duct (D) were fitted to determine the empirical mathematical model as shown in the Figure 55. Since it was not possible to find a true power of the thermoelectric devices, fitting the empirical equations to the experimental results could archive the approximate power of the thermoelectric devices.
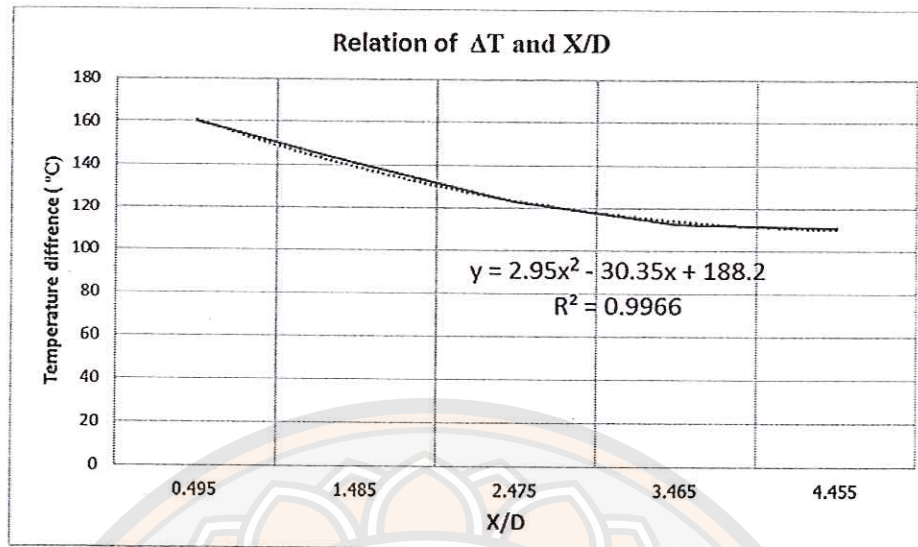
Figure 55 The relationships of temperature difference and X/D.

The empirical mathematical model from the experiment can be derived as follows.

$$P = 0.035 \times (2.95(\tfrac{X}{D})^2 - 30.35(\tfrac{X}{D}) + 188.2)$$

When,

P	=	The power of thermoelectric devices.
(ΔT)	=	The temperature difference between the two sides.
(X/D	=	The perimeter of the duct (X) and the distance from the inlet of a heat duct to measured (D).

The equation can be used to calculate the power of thermoelectric generation on the duct.

$$P = 0.035 \times (2.95(0.495)^2 - 30.35(0.495) + 188.2)$$

$$P = 6.03\ Watt$$

The power output from the equation was approximately from measured about 6.02 Watt, error 0.16%.

The economic analysis

The biomass gasifier system. The economic life was 25 years and 8% discount rate. The results of comparison between the original biomass gasifier system, the thermoelectric power generation system and the integrated system were shown as follows;

Table 23 The comparison of the economic analysis between each system.

Economic Indicator	The original biomass gasifier system	The thermoelectric power generation system	The integrated system
Internal Rate of Return (IRR)	10%	8%	10%
Net Present Value (NPV)	1,297,890 THB	21,662 THB	1,319,551 THB
Payback period (PB)	15 years 5 months	14 years 10 months	15 years 5 months

According to the results shown in the Table 23, all power generation systems were economically reasonable to invest money in these projects. However, the IRR of the original biomass gasifier system and the integrated system were greater than that of the thermoelectric power generation system. Even though the Net Present Value indicated that these power generation systems return positive benefits, the integrated system had the highest NPV. Thus, the integrated system is a good choice for investment. Additionally, the payback period indicated that all power generation system are equally attractive for investment for at least 25 years.

CHAPTER V

CONCLUSION

The application of thermoelectric devices for power generation from waste-heat of a small-scaled biomass power plant was proposed here. In this study, performance of thermoelectric devices, suitable designs and performance of a heat duct were investigated. The economic analysis was included in the thesis to explore whether it is economically reasonable for investment.

CONCLUSION

1. A total thermal energy produced from a biomass gasifier system was 42.547 kW, while waste-heat was 23.288 kW. The thermoelectric power generators could recover only 1.254 kW and generated 0.065 kW of electricity, with 5.18% efficiency. The newly-design biomass gasifier system proposed in this research can produced the total electricity of 10.065 kW.

2. There were three types of heat ducts designed in this research, which were a circular, a triangular and a square cross-sectional ducts. Each type had a cross-sectional area of 10x10 cm^2. A square cross-sectional duct was the most suitable geometry, because the temperatures along its length were nearly equal. By having a stable temperature profile, a square duct was possible to generate the highest amounts of electricity. Since a turbulent flow improved the efficiency of heat transfer. The turbulent flow inside a heat duct was created by reduction of a cross-sectional area with a swirl core. At 180°C heat transfer of a heat duct was 16.47%, while at 280°C heat transfer of a heat duct was 22.12% with thermal conductivity of 0.0344 W/m·°C. Moreover, at 150°C the heat transfer per unit area of a heat duct was 2.56 W/cm^2.

3. According to the economic analysis, a payback period of the original biomass gasifier power plant and a thermoelectric power generation system was 15 years 5 months and 14 years 10 months, respectively. Thus, a payback period of the proposed gasifier system was 15 years 5 months.

RECOMMENDATION

1. A synthetic gas or syngas from a biomass gasifier system was produced by reacting biomass with high temperature under limited amounts of oxygen without combustion. Most of the thermal energy produced from a biomass gasifier system loses into waste-heat by a cooling system. This waste-heat could be recovered to utilize as an energy source, for example, by using thermoelectric devices. Even though this study suggests a possible way to convert waste-heat into electricity, to improve the performance and efficiency of the gasifier system further researches and development are necessary.

2. To reach the highest efficiency of thermoelectric devices, temperature differences between the two sides (hot and cool sides) should not less than 200 °C or 250 °C depending on the specification.

3. Materials with high thermal conductivity and resistance to heat corrosion are suitable for making a heat duct. According to these properties, copper is the most suitable material.

4. Temperature variation on the surface of a heat duct was not high due to non-uniform heating of gas flow along the duct. The efficiency of heat transfer can be improved by installation of a swirl core or a wedge to obstructed gas flow. This will create a turbulent which increases the average temperature on the surface of a heat duct.

5. Even though a thermoelectric device is expensive, it can convert thermal energy into electricity more easily than other methods. The thermoelectric devices can be used for long term operation with a long useful lifetime. It is also widely used in the industrial sector and will become cheaper in the future.

REFFERENCES

REFFERENCES

[1] Energy Policy and Planning Office. (2013). **Energy Statistics of Thailand 2012.** Bangkok: Ministry of Energy.

[2] Energy Policy and Planning Office. (2012) **Annual report 2011.** Bangkok: Ministry of Energy.

[3] Office of Agricultural Economics. (2013). **Agricultural Statistics of Thailand 2012**. Bangkok: Ministry for Agricultural and Cooperative.

[4] Chuang Yu. (2009). Thermoelectric Automotive Waste Heat Energy Recovery Using Maximum Power Point Tracking. **Energy Conversion and Management,** 50, 1506-1512.

[5] Mckendry, Peter. (2002). Energy production from biomass Part 1: overview of Biomass. **Bio resource Technology,** 83(1), 37-46.

[6] Jared, P. Ciferno and John J. Marano. (2002). **Benchmarking Biomass Gasification Technology for fuel, chemical and hydrogen production.** USA: U.S. Department of Energy, national Energy Technology Laboratory.

[7] NL Agency. (2013). **Sustainable biomass and bioenergy in the Netherlands Nnual report 2012.** Netherlands: Ministry of economic affairs.

[8] Wattanapong Rakvichian, Bongkot Prasit, Sukrudee Nathakaranakule and Pisit Maneechot. (2004). **Development of solar tunnel dryer for agricultural product.** Phitsanulok: School of Renewable Energy Technology, Naresuan University.

[9] B. L. Wornsnop. (1960). **Applications of thermoelectricity.** England: Great Britain.

[10] Ahiska, Rasit, Dislitas and Serkan. (2006). Microcontroller Based Thermoelectric Generator Application. **Gazi University, Journal of Science Apr 2006,** 19(2), 135-141.

[11] D. M. Rowe. (2006). **Thermoelectric handbook macro to nano.** USA: Taylor & Francis Group, CRC Press, New York.

[12] Clemens J. M. Lasance. (2006). The Seebeck Coefficient. **Electronic cooling, Article.** Retrieved November 1, 2006, from http://www.electronics-cooling.com/2006/11/the-seebeck-coefficient/

[13] D.M.Rowe. (1995). **Handbook of Thermoelectric**. Taylor & Francis Group, USA: CRC Press, New York.

[14] Frederik A. Leavitt, Norbert B. Elsner and Jonn C. Bass. (2009). Application and Testing of Hi-Z Thermoelectric Modules. **Hi- Z Technology.** USA: San Diego.

[15] Heat Transfer (Energy Engineering). (2014). **What-When-How,** Article, Retrieved June 1, 2014, from http://what-when-how.com/ energy-engineering/ heat-transfer-energy-engineering/

[16] Heat Exchangers Classification (Types). (2011). **Mechanical Engineering,** Article, Retrieved June 1, 2014, from http://mechanicalgalaxy. blogspot.com/2011/05/heat-exchangers-classification-types.html

[17] Brogan R.J. (2014). **Heat exchangers.** Retrieved February 13, 2013, from http://www.thermopedia.com/content/832/

[18] Laminar vs Turbulent. (2014). **The pillars curriculum for mechanical** Article, Retrieved June 1, 2014, from, http://pillars.che.pitt.edu/ student/slide.cgi?course_id=10&slide_id=14.0

[19] J C. Bass, N. B. Elsner and S. Ghamaty. (1995). **Performance of the 1 kW thermoelectric generator for diesel engines**. new york: Thirteenth International Conference on Thermoelectric, AIP Press.

[20] K. Ikoma, M. Munekiyo, K. Furuya, M. Kobayashi, T. Izumi and K. Shinohara. (1996). **develop a prototype generator for gasoline engine vehicle.** Japan: Nissan motor group co. ltd, Yokosuka.

[21] Chih Wu. (1996). Analysis of Waste-Heat Thermoelectric Power Generators. **Applied Thermal Engineering,** 16(1), 63-69.

[22] Jin-Kuk Kim and Robin Smith. (2001). Cooling Water System Design. **Chemical Engineering Science,** 56, 3641-3658.

[23] Douglas T. Crane and Gregory S. Jackson. (2004). Optimization of Cross Flow Heat Exchangers for Thermoelectric Waste Heat Recovery. **Energy Conversion and Management,** 45, 1565-1582.

[24] Chuang Yu and K.T. Chau. (2009). Thermoelectric Automotive Waste Heat Energy Recovery Using Maximum Power Point Tracking. **Energy Conversion and Management,** 50, 506-1512.

[25] Panya Yodovard. (2000). **Thermoelectric power generation.** Bangkok: King Mongkut's Institute of Technology Thonburi.

[26] Somchai Maneewan. (2004). **Mathematical modeling of a roof-integrated solar thermoelectric generation (rsteg) system for cooling load reduction.** Bangkok: King Mongkut's Institute of Technology Thonburi.

[27] Xiaolong Gou, Heng Xiao and Suwen Yang. (2010). Modeling Experimental Study and Optimization on Low-temperature Waste Heat Thermoelectric Generator System. **Applied Energy,** 87, 3131-3136.

[28] Basel I. Ismail and Wael H. Ahmed. (2009).Thermoelectric Power Generation Using Waste-Heat Energy as an Alternative Green Technology. **Electrical Engineering,** 2, 27-39.

[29] Gao Min and David M. Rowe. (1995). **Peltier devices as generators.** USA: Taylor & Francis Group, CRC Press, New York.

[30] Takenobu Kajikawa. (2006). **Thermoelectric power generation system recovery industrial waste heat.** USA: Taylor & Francis Group, CRC Press, New York.

[31] Walter Short, Daniel J. Packey and Thomas Holt. (1995). **A manual for the economic evaluation of energy efficiency and renewable energy technologies.** USA: National Renewable Energy Laboratory.

[32] M. G. Kanatzidis. (2000). Dealing with the uncovery of CsBi4Te6 (a new Material for low-Temperature Applications). **Science,** 287, 1024.

[33] Kin-ichi Uemura. (1995). **Commercial pentier module.** USA: Taylor & Francis Group, CRC Press, 621. New York.

[34] Kakuei Matsubara and Mitsuru Matsuura. (2006). **A Thermoelectric Application to vehicles**. USA: Taylor & Francis Group, CRC Press, New York.

[35] E. F. Thacher, B. T. Helenbrook, M. A. Karri and Clayton J. Richter. (1999). **Testing an automobile exhaust thermoelectric generator in a light truck**. USA: Clarkson University, Potsdam, New York.

[36] Charles Y. Wereko-Brobby and Essel B.Hagan. (1996). **Biomass conversion and technology**. England: UNESCO, John Willey & Sons.

[37] Aleksander S. Kushch, John C. Bass, Saeid Ghamaty, Norbert B. Elsner, Richard A. Bergstrand, David Furrow, et al. (2002). **Thermoelectric development at Hi-Z technology**. USA: Hi-Z Technology

[38] McKendryPeter. (2002). Energy Production from Biomass Part 2: Overview of Biomass. **Biosource Technology,** 83(1), 37-46.

[39] Bhaskar Kumar. (2011). **Lamina Transitional and Turbulent Flows 10th Indo-German Winter academy 2011.** Retrieved September 14, 2013, from http://www.leb.eei.uni-erlangen.de /winterakademie/2011/ report/content/course01/pdf/0103.pdf

[40] B. C. Sales, D. Mandrus and R. K. Williams. (1996). Covering the Antimonies LnM4Sb12 as Thermoelectric. **Science,** 272, 1325.

[41] Jihat G. Haidar and Jamil I. Ghojel, (2001). Waste Heat Recovery from the Exhaust of Low-power Diesel Engine using Thermoelectric Generators. In **20th International Conference on Thermoelectric** (pp. 413-417). Australia: Department of Engineering, Monash University.

[42] Young, Hugh D. (1992). **Values for diamond and silica aerogel**. N.P.: Handbook of Chemistry and Physics.

[43] Bongkot prasit. (2013). **Low cost saturated mixture stream production by biomass combustion for low temperature agro-industry.** Phitsanulok: School of Renewable Energy Technology, Naresuan University.

[44] Cengel, Y. A. (2006). **Heat and mass transfer.** New York: McGraw-Hill.

[45] Brogan, R. J. (2013). **Heat Exchangers.** Retrieved June 1, 2014,
from http://www. thermopedia.com/content/832/

[46] University of Pittsburgh, Department of Chemical and Petroleum
Engineering. (2008). **Laminar vs Turbulent**. Retrieved
July 10, 2014, from http://pillars.che.pitt.edu/files/course_10/
figures/lam_turb.gif

[47] G. Jeffrey Snyder1 and Eric S. Toberer. (2008). Complex thermoelectric
materials. **Nature Materials**, 7, 105–114.

[48] Moffat, R. (1997). Notes on Using Thermocouples. **Electronics Cooling.**
Retrieved July 10, 2014, from http://www.electronics- cooling.com/
1997/01/notes-on-using-thermocouples/

[49] P. De Groote. (1995). Maintenance performance analysis: A Practical
Approach. **Journal of Quality in Maintenance Engineering,**
1(2), 4–24.

[50] Finite Element Analysis Pipe Flow with ANSYS. (2013). **Engineers' handbook**.
Retrieved July 10, 2014, from http://www.engineershandbook.net/
finite-element-analysis-pipe-flow-ansys/

[51] Curtis Gulaga. (2014). **Vortex Shedding Meters.** Business Development
Manager CB Engineering, Article, Retrieved August 10, 2014,
from http://www.cbeng.com/resources/whitepaper/vortexmetersforgas.pdf

APPENDIX

APPENDIX A HEAT DUCT DESIGN AND CALCULATION

A circular, a triangular and a square cross-sectional duct were designed to fit with the thermoelectric device as shown in the Figure 56. The heat duct surface was flat for install thermoelectric module. The thermal conductivity of each geometries can be calculated by the heat conduction equation or Fourier's Law as follows;
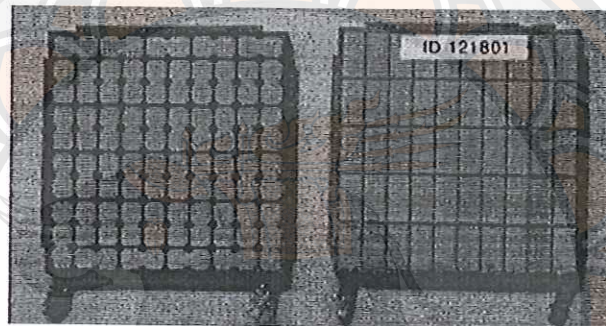
$$q_x = -kA \frac{\partial T}{\partial k}$$

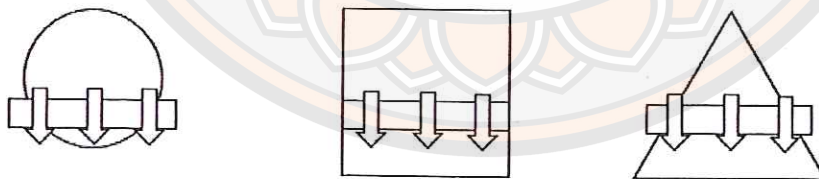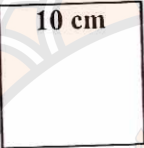**Figure 56 Shape of the thermoelectric device.**
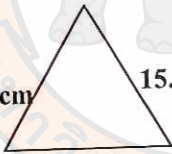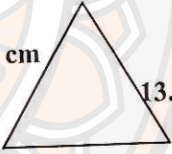
Figure 57 Surface of heat ducts for the installation of thermoelectric devices.

On the surface of the circular duct, triangular duct and rectangular duct can be see that the pipe surface of the triangular shape and squares shape are the areas to expose thermoelectric much that the Table 24 was the consider the area of the triangle duct shape and squares duct shape.

Table 24 Comparison the circumference and cross sectional area of duct.

Duct shape	circumference (Fix area 100 cm^2)	Area (Fix circumference 40 cm)
Square	10 cm, 10 cm (square) 10+10+10+10 = **40 cm**	10 cm, 10 cm (square) 10 x 10 = **100 cm^2**
Triangular	15.2 cm, 15.2 cm, 15.2 cm (triangle) 15.2+15.2+15.2= **45.6 cm**	13.3 cm, 13.3 cm, 13.3 cm (triangle) 1/2 x base x high = **76.6cm^2**

According to the Table 24, compare the duct shape by giving the same area, which the circumference of the square duct is shorter than a triangular duct but the area was smaller. Consider the circumferential of rectangular duct, the cross-section area was much more than triangular duct. The square duct pipe was selected to use in the experiments of the actual system. Consider when the design flow in pipes was not circular. In experiment to use the turbulent flow when analyze the effect of heat transfer of hot gas flow in laminar and turbulent flow by Nusselt number as equation below.

$$Nu = 3.66 + \frac{0.065(D_h/L)E_e P_r}{1+0.04((D_h/L)R_e P_r)^{2/3}}$$ (Laminar flow)

$$Nu = \frac{hD_h}{K} = 0.023 Re^{0.8} Pr^{0.3}$$ (Turbulent flow)

When consider equation shown that turbulent flow will provide value of the Nusselt number higher. Represent the convection over than that as the equation shown.

$$Re = \frac{V_{avg} D_h}{v}$$

When the gas flow in non-circular duct shape by consider Re > 10,000

$$V_{avg} = \frac{\dot{V}}{A_c}$$

$$D_h = \frac{4A_c}{P} = \frac{4a^2}{4a} = a$$

V is value of the kinetic viscosity consider the heat from the burning temperature 150 ° C at a pressure of 1 atm which consider the assumption based on the air used for combustion with excess air in volume over the air to complete combustion up over to double. Thus, it assumes the properties of the hot gas that occur after burning. Hot air after combustion has the properties as shown in the Table 25.

Table 25 Property of air at 1 atm pressure.

Temp $T, °C$	Density $p, kg/m^3$	Specific heat $C_p, \dfrac{j}{kg}k$	Thermal conductivity $k, \dfrac{W}{m}k$	Thermal diffusivity $\alpha, m^2/s$	Dynamic viscosity $\mu, \dfrac{kg}{m}s$	Kinematic Viscosity $v, m^2/s$	prandtl number Pr
100	0.9458	1009	0.03095	3.243×10^{-5}	2.181×10^{-5}	2.306×10^{-5}	0.7111
120	0.8977	1011	0.03235	3.565×10^{-5}	2.164×10^{-5}	2.522×10^{-5}	0.7073
140	0.8542	1013	0.03374	3.898×10^{-5}	2.345×10^{-5}	2.745×10^{-5}	0.7041
160	0.8148	1016	0.03511	4.241×10^{-5}	2.420×10^{-5}	2.975×10^{-5}	0.7014

$$\mathcal{V} = 2.86 \times 10^{-5} \, m^2/s$$

The design was set the square duct size 10 x10 cm the value $D_h = 0.1m$ and flow rate of hot gas is 257 CFM or 7.281 CMM.

$$V_{avg} = \frac{\dot{V}}{A_c} = \frac{7.281}{(0.1)^2(60)} = 12.135 \, m/s$$

Therefore

$$Re = Re = \frac{V_{avg}D_h}{v} = \frac{12.135(0.1)}{2.86 \times 10^{-5}} = 42{,}430.07$$

When Re is more than 10000. Consider, the turbulent flow on the length of pipe as equation.

$$L_h \approx L_t \approx 10D = 10(01) = 1 \, m.$$

Consider the length of the resulting turbulent flow is too long, thus reducing the cross-sectional area by putting the wedge and ribbon blade inside the duct. The length to cause turbulent flow is reduce D_h =0.04m therefore length of duct to cause turbulent flow is reduce as shown in the Figure 58.

$$L_h \approx L_t \approx 10D = 10(0.04) = 0.4 \, m. = 40 \, cm.$$
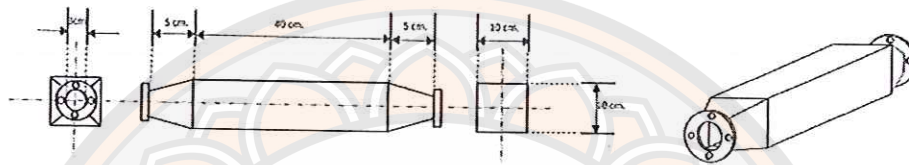
Figure 58 Square duct dimension.

Thermoelectric will be install during the length of duct 40 cm. The size is 7x7 cm 10 module on each side and two rows of two sides of the duct, as shown in the Figure 60.
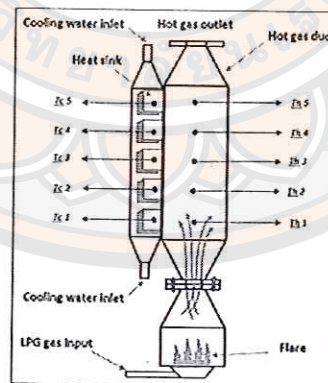
Figure 59 Thermoelectric install on the hot gas duct.

When consider the Nusselt number by Equation.

$$Nu = \frac{hD_h}{K} = 0.023Re^{0.8}Pr^{0.3}$$

When $\quad Pr = 0.70275$

$$Nu = 0.023(42,430.07)^{0.8}(0.70275)^{0.3} = 104.21$$

Therefore, the thermal conductivity is

$$K = 0.034425 \; W/m \; °C$$

When

$$h = Nu\frac{K}{D_h} = (104.21)\frac{0.034425}{0.04} = 89.69 \; W/m^2 \; °C$$

and

$$A_s = pL = 4aL = 4(0.1)(0.4) = 0.16 \; m^2$$

$$\dot{m} = \rho\dot{V} = 0.8345 \, (0.12135) = 0.1.1 \; kg/s$$

The heat transfer was the temperature of the gas equal to 110°C. Temperature of the gas at the entrance is 150°C. It can be found from the following equation.

$$\dot{Q} = \dot{m}c_p(T_e - T_i)$$

$$= (0.101kg/s) \, (1,014.5 \, J/kg \, °C) \, (110\text{-}150) \; °C$$

$$= \text{-}4,098.58 \; W$$

$$= \text{-}4.09858 \; kW$$

Amount of heat transfer per unit area is

$$q_s = \frac{\dot{Q}}{A_s} = \frac{4,089.58}{0.16} = 25,616.125 \frac{W}{m^2} = 2.56 \frac{W}{cm^2}$$

In the analysis of heat transfer in this case define as q_s is constant because gas does not change the status and then during the steady state can consider the q_s that flow out of the pipe is constant.

The coolant hose is design to meet the hot gas duct. cross-sections is using the same square duct and pipe cross section 9x8 cm in length with 38 cm. as shown in the Figure 60. It has cooling fins five positions, which correspond to the location of install thermoelectric module as shown in the Figure 61 as heat is apply, it can be made of heat through the pipes transfer to thermoelectric by convection cooling pipes. It has better than did not install. Define by the water coolant temperature at the entrance is 30 °C.
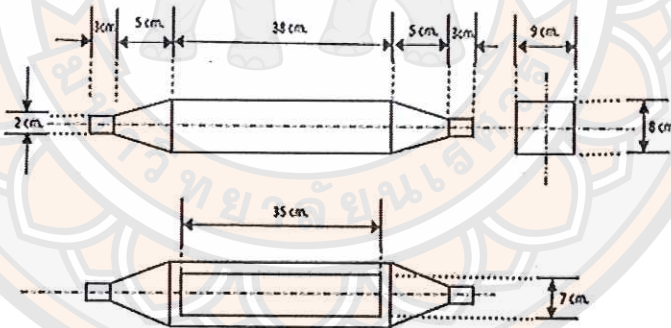
Figure 60 Water cooling pipe dimension.
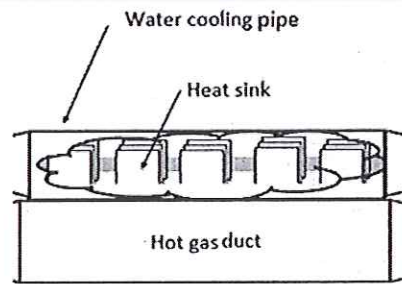
Figure 61 Heat sink contact on the cold side of thermoelectric module.

Analysis of heat exchanger tube and heat transfer to the coolant pipe considers equations of thermal balance occur.

$$\dot{Q} = \dot{m}_c c_{pc}(T_{c,in} - T_{c,out})$$

And
$$\dot{Q} = \dot{m}_h c_{ph}(T_{h,out} - T_{h,in})$$

when
$$\dot{m}_h c_{ph}(T_{h,out} - T_{h,in}) = -4{,}098.58\ W$$

The cross section of the coolant pipe size 9x8 cm. = 72 cm^2 = 0.0072 m^2

The design speed of water equal to 6 cm/s. Is equal to the mass flow rate.

$$\dot{m} = \rho AV = (996)(0.0072)(0.06) = 0.49\ kg/s$$

Value
$$c_p = 4{,}178\ j/kg\ °C$$

$$-4{,}098.58 = (0.49)4{,}178(30 - T_{c,out})$$
$$T_{c,out} = 32°C$$

Table 26 Property of saturated water.

Temp. T, °C	Saturation Pressure P_{sat}, kPa	Density ρ, kg/m³		Enthalpy of Vaporization h_{fg}, kJ/kg	Specific Heat c_p, J/kg · K		Thermal Conductivity k, W/m · k		Dynamic Viscosity μ, kg/m · s		Prandtl Number Pr		Volume Expansion Coefficient β, 1/K
		Liquid	Vapor		Liquid	Vapor	Liquid	Vapor	Liquid	Vapor	Liquid	Vapor	Liquid
0.01	0.6113	999.8	0.0048	2501	4217	1854	0.561	0.0171	1.792×10^{-3}	0.922×10^{-5}	13.5	1.00	-0.068×10^{-3}
5	0.8721	999.9	0.0068	2490	4205	1857	0.571	0.0173	1.519×10^{-3}	0.934×10^{-5}	11.2	1.00	0.015×10^{-3}
10	1.2276	999.7	0.0094	2478	4194	1862	0.580	0.0176	1.307×10^{-3}	0.946×10^{-5}	9.45	1.00	0.733×10^{-3}
15	1.7051	999.1	0.0128	2466	4185	1863	0.589	0.0179	1.138×10^{-3}	0.959×10^{-5}	8.09	1.00	0.138×10^{-3}
20	2.339	998.0	0.0173	2454	4182	1867	0.598	0.0182	1.002×10^{-3}	0.973×10^{-5}	7.01	1.00	0.195×10^{-3}
25	3.169	997.0	0.0231	2442	4180	1870	0.607	0.0186	0.891×10^{-3}	0.987×10^{-5}	6.14	1.00	0.247×10^{-3}
30	4.246	996.0	0.0304	2431	4178	1875	0.615	0.0189	0.798×10^{-3}	1.001×10^{-5}	5.42	1.00	0.294×10^{-3}
35	5.628	994.0	0.0397	2419	4178	1880	0.623	0.0192	0.720×10^{-3}	1.016×10^{-5}	4.83	1.00	0.337×10^{-3}

The estimated temperature at the exit of the cooling water is 32°C.

The analysis of the balance of the heat generate by consider the effect of heat transfer per unit. The area of the pipe is heat transfer to the coolant pipe.

When consider from the requirements. HZ-14 Thermoelectric types use in the design of this.
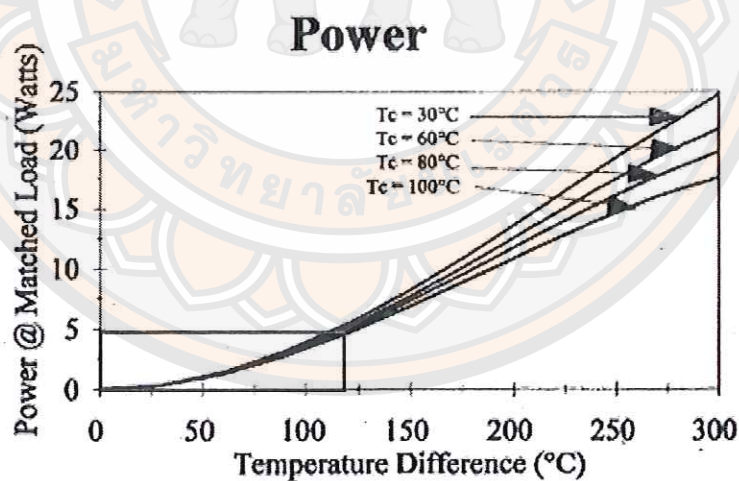
Figure 62 Thermoelectric power generation characteristic.

The temperature difference between both sides is 200 ˚C.

The heat flux $9.54\ W/cm^2$ can generate electric power 14 watt.

The difference between the temperature 120 ˚C by design at different.

Design layout piping hot gas at 150 ˚C and at a flow equal to 30 ˚C.

Power output is about 4.8 watt compare to the estimate proportion of Heat Flux is $2.74\ W/cm^2$.

Consider the effect of the amount of heat discharge per unit area is calculate$\dot{q}_s = 2.56\ W/cm^2$ and the heat transfer per unit area is derive from the specifications. Thermoelectric company Hi-Z Technology, Inc. is a tolerance of about $0.18\ W/cm^2$ or about 6.56 %.

Therefore the design is analyze on the thermal balance occurs, then there is not much discrepancy. The result of a calculation design to create pieces for use in experiment.
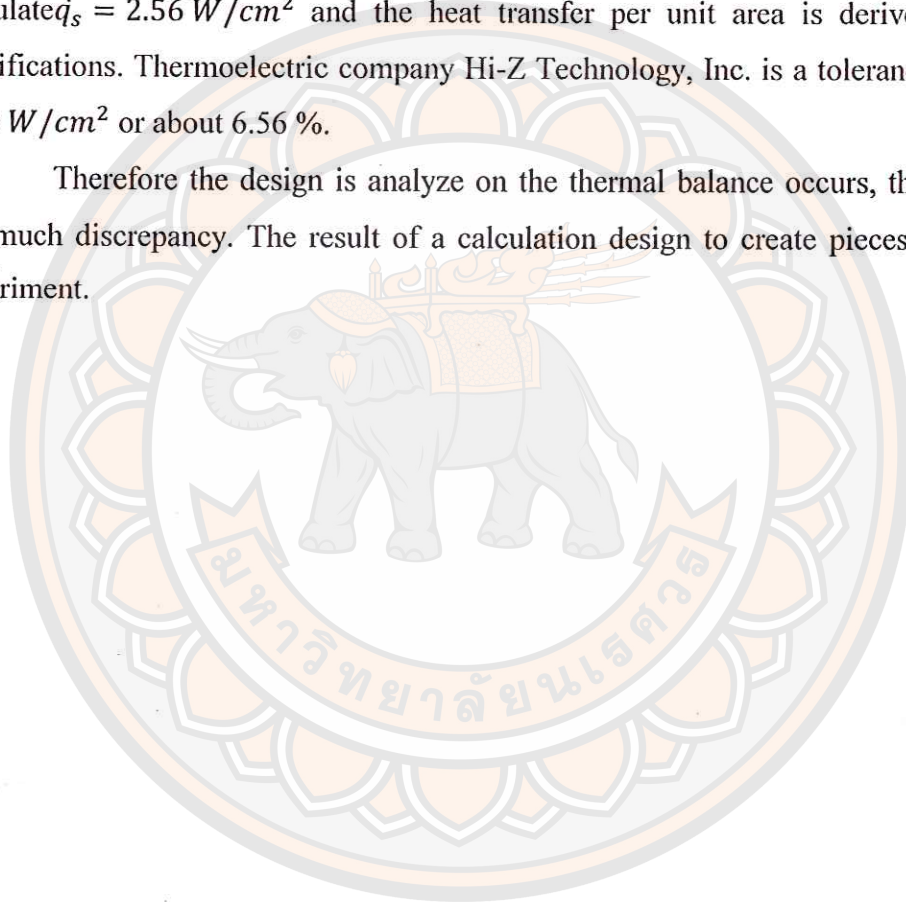
APPENDIX B MASS BALANCE AND ENERGY BALANCE ANALYSIS.

Mass balance and energy balance are used in a simple steady flow process as shown the Figure 63. It was working with the influx only one way through the control volume without collection of mass and energy. The control volume any location within the volume is constant time independent. In cross section of pipe 1-1 is inlet 2-2 is outlet. The fluid that heat will be passing flow a control area as the Figure 63.
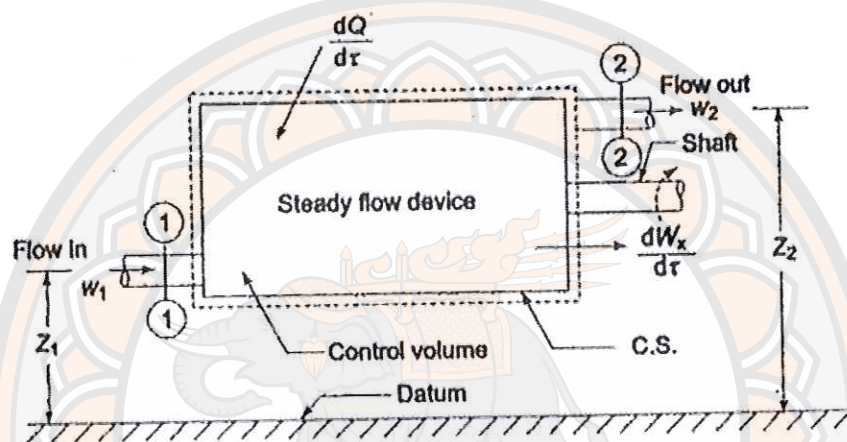
Figure 63 Steady flow process constant.

The cross section 1-1 and 2-2 has the data as follow.

A_1, A_2 is cross section of inlet outlet pipe(m^2)

$\dot{m}_1, \dot{m}_2$ is flow rate of fluid ($\frac{Kg}{s}$)

P_1, P_2 is pressure of inlet outlet ($\frac{N}{m^2}$)

V_1, V_2 is volume of fluid flow ($\frac{m^3}{Kg}$)

Z_1, Z_2 is different level of inlet outlet (m)

$\frac{dQ}{d\tau}$ is heat transfer rate passes surface control ($\frac{J}{s}$)

$\frac{dW_x}{d\tau}$ is power transfer rate passes surface control($\frac{J}{s}$)

By τ is the time in second unit and subscript 1, 2 is inlet-outlet of volume control.

Mass Balance

The law of conservation of mass, the flow rate of the working substance is equal to the rate the control volume the working fluid as shown in the equation.

$$\dot{m}_1 = \dot{m}_2$$

When

$$\dot{m}_1 = \frac{AV}{V}$$

When   replace value in equation.

$$\frac{A_1 V_1}{V_1} = \frac{A_2 V_2}{V_2}$$

or
$$\rho_1 A_1 V_1 = \rho_2 A_2 V_2$$

By equation present is call equation of continuity.

Energy Balance

In transfer flow, there are two types of internal and external flow. All work is transferred across the control surface. In engineering worked, it is considered external. Because the shear (shear work) including a shaft and electrical (electrical work). In the Figure 64 is only the outside work by a shaft (W_x). The mass of the fluid displace by the entrance is dm_1 and exit is dm_2 but work of mass flow is

$-p_1 V_1 V dm_1$ The mass of the fluid displace by the entrance

and

$+p_2 V_2 dm_2$ The mass of the fluid displace by the exit.

Therefore total is transferred to the system as shown below.

$$W = W_x - p_1 V_1 V dm_1 + p_2 V_2 dm_2$$

When write in the form of rate with respect to time as follows.

$$\frac{dW}{d\tau} = \frac{dW_x}{d\tau} - p_1 V_1 \frac{V dm_1}{d\tau} + p_2 V_2 \frac{dm_2}{d\tau}$$

or

$$\frac{dW}{d\tau} = \frac{dW_x}{d\tau} - \dot{m}_1 p_1 V_1 + \dot{m}_2 p_2 V_2$$

From the law of energy conservation. When the sum of the energy, the working fluid flow rate at inlet of the control volume is equal to the sum of the rate on the flow of energy working at the exit of the control volume, which can be expressed as the following the equation.

$$\dot{m}_1 e_1 + \frac{dQ}{d\tau} = \dot{m}_2 e_2 + \frac{dW}{d\tau}$$

Replace

$$\frac{dW}{d\tau} = \frac{dW_x}{d\tau} - \dot{m}_1 p_1 V_1 + \dot{m}_2 p_2 V_2$$

In equation is

$$\dot{m}_1 e_1 + \frac{dQ}{d\tau} = \dot{m}_2 e_2 + \frac{dW_x}{d\tau} - \dot{m}_1 p_1 V_1 + \dot{m}_2 p_2 V_2$$

$$\dot{m}_1 e_1 + \dot{m}_1 p_1 V_1 + \frac{dQ}{d\tau} = \dot{m}_2 e_2 + \dot{m}_2 p_2 V_2 + \frac{dW_x}{d\tau}$$

When e_1 and e_2 is the energy carries in and out of the control volume per unit mass of fluid. Specific energy e can write that.

$$e = e_K + e_p + u$$

$$= \frac{V^2}{2} + Z_g + u$$

Replace e in equation is

$$\dot{m}_1 e_1 + \dot{m}_1 p_1 V_1 + \frac{dQ}{d\tau} = \dot{m}_2 e_2 + \dot{m}_2 p_2 V_2 + \frac{dW_x}{d\tau}$$

$$\dot{m}_1 \left(\frac{V_1^2}{2} + Z_1 g + u_1 \right) + \dot{m}_1 p_1 V_1 + \frac{dQ}{d\tau} = \dot{m}_2 \left(\frac{V_2^2}{2} + Z_2 g + u_2 \right) + \dot{m}_2 p_2 V_2 + \frac{dW_x}{d\tau}$$

or

$$\dot{m}_1 \left(\frac{V_1^2}{2} + Z_1 g + u_1 \right) + p_1 V_1 + \frac{dQ}{d\tau} = \dot{m}_2 \left(\frac{V_2^2}{2} + Z_2 g + u_2 \right) + p_2 V_2 + \frac{dW_x}{d\tau}$$

When $\qquad h = u + pV$

$$\dot{m}_1 \left(\frac{V_1^2}{2} + Z_1 g + h_1 \right) + \frac{dQ}{d\tau} = \dot{m}_2 \left(\frac{V_2^2}{2} + Z_2 g + h_2 \right) + \frac{dW_x}{d\tau} \qquad (1)$$

When a process flow constant.

$$\dot{m}_1 = \dot{m}_2 \quad \text{or} \quad m^\cdot = \dot{m}_1 = m_2 = \frac{dm}{d\tau}$$

Find the equation above $\frac{dm}{d\tau}$ is

$$\frac{\dot{m}_1 (\frac{V_1^2}{2} + Z_1 g + h_1)}{\frac{dm}{d\tau}} + \frac{\frac{dQ}{d\tau}}{\frac{dm}{d\tau}} = \frac{\dot{m}_2 (\frac{V_2^2}{2} + Z_2 g + h_2)}{\frac{dm}{d\tau}} + \frac{\frac{dW_x}{d\tau}}{\frac{dm}{d\tau}}$$

$$\frac{\dot{m}_1 (\frac{V_1^2}{2} + Z_1 g + h_1)}{\dot{m}_1} + \frac{dQ d\tau}{d\tau \, dm} = \frac{\dot{m}_2 (\frac{V_2^2}{2} + Z_2 g + h_2)}{\dot{m}_2} + \frac{dW_x d\tau}{d\tau \, dm}$$

Equation is

$$\left(\frac{V_1^2}{2} + Z_1 g + h_1\right) + \frac{dQ}{dm} = \left(\frac{V_2^2}{2} + Z_2 g + h_2\right) + \frac{dW_x}{dm} \qquad (2)$$

Equations 1 and 2 is called the equation of power flow constant steady flow energy equations (S.F.E.E) For the flow of working fluid at the inlet and outlet of the control volume as in Equation 2 is a flow of energy per unit mass of fluid (J/kg) and Equation 1 is the energy of the flowing fluid per unit time. $(J/, w)$

From Equation 2 can be written in terms of the difference as follows.

$$\frac{dQ}{dm} - \frac{dW_x}{dm} = \left(\frac{V_2^2}{2} + Z_2 g + h_2\right) - \left(\frac{V_1^2}{2} + Z_1 g + h_1\right)$$

$$q - W_x = (h_2 - h_1) + \left(\frac{V_2^2 - V_1^2}{2}\right) + g(Z_1 - Z_1)$$

When q, W_x is the energy transfer per unit of mass. Derivatives of the equation can be write SFEE.

$$dq - dW_x = dh + V dV + g dZ$$

Power conversion efficiency (energy conversion efficiency) is the ratio between energy outputs of the energy conversion by energy input into the converter. Because inherent in the process of converting the energy is the energy loss. (convert into energy that does not need it), can always be expressed as an equation.

$$Energy\ conversion\ efficiency\ (\%) = \frac{Energy\ output}{Eneregy\ input} \times 100$$

Analysis balance and transformation of energy (energy balance, energy conversion) of the new system was designed as shown in the Figure 64 by consider

1) Biomass is heat 2) gas from waste heat conversion into electricity by thermoelectric and 3) the gas converted to electricity. The engine and generator of 10 kW.
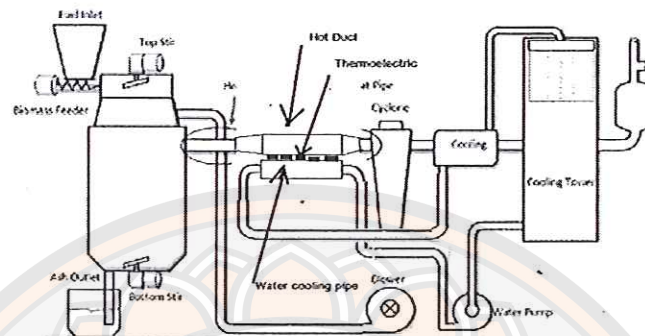
Figure 64 Biomass gasification system integrated with thermoelectric system.

When consider the biomass gasifier system. It can find energy balance by equation as follow.
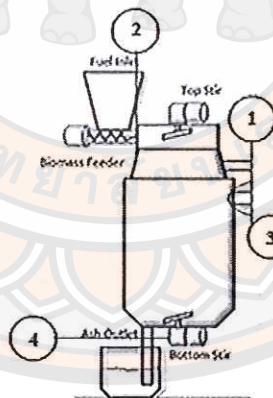
Figure 65 Biomass gasifier furnace.

$$\dot{m}_1 \left(\frac{V_1^2}{2} + Z_1 g + h_1 \right) + \dot{m}_2 \left(\frac{V_2^2}{2} + Z_2 g + h_2 \right) + \frac{dQ}{d\tau}$$

$$= \dot{m}_3 \left(\frac{V_3^2}{2} + Z_3 g + h_3 \right) + \dot{m}_4 \left(\frac{V_4^2}{2} + Z_4 g + h_4 \right) + \frac{dQ_x}{d\tau}$$

When
Point 1 is channel of air flow.

Point 2 is influx of biomass channels.

Point 3 is outflow of hot gas channel.

Point 4 is a flow of ash channel.

Consider the volume control.

Δ KE $\cong$ 0 because point 1 to point 3 and point 2 to point 4, the effect of the speed difference is small., Δ PE $\cong$ 0 because point 1 to point 2, when compare with point 3 to point 4, the effect of the height difference is small and point 4 of ash flow channel to set the value of the energy of the charcoal is low.

$dQ/d\tau$ is the heat transfer passes surface control(j/s)

$dW_x/d\tau$ is the energy transfer passes surface control (j/s)

When consider the biomass gasifier electric equipment are uses the energy consumption as shown on the Table 26.

**Table 27 Energy consumption the equipment of biomass gasifer.**

Motor	Power(W)	Nomenclature
1.Blower	638	E_{blower}
2.Water pump	374	$E_{water\ pump}$
3.Top stir motor	286	$E_{top\ stir}$
4. Bottom Stir motor	286	$E_{bottom\ stir}$
5 Biomass feeder motor	308	E_{auger}
Total	**1,892**	E_{total}

The energy balance of biomass gasifier can be find by equation.

$$\dot{m}_1(h_1) + \dot{m}_2(h_2) + \frac{dQ}{d\tau} = \dot{m}_3(h_3) + (E_{blower} + E_{water\ pump} + E_{top\ stir} + E_{auger})$$

$$\dot{m}_1(h_1) + \dot{m}_2(h_2) + \frac{dQ}{d\tau} = \dot{m}_3(h_3) + (E_{Total})$$

When set to mass flow rate of the biomass is 4 kg / hr, equivalent to 0.0011 kg/s. The heating value of biomass fuels are used in the dry (Dry wood) with a heating value of 19 MJ / kg.

Volumetric flow rate of hot gas and air at 257 CFM or 7.281CMM.

Square duct size 10X10 cm from the pipe is design, temperature of the hot gas at 150 ° C at a pressure of 1 atm is = 0.12135 m^3/ s and = 0.101 kg / s for h3 = 421.16 kJ / kg.

Inlet duct at a temperature of 30°C from Table features air =1.164 kg/ m^3 (30°C at a pressure of 1 atm) is = 1.164 (0.12135) = 0.141 kg / s for h2 = 305.22 kJ / kg.

From equation $\qquad \dot{m}_1(h_1) + \dot{m}_2(h_2) + \frac{dQ}{d\tau} = \dot{m}_3(h_3) + (E_{Total})$

Change to $\qquad \dot{m}_1(HHV_{1,mass}) + \dot{m}_2(h_2) + \frac{dQ}{d\tau} = \dot{m}_3(h_3) + (E_{Total})$

0.0011 (kg/s) 19,000 (kJ/kg) + 0.141 (kg/s) 305.22 (kJ/kg) + $\frac{dQ}{d\tau}$ = 0.101 (kg/s) 421.16(kJ/ kg) + (-1.892) kW

20.9 kW + 43.036 kW + 1.892 kW + $\frac{dQ}{d\tau}$ = 42.54 kW

$$\frac{dQ}{d\tau} = 42.54 \text{ kW-}(20.9 \text{ kW} + 43.036 \text{ kW} + 1.892 \text{ kW})$$

$$\frac{dQ}{d\tau} = -23.288 \text{ kW}$$

The heat loss rate of biomass gasified about 23.288 kW.

Power conversion efficiency (energy conversion efficiency) of the furnace in conversion of the biomass gasifier with air in a combustion gas and the heat loss that occurs can be found from the following equation as shown in the Figure 66.

$$\text{Energy conversion efficiency} (\%) = \frac{42.54}{65.828} \times 100 = 64.623\%$$

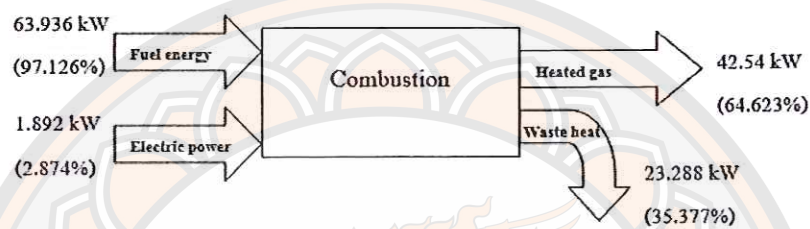**Figure 66 Energy conversion of gasifier.**

Turning biomass fuel with air in a combustion gas and heat loss occurs.

Gas Conversion of Waste Heat into Electricity with Thermoelectric devices

Consider most of the gas from the waste heat convert into electricity with thermoelectric device. The energy balance can be expressed as follows;
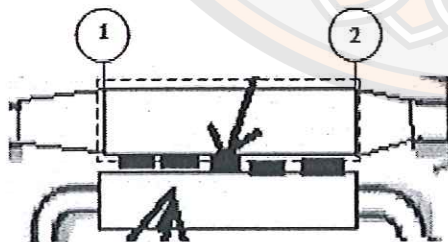
Figure 67 Waste heat recovery by thermoelectric device.

Where

Point 1 is the first hot gas flow in duct.

Point 2 is hot gas outflow from duct.

$$\dot{m}_1 \left(\frac{V_1^2}{2} + Z_1 g + h_1 \right) + \frac{dQ}{d\tau} = \dot{m}_2 \left(\frac{V_2^2}{2} + Z_2 g + h_2 \right) + \frac{dW_X}{dm}$$

When control the volume of hot gas flow.

$\Delta KE \cong 0$ point 1 and point 2, as a result of the speed difference is small

$\Delta PE \cong 0$ because point 1 to point 2 in the class

$dW_x/d\tau = 0$, because no net rate of flow through the control surface

$dQ/d\tau$ Net rate of heat transfer through the surface control. (j/s)

The energy balance of hot gas can be expressed as follows;

$$\dot{m}_1(h_1) + \frac{dQ}{d\tau} = \dot{m}_2(h_2)$$

Where $\dot{m}_1 = \dot{m}_2 = \dot{m} = 0.101 \ kg/s$

Heat transfer is the temperature of the gas equal to 110 ˚C while the temperature of the gas at the entrance equal to 150 ° C.

$$\frac{dQ}{d\tau} = \dot{m}(h_2 - h_1) = \dot{m}c_p(T_2 - T_1)$$

$$= (0.101 \ kg/s) \ (1{,}014.5 \ J/kg \ ˚C) \ (110\text{-}150) \ ˚C$$

$$= -4{,}098.58 \ W$$

$$= -4.09858 \ kW$$

Net rate of heat loss of hot gas is 4.09858 kW.

Consider conversion of heat into electricity with thermoelectric devices. The energy balance can be expresses as shown in the Figure 68.
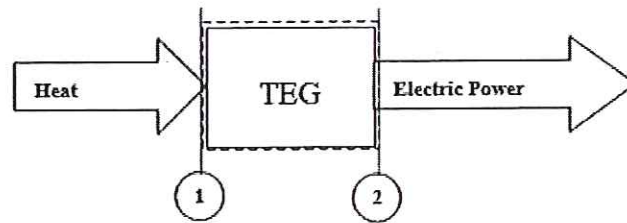
Figure 68 Heat conversion to electricity.

Where

Point 1 is the first surface in contact with the thermoelectric device

Point 2 is two wires from the thermoelectric device.

$$\dot{m}_1\left(\frac{V_1^2}{2} + Z_1 g + h_1\right) + \frac{dQ}{d\tau} = \dot{m}_2\left(\frac{V_2^2}{2} + Z_2 g + h_2\right) + \frac{dW_X}{d\tau}$$

If considering the volume control, fluid volume control does not flow.

$dW_x/d\tau$ The rate of flow through the control surface.

$dQ/d\tau$ Net rate of heat transfer through the surface control. (j/s)

Amount of heat transfer per unit area of heat ducts is not equal

$$\dot{q}_s = \frac{\dot{Q}}{A_s} = \frac{4,098.58}{0.16} = 25,616.125 \; \frac{W}{m^2} = 2.56 \; \frac{W}{cm^2}$$

Thermoelectric space heating is equal to (7X7) x10 = 490.cm^2

The estimation of the amounts of heat from the thermoelectric device is

$$2.56 \frac{w}{cm^2}(490)cm^2 = 1,254.4 \; W = 1.2544 \; kW$$

According to the specification of the thermoelectric company Hi-Z Technology, Inc. The thermoelectric device has a heat flux of $2.56 \ W/cm^2$ while the electric power was 6.5 watt per each device. If 10 thermoelectric devices were installed, the total power output would be 65 W.

If considering the energy balance equation by multiplying the coefficient of thermal energy into electrical energy can be expressed as follows.

$$\eta_{TEG} \frac{dQ}{d\tau} = \frac{dW_x}{d\tau}$$

$$\eta_{TEG} 1{,}254.4W = 65W$$

$$\eta_{TEG} = 65/1{,}254.4W = 0.0518$$

Power conversion efficiency (energy conversion efficiency) of gas from waste-heat into electricity with thermoelectric devices can be derived into the following equation as shown in the Figure 69.

$$\text{Energy conversion efficiency (\%)} = \frac{65}{1{,}254.4} \times 100 = 5.18\%$$
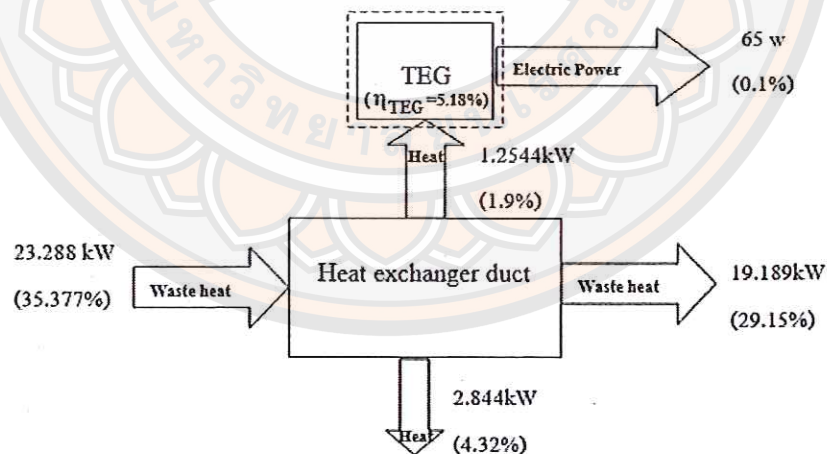
Figure 69 Block diagram of the energy conversion.

Energy conversion from heat into electricity with thermoelectric devices by using the engine and a 10 KW power generator.

Consider if the most of waste-heat convert into electricity by using the thermoelectric devices, the energy balance can be expresses as follows;
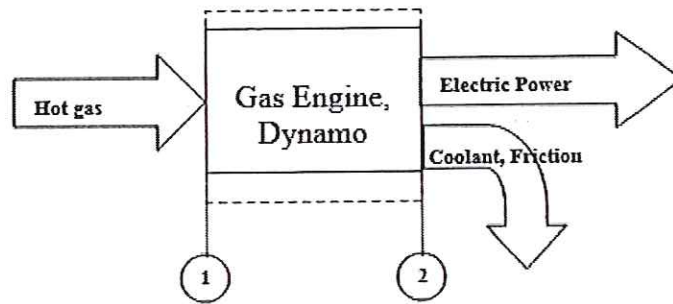
Figure 70 Energy conversion of a biomass power plant.

Where,

Point 1 is the first entrance of the hot gas before entering the engine.

Point 2 is the two wires from the generator.

$$\dot{m}_1\left(\frac{V_1^2}{2} + Z_1 g + h_1\right) + \frac{dQ}{d\tau} = \dot{m}_2\left(\frac{V_2^2}{2} + Z_2 g + h_2\right) + \frac{dW_X}{d\tau}$$

Analysis of the volume control will not consider the exhaust gases from the combustion. It can be integrated with the fluid volume control solution.

$dW_x/d\tau$ Net rate of flow through the control surface, in addition to electric power. (W)

$dQ/d\tau$ Net rate of heat transfer through the control surface. (j/s) Friction heat emitted from the engine and heat transfer from the exhaust gases.

KE1 $\cong 0$ the first point, the effect of speed is not fast.

PE1 $\cong 0$ the first point, the effect of is not high.

The 10 kW system can be expressed by the equations as follows;

$$\dot{m}_1(h_1) + \frac{dQ}{d\tau} = \frac{dW_X}{d\tau}$$

$$0.101\ (kg/s)\ 421.16(kJ/kg) + \frac{dQ}{d\tau} = 10\ kW$$

$$42.537 \ kW + \frac{dQ}{d\tau} = 10 \ kW$$

$$\frac{dQ}{d\tau} = -32.537 \ kW$$

Thus, the net rate of heat transfer through the control surface is friction heat emitted from the engine. The heat transfer from the exhaust gas was 32.537 kW. The efficiency power conversion (energy conversion efficiency) of gas into electricity by the engine and generator was 10 kW. The energy conversion efficiency can be obtained from the following equations as shown in the Figure 71.

$$\text{Energy conversion efficiency}(\%) = \frac{10}{42.537} \times 100 = 23.509\%$$
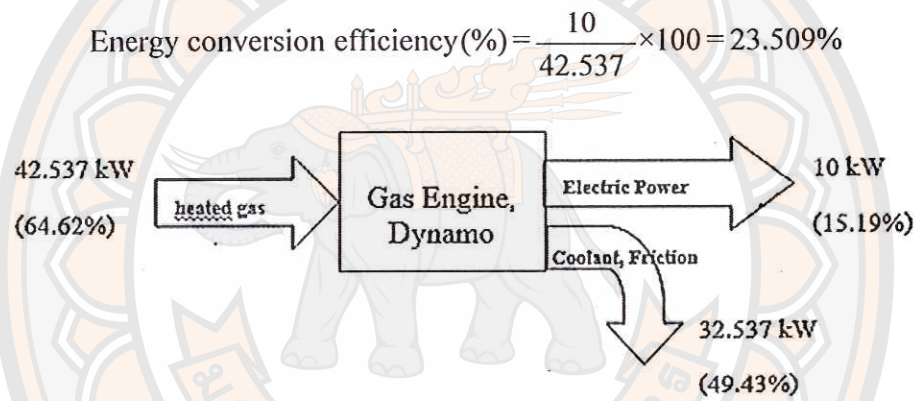
Figure 71 Conversion of thermal energy into electricity by the engine.
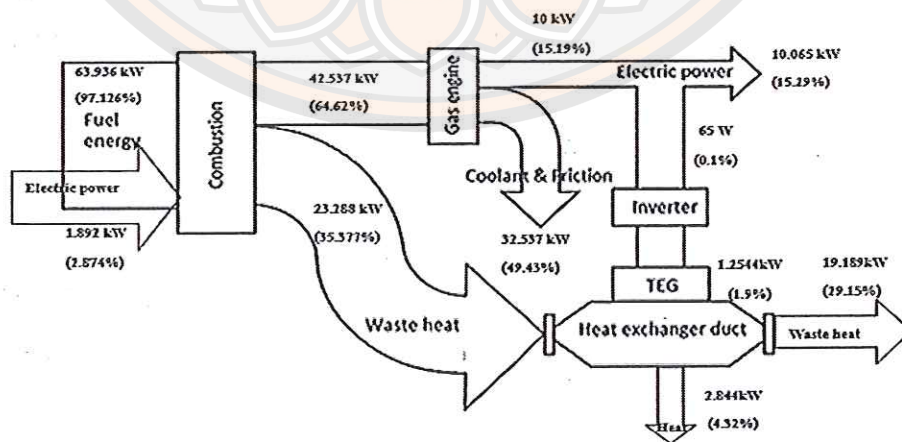
Figure 72 Energy balance of the power plants system.

Table 28 Result of energy balance and energy conversion analysis.

Process	Input (kW)	Output (kW)	energy conversion efficiency
Combustion	Fuel energy= 63.936 kW Electric power= 1.892 kW	hot gas=42.537 kW Waste heat=23.288 kW	64.623%
Heat exchanger duct	Waste heat =23.288 kW	Waste heat= 19.189kW Heat= 4.0984kW	17.599%
TEG	Heat = 1.2544kW	Electric power = 0.065 kW	5.18%
Gas Engine, Dynamo	hot gas =42.537 kW	Electric Power =10 kW Coolant, Friction and exhaust = 32.537 kW	23.509%
Original System Total	Fuel energy= 63.936 kW Electric power= 1.892 kW	Electric Power =10 kW	15.191%
New System Total	Fuel energy= 63.936 kW Electric power= 1.892 kW	Electric Power=10.065 kW	15.29%

APPENDIX C BIOMASS GASIFIER SYSTEM SPECIFICATION

A biomass gasifier system consists of a gas production unit and an electric control unit

1. Gas produce unit

The down draft gasifier component within 6 parts, fuel feed system, a burner system, a particles separate system, gas separation systems, gas storage, gas and vacuum systems.

Details:

1.1 The fuel feeding system consists of AC motor 1 HP 220 V, 50 Hz, 1 Phase, gear box ratio 1:60, Spiral feeder diameter of 4 inch automatic operation and fuel feeding tray capacity of 0.5 m^3.

1.2 Chamber has the following components, layer burning with thick steel (3 mm. thick, a diameter of 170 mm., a height of 370 mm.). Internal parts construction with high tension steel SKD11 temperature durable 1,100 degree Celsius, gas tank made from thick steel 2 mm. diameter 370 mm. high 550 mm. Ash ejection unit using a motor 1/4 HP, 220 V, 50 Hz, 1 phase automatic operation gear box ratio 1:60 and fuel cycling unit use motor 1/4 HP 220 V 50 Hz 1 phase automatic operation gear box ratio 1:60.

1.3 Particles separation unit cyclone type construction from iron gas inlet-outlet pipe diameter 3 inch long   500 mm.

1.4 Gas separate unit consists with cooling tower 10 ton, water pump use motor 1/4 HP 220 V 50 Hz 1 phase water inlet-outlet pipe diameter 1 inch water tank construction from metal sheet thick 2 mm. diameter 200 mm. high 750 mm., Tank pad, wood vinegar construction from metal sheet width 200 mm. Length 270 mm. high 200 mm., Filter tank construction from metal sheen thick 2 mm. diameter 245 mm. high 400 mm., Low pressure tank construction from metal sheet thick 2 mm. diameter 490 mm. high 400 mm.

1.5 Gas tank construction from metal sheet in 2 layer   external layer capacity 200 liter contain water for floating internal gas tank capacity 100 liter, gas inlet on bottom external tank, gas out let from the top of internal tank install valve control and by pass valve to other tank .

1.6 Gas suction system consists with gas pipe made from iron diameter 2 inch, install with Blass valve 2 inch, diameter of fan 320 mm. and centrifugal motor 1 HP 220 V 50 Hz 1 phase speed 2,950 rpm.

2. Control system

AC power 220 V, 50 Hz, 1 phase

Detail of equipments

2.1 Cabinet box (width 200 mm., length 500 mm., height 600 mm.)

2.2 Magnetic contractor 5 units.

2.3 Overload control 4 units.

2.4 Relay 7 units.

2.5 Programmable logic control 1 unit.

2.6 Temperature panel display.

2.7 Selector switch. (manual and automatic control)

2.8 Pilot lamp operation display.

2.9 Burglar alarm when system error.

APPENDIX D GEOMETRICAL CHARACTERISTIC OF
THERMOELECTRIC DEVICES

	Value	Tolerance
Width and Length	2.47 in. (6.27 cm)	±0.005 (0.25)
Thickness	0.2 in. (0.508 cm)	±0.005 (0.25)
Weight	82 grams	±3 grams
Compressive Yield Stress	10 ksi (70 Map)	Minimum
Number of active couples	49 couples	--
Thermal Properties		
Design Hot Side Temperature	230°C (450°F)	±10 (20)
Design Cold Side Temperature	30°C (85°F)	±5 (10)
Maximum Continuous Temperature	250°C (480°F)	--
Minimum Continuous Temperature	None	--
Maximum Intermittent Temperature	400°C (750°F)	+0.001
Thermal Conductivity1	0.024 W/cm*K	±0.5
Heat Flux1	9.54 W/cm2	
Electrical Properties (as a generator)1		
Power2 (typically > 14 Watts)	14 Watts	Minimum
Load Voltage	1.65 Volts	±0.1
Internal resistance	0.15 Ohms	±0.05
Current	8 Amps	±1
Open Circuit Voltage	3.5 Volts	±0.3
Efficiency	4.5%	minimum

1At design temperatures.

2At matched load, please refer to the graphs for properties at various operating. temperature and conditions.http://www.hi-z.com/uploads/2/3/0/9/23090410/hz-14.pdf

APPENDIX E   PROPERTIES TABLE OF STAINLESS STEEL, METALS AND OTHER CONDUCTIVE

material	Electrical		Thermal		Density (g/cm3)	Melting point or degradation(°C)
	conductivity (10.E6 Siemens/m)	resistivity (10.E-8 Ohm.m)	Conductivity (W/m.k)	expansion coef.10E-6(k-1) from 0 to 100°C		
Silver	62,1	1,6	420	19,1	10,5	961
copper	58,5	1,7	401	17	8,9	1083
Gold	44,2	2,3	317	14,1	19,4	1064
Aluminum	36,9	2,7	237	23,5	2,7	660
Molybden	18,7	5,34	138	4,8	10,2	2623
Zinc	16,6	6,0	116	31	7,1	419
Lithium	10,8	9,3	84,7	56	0,54	181
Tungsten	8,9	11,2	174	4,5	19,3	3422
Brass	15,9	6,3	150	20	8,5	900
Carbon (ex PAN)	5,9	16,9	129	0,2	1,8	2500
Nickel	14,3	7,0	91	13,3	8,8	1455
Iron	10,1	9,9	80	12,1	7,9	1528
Palladium	9,5	10,5	72	11	12	1555
Platinum	9,3	10,8	107	9	21,4	1772
Tin	8,7	11,5	67	23,5	7,3	232
Bronze 67Cu33Zn	7,4	13,5	85	17	8,8	1040
Carbon steel	5,9	16,9	90	12	7,7	1400
Lead	4,7	21,3	35	29	11,3	327
Titanium	2,4	41,7	21	8,9	4,5	1668
St.Steel316L EN1.4404	1,32	76,0	15	16,5	7,9	1535
St. Steel 304 EN1.4301	1,37	73,0	16,3	16,5	7,9	1450

| material | Electrical | | Thermal | | Density (g/cm3) | Melting point or degradation(°C) |
	conductivity (10.E6 Siemens/m)	resistivity (10.E-8 Ohm.m)	Conductivity (W/m.k)	expansion coef.10E-6(k-1) from 0 to 100°C		
Mercury	1,1	90,9	8	61	13,5	-39
Fe. Cr. Alloy	0,74	134	16	11,1	7,2	+-1440
St. Steel 310 EN1.4841	1,28	78	14,2	17	7,75	2650

http://www.tibtech.com/conductivity.php

APPENDIX F SEEBECK COEFFICIENT OF MATERIAL.

Metals	Seebeck Coefficient	Semiconductors	Seebeck Coefficient
	µV/K		µV/K
Antimony	47	Se	900
Nichrome	25	Te	500
Molybdenum	10	Si	440
Cadmium	7.5	Ge	300
Tungsten	7.5	n-type Bi_2Te_3	-230
Gold	6.5	p-type $Bi_{2-x}Sb_xTe_3$	300
Silver	6.5	p-type Sb_2Te_3	185
Copper	6.5	PbTe	-180
Rhodium	6.0	$Pb_{03}Ge_{39}Se_{58}$	1670
Tantalum	4.5	$Pb_{06}Ge_{36}Se_{58}$	1410
Lead	4.0	$Pb_{09}Ge_{33}Se_{58}$	-1360
Aluminum	3.5	$Pb_{13}Ge_{29}Se_{58}$	-1710
Carbon	3.0	$Pb_{15}Ge_{37}Se_{58}$	-1990
Mercury	0.6	$SnSb_4Te_7$	25
Platinum	0	$SnBi_4Te_7$	120
Sodium	-2.0	$SnBi_3Sb_1Te_7$	151
Potassium	-9.0	$SnBi_{2.5}Sb_{1.5}Te_7$	110
Nickel	-15	$SnBi_2Sb_2Te_7$	90
Constantan	-35	$PbBi_4Te_7$	-53
Bismuth	-72		

APPENDIX G   THERMAL CONDUCTIVITY OF THERMOELECTRIC MATERIALS.

Materials	Lattice thermal		
	Energy gap (eV)	conductivity $(W\ m^{-1}k^{-1})$	δ $((eV)^{\frac{1}{2}}/Wm^{-1})$
GaSb	0.67	27	0.101
Bi2Te3	0.15	1.6	0.81
Sb2Te3	0.30	2.4	0.76
PbTe	0.32	2.0	0.94
PbSe	0.25	1.7	0.98
CdTe	1.50	7.5	0.54
InAs	0.35	29	0.068
InSb	0.17	15	0.092
ZnSb	0.6	17	0.16
InP	1.25	80	0.047
Ge	0.65	63	0.043
Si	1.15	113	0.032
Si- Ge[1]	0.97	7.6	0.432
Si- Ge[2]	0.97	3.3	0.99
Mg_2Ge	0.60	13	0.20
Mg_2Si	0.70	10.5	0.26
Mg_2Sn	0.30	16	0.114
AgPb18SbTe20	0.30	1.99	0.92
GaAs	1.42	37	0.107

[1]$Si_{70}Ge_{30}$ Alloy single crystal; [2]ne grained material (~5 μm).

Room temperature of energy gap.

http://www.ias.ac.in/pramana/v65/p469/fulltext.pdf

APPENDIX H THERMOCOUPLE TYPE APPLICATION.

Thermocouple type	Conductors	Temperature range (°C)	Typical specified temperature range (°C)	Seebeck coefficient at 20°C (μV/°C)	Application environments
E	Chromel (+) constantan (−)	−270 to +1000	−200 to +900	62	Oxidizing, inert, vacuum
J	Iron (+) constantan (−)	−210 to +1200	0 to 760	51	Caccuum, oxidizing, reducing, inert
T	Copper (+) constantan (−)	−270 to +400	−200 to +371	40	Corrosive, moist, subzero
K	Chromel (+) alumel (−)	−270 to +1370	−200 to +1260	40	Inert
N	Nicrosil (+) nisil (−)	−270 to +1300	0 to 1260	27	Oxidizing
B	Platinum (30% rhodium)(+) Platinum (6% rhodium) (−)	0 to 1820	0 to 1820	1	Oxddizing, inert
S	Platinum (10% rhodium) (+) platinum (−)	−50 to +1760	0 to 1480	7	Oxidizing, inert
R	Platinum (13% rhodium) (+) platinum (−)	−60 to +1760	0 to 1480	7	Oxidizing, inert

http://www.edn.com/electronics-blogs/bakers-best/4368765/Designing-with-temperature-sensors-part-four-thermocouples